

Smal Bank

Nieuwpoort Bank

Westdiep

Trapegeer

Broersbank

Potje

Den Oever



Flanders
State of
the Art

20_017_1
FHR reports

Understanding the coastal resilience of the Belgian West Coast

Set-up of a 1D coastline model

DEPARTMENT
MOBILITY &
PUBLIC
WORKS

www.flandershydraulicsresearch.be

Understanding the coastal resilience of the Belgian West Coast

Set-up of a 1D coastline model

Dujardin, A.; Montreuil, A.-L.; Trouw, K.; Dan, S.; De Maerschallck, B.; Houthuys, R.; Verwaest, T.

Legal notice

Flanders Hydraulics Research is of the opinion that the information and positions in this report are substantiated by the available data and knowledge at the time of writing.
 The positions taken in this report are those of Flanders Hydraulics Research and do not reflect necessarily the opinion of the Government of Flanders or any of its institutions.
 Flanders Hydraulics Research nor any person or company acting on behalf of Flanders Hydraulics Research is responsible for any loss or damage arising from the use of the information in this report.

Copyright and citation

© The Government of Flanders, Department of Mobility and Public Works, Flanders Hydraulics Research 2022
 D/2022/3241/184

This publication should be cited as follows:

Dujardin, A.; Montreuil, A.-L.; Trouw, K.; Dan, S.; De Maerschalck, B.; Houthuys, R.; Verwaest, T. (2022). Understanding the coastal resilience of the Belgian West Coast: Set-up of a 1D coastline model. Version 3.0. FHR Reports, 20_017_1. Flanders Hydraulics Research: Antwerp

Reproduction of and reference to this publication is authorised provided the source is acknowledged correctly.

Document identification

Customer:	Flanders Hydraulics Research	Ref.:	WL2022R20_017_1
Keywords (3-5):	coastal resilience, shoreface-connected ridge, sea level rise, 1D coastline model		
Knowledge domains:	erosiebescherming kust > morfodynamiek zachte zeewering > numerieke modelleringen		
Text (p.):	68	Appendices (p.):	14
Confidential:	<input checked="" type="checkbox"/> No	<input checked="" type="checkbox"/> Available online	

Author(s):	Dujardin, A., Montreuil, A.-L., Trouw, K., Verwaest, T.
------------	---

Control

	Name	Signature
Reviser(s):	Dan, S.	Getekend door:Sebastiaan Dan (Signature) Getekend op:2022-09-19 20:29:01 +02:0 Reden:Ik keur dit document goed 
	De Maerschalck, B.	Getekend door:Barth De Maerschalck (Sig) Getekend op:2022-09-21 09:57:46 +02:0 Reden:Ik keur dit document goed 
	Houthuys, R.	Getekend door:Rik Houthuys (Signature) Getekend op:2022-10-06 10:44:27 +02:0 Reden:Ik keur dit document goed 
Project leader:	Verwaest, T.	Getekend door:Toon Verwaest (Signature) Getekend op:2022-09-19 16:58:46 +02:0 Reden:Ik keur dit document goed 

Approval

Head of Division:	Bellafkih, K.	Getekend door:Abdelkarim Bellafkih (Sig) Getekend op:2022-09-20 11:38:09 +02:0 Reden:Ik keur dit document goed 
-------------------	---------------	---



Abstract

The CREST project (Monbaliu *et al.*, 2020) showed that topo-bathymetric monitoring carried out in the past 30 years revealed that the amount of sand in the active zone of the Belgian West Coast increased substantially. Correcting for sand works carried out, the rate of natural feeding of the area was estimated to be 10 mm/year, which is significantly more than the local sea level rise rate of 2 to 3 mm/year. One concludes that this coastal zone, with a length of ca. 16 km, has shown a natural resilience against sea level rise. The question remains which processes govern this behavior and where natural input of sand to the system occurs.

Using available coastal monitoring data as well as a state of the art sand transport model for the Belgian coast, it was revealed that natural processes drive complex transport patterns in the channel and the nearshore bank, resulting in a cross-shore natural feeding from off-shore to the coastline. The spatial distribution of this cross-shore natural feeding is determined by the existence of a channel – sand bank system.

The outcome of this research is a conceptual model for the large scale sand exchange in the study area which is implemented in a 1D coastline model. The most important element in these models is the cross-shore natural feeding of the active zone via a shoreface connected ridge amounting to 95,000 m³/year in the period 2000-2020.

Contents

Abstract	III
Contents	V
List of tables.....	VII
List of figures	VIII
1 Introduction.....	1
2 Morphological data-analysis	2
2.1 Introduction.....	2
2.2 Methodology	2
2.2.1 Morphological data and analyses.....	2
2.2.2 Volumetric analyses of the morphological zones.....	4
2.3 Results	6
2.3.1 Morphological changes and evolution	6
2.3.1.1 Onshore zone (active zone and landward dune zone).....	6
2.3.1.2 Onshore-offshore zone.....	7
2.3.2 Comparison between Scaldis model and observed morphological changes	10
2.3.3 Nieuwpoort harbour.....	16
2.3.4 Volumetric changes of the morphological zones	18
2.4 Human interventions.....	22
2.4.1 Beach management.....	22
2.4.2 Dredging and dumping work	24
3 1D Shoreline model	30
3.1 Introduction.....	30
3.2 Input data and boundary conditions	31
3.2.1 Bathymetry	31
3.2.2 Wave climate	37
3.2.3 Tidal currents.....	41
3.2.4 Grain size distribution.....	44
3.2.5 Sediment fluxes: Scaldis Coast	45
3.3 Model set-up	47
3.3.1 UNIBEST-LT	47
3.3.2 UNIBEST-CL.....	52

3.4	Sea level rise	56
3.4.1	Effect of SLR on the littoral drift	56
3.4.2	Application of the Bruun-rule	60
4	Discussion and Conclusions	62
4.1	Discussion	62
4.2	Conclusion	65
5	References	67
	Appendix A	A1
	Appendix B	A2
	Appendix C	A4
	Appendix D	A5
	Appendix E	A9
	Appendix F	A10
	Appendix G	A11
	Appendix H	A14

List of tables

Table 1 – Description of the landward and active morphologic zones.	5
Table 2 – Surveys period.....	16
Table 3 – Sand budgets for the landward and active morphological zones between 2000 and 2020.	19
Table 4 – The observed volumetric changes in the morphologic zones for the landward boundary and active zones. Erosion is red, accretion is green and no significant change in grey.	21
Table 5 – Examples of estimated sand input per human interventions.....	22
Table 6 – Directly reported dredging activities in the entrance and harbour of Nieuwpoort from 2016-2020 from the BIS database	26
Table 7 – Determined dredged sand volume in the entrance of Nieuwpoort from 2016-2020.....	29
Table 8 – Tide measurement campaigns at the Belgian west coast.	41
Table 9 – average grain size distributions on the beach.	44
Table 10 – Scaldis Coast runs.....	45
Table 11 – Target littoral drift	50
Table 12 – Calibration parameters	51
Table 13 – Littoral drift (x1000 m ³ /year).....	54
Table 14 – and sedimentation volumes (x1000 m ³ /year)	54
Table 15 – Littoral drift without and after 1 m SLR	56
Table 16 – Model input according to Bruun-rule.	60
Table 17 – Results from volumetric analysis. Sand balances for three sections (shown on Figure 49).....	62

List of figures

Figure 1 – A) Map indicating bathy-topographic coverage of the study zones, B) data timeline.....	3
Figure 2 – Delimitation of the morphologic zones along the west Belgian coast.....	4
Figure 3 – A) DEM in 2010, B) 2016, C) DoD between 2010-2016 and D) linear trend between 2010-2016. ...	6
Figure 4 – A) DEM in 2006, B) 2014, C) DoD and D) linear trend between 2006-2014.....	7
Figure 5 – A) Time series of topographic profiles in the onshore-offshore zone perpendicular to the coast from 2006-2014, B) zoom on the profile presenting the difference of elevation of the surveys between 2006 and 2014 and standard deviation over this period.	9
Figure 6 – Time series of topographic profiles in the onshore-offshore zone across the sand banks, presenting the difference of elevation of the surveys between 2006 and 2014 and standard deviation over this period.	10
Figure 7 – A) Initial and B) final modelled bed considered in Scaldis model for only wave and tidal processes	12
Figure 8 – A) Initial and B) final modelled bed considered in Scaldis model for only tidal processes.	12
Figure 9 – A) Simulation of bed evolution results of the Scaldis model considering wave and tidal processes, B) observed morphological change between 2015-2016, C) difference between Scaldis model and observed results.	13
Figure 10 – A) Simulation of bed evolution results of the Scaldis model considering only tidal processes, B) observed morphological change between 2015-2016, C) difference between Scaldis model and observed results.	13
Figure 11 – A) Simulation of bed evolution results of the Scaldis model considering wave and tidal processes, B) observed morphological change for the offshore zone between 2013-2014, C) difference between Scaldis model and observed results.	14
Figure 12 – Comparison between the observed bed evolution and Scaldis model after 1 year along profile 3 perpendicular to the coast.	15
Figure 13 – Comparison between the observed bed evolution and Scaldis model after 1 year along a profile oblique to the coast.....	15
Figure 14 – A) DEM in 2010, B) 2016, C) DoD between 2010-2016 and D) linear trend between 2010-2016.	17
Figure 15 – DoD between 2000-2020 along the study site with the defined morphological zones.....	20
Figure 16 – Principle sketch of types of human interventions.....	23
Figure 17 – Dredging timeline in Nieuwpoort harbour and entrance from 2009 to 2020.....	24
Figure 18 – Example of vertical profile of a hopper well densimeter (HWD) in the Nieuwpoort entrance, red line. The blue line corresponds to sand material threshold. Inset: location of the measurement	25
Figure 19 – Map of location of dredging and dumping zones based on common, area dredged between 2016-2020.	25
Figure 20 – Example of intensity map for the dredged sand material (excluded silt) in 2016	27

Figure 21 – Maps of determined yearly dredged sand volume from 2016 to 2020 28

Figure 22 – Map of the determined average yearly dredged sand volume from 2016 to 2020..... 29

Figure 23 – Example of output generated by the UNIBEST-LT module..... 31

Figure 24 – Investigation of cross-shore profile dynamics using semi-annual topo-bathymetric monitoring data. Example of the cross-shore profile “transect 18”, located in coastal section 8 – “Verkaveling Westhoek”, illustrating the method used. 33

Figure 25 – Investigation of cross-shore profile dynamics using semi-annual topo-bathymetric monitoring data. Example of the cross-shore profile “transect 59”, located in coastal section 24 – “Sint-Idesbald”, illustrating the method used. 33

Figure 26 – Elevation of the morphological Depth of Closure and dunefoot in the study area. MHW – Mean High Water; MLW – Mean Low Water. 34

Figure 27 – Definition of Momentary Coastline 34

Figure 28 – Evolution of the location of the dune foot (5.9 m TAW), the depth of closure (-4 m TAW) and derived Momentary CoastLine. 35

Figure 29 – Evolution of the location of the mean low water line (+0.18 m TAW) and high water line (+4.51 m TAW)..... 36

Figure 30 – Wave climate at Westhinder. 38

Figure 31 – Wave conditions at Westhinder per calendar year..... 40

Figure 32 – Measured tidal ellipses at the West coast..... 42

Figure 33 – Measured tidal ellipses at Potje 2 and Oostduinkerke Bad..... 42

Figure 34 – Tidal currents and water levels, binned and averaged in respect to the moment of high water in Nieuwpoort..... 43

Figure 35 – Map of median grain size, on the basis of kriging interpolation with an external drift. 44

Figure 36 –Yearly averaged sediment fluxes (calculated from Scaldis Coast HSW112) on the boundaries and profiles of the UNIBEST model. 46

Figure 37 – Illustration of the 6 profiles implemented in UNIBEST-LT and the applied wave climate. 47

Figure 38 – Location of the 6 profiles, wave climate boundary points and two tidal boundaries implemented in UNIBEST-LT. 47

Figure 39 – Comparison of the sediment transport rates using different formulations in Unibest with the results of Scaldis-Coast (HSW112), for a relatively deep profile..... 49

Figure 40 – Comparison of the sediment transport rates using different formulations in Unibest with the results of Scaldis-Coast, for a relatively shallow profile..... 49

Figure 41 – Net alongshore transport (Scaldis Coast model) 53

Figure 42 – Littoral drift after 1,2 and 5 years..... 54

Figure 43 – Coastline propagation/retreat with and without nourishments..... 55

Figure 44 – Littoral drift for profile 8 for a climate condition with high waves 57

Figure 45 – Yearly total littoral drift for profile 78 58

Figure 46 – Littoral drift along the coast after 5 years without and with SLR..... 59

Figure 47 – Coastline accretion/erosion per year between the 2nd and 5th year without and with SLR..... 59

Figure 48 – Total accretion/sedimentation over the next 30 years without SLR and by applying the Bruun rule for SLR of 8 mm/year 61

Figure 49 – Distinguishing three sections in the study area based on sand balances. 62

Figure 50 – Variability of the slope of the active beach and shoreface zone in the study area. 63

Figure 51 – Conceptual model for the large scale sand exchanges in the study area. 64

1 Introduction

This research project has two objectives. Firstly, we want to explain our observations of resilience to sea level rise of the Belgian West coast. In a previous research on the Belgian coast (CREST project, Monbaliu et al 2020), we compared the sea level rise in the past 30 years, with the change in sand volume in the beaches, active foreshores and dunes for the Belgian West Coast. The result was a much larger growth rate of 10 mm/year compared to a sea level rise of 2 to 3 mm/year. So there must be a natural feeding into this zone to compensate for the difference. But, how much comes from along shore, how much comes from cross-shore, and is this resilience uniform over the area considered? We want to solve these questions.

Secondly, our goal is to establish a morphological model on the time scale of decennia to centuries. Such models can be tools for predicting morphological effects of sea level rise, as well as effects of large infrastructure works. The model should be able to predict, for example, the retreat of a coastline, according to Bruun rule, but also progradation of a coastline in cases where natural feeding is dominating the Bruun rule effect (Bruun, 1962). How are we approaching this? We approach it by establishing a 1D coastline model. This means that we adopt the concept of equilibrium profile and that the behavior of the coastline is described by equation (Eq. 1) from Stive (2004).

$$C_p h_* = \frac{\partial \text{MSL}}{\partial t} L_* - (q_{x,\text{sea}} - q_{x,\text{dune}}) + \frac{\partial Q_y}{\partial y} - s$$

where x and y are cross-shore and alongshore distance, respectively; C_p = coastline retreat rate [m/y]; h_* = active height of the profile [m]; $\partial \text{MSL}/\partial t$ = sea level rise rate [m/y]; L_* = width of the active zone [m]; $q_{x,\text{sea}}$ = cross-shore feeding of the active zone from the neighbouring sea bottom [$\text{m}^3/\text{m}/\text{y}$]; $q_{x,\text{dune}}$ = flux towards the dunes [$\text{m}^3/\text{m}/\text{y}$]; Q_y = littoral drift [m^3/y]; and s = nourishment intensity [$\text{m}^3/\text{m}/\text{y}$].

The position of the coastline on the left side of the equation multiplied with the active height of the profile is described by a summation of influences by five different processes on the right side of the equation. The first term corresponds to the Bruun rule (Bruun, 1962). The second term is cross-shore feeding to the active zone from the sea bottom. The third term is aeolian loss to the dunes. The fourth term represents the gradients in littoral drift. The fifth and last term is human interventions, nourishments or sand extractions.

The main result of this research is a conceptual model for the large scale sand exchange in the study area which is implemented in a 1D coastline model. The most important element in these models is the cross-shore natural feeding of the active zone via a shoreface connected ridge amounting to 95,000 m^3/year in the period 2000-2020.

Materials and Methods:

- Digital elevation models, wave and tidal data, grain size measurements and descriptions of human interventions, for our study area and considered period from 2000 to 2020 (20 years) are provided by Coastal Division.
- For the 1D coastline model, we use Deltares software Unibest-CL+ (Deltares, 2020). Profiles are taken from a published data-set with 100 m spacing (Roest, 2019), which is derived from the ca. yearly topo-bathymetric monitoring data.

2 Morphological data-analysis

2.1 Introduction

A morphological data-analysis is conducted in order to quantify the volumetric changes in the coastal zone. Observations are based on topo-bathymetric surveys and LiDAR data provided by Coastal Division and the derived volumetric changes are corrected for the human interventions like beach nourishments (data provided by Coastal Division) and dredging works in the access channel to Nieuwpoort harbour (data provided by Maritime Access).

The observed volumetric changes will serve as validation dataset of the 1D coastline model, while the human interventions serve as an input for the same model (see §3.3.2).

2.2 Methodology

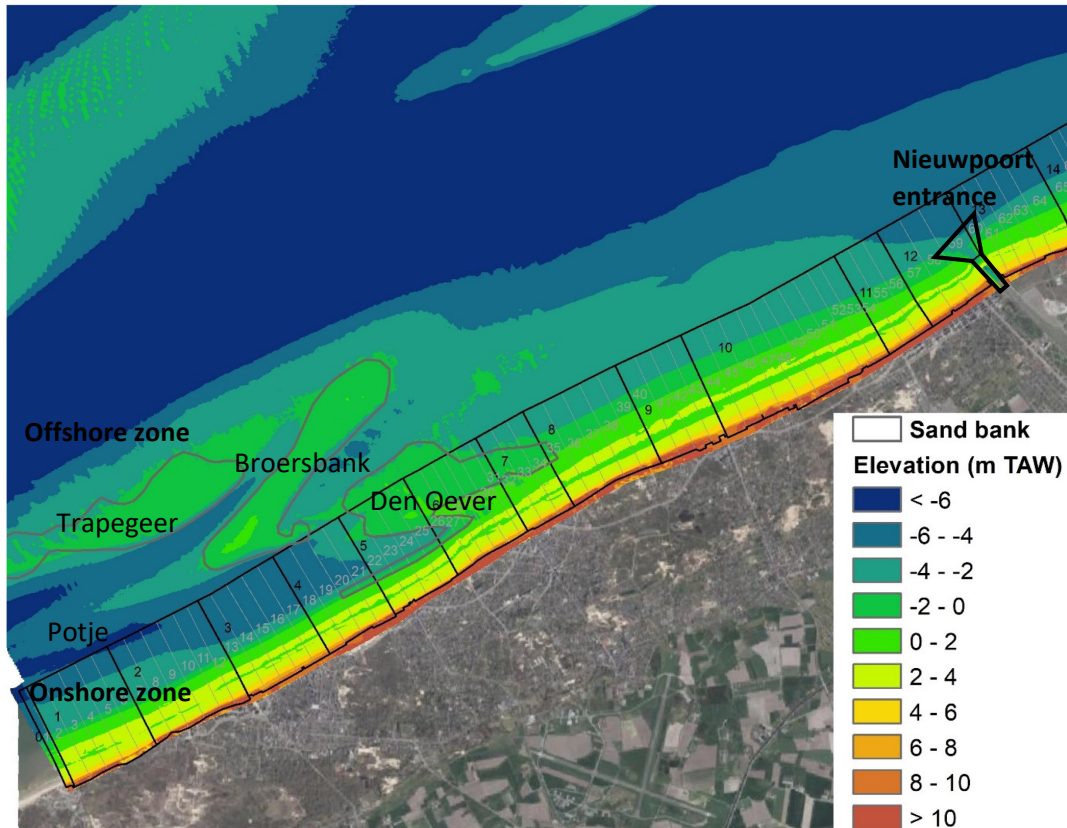
2.2.1 Morphological data and analyses

Bathy-topographic data consists of airborne LiDAR surveys covering the beach and single-beam bathymetric surveys of the shoreface which was provided by Coastal Division (Figure 1 A). Also, bathymetric data covering the entrance of Nieuwpoort harbour and the offshore zone (up to -10 m TAW) along the study site were acquired and retrieved from Caris database on the Triton server owned by Vlaamse Hydrografie. Figure 1 B presents the data timeline of the acquired datasets. The onshore zone covers the area from the dunes to -4 m TAW, followed by the offshore zone of deeper elevations (< -4 m TAW).

For every survey, a digital elevation model (DEM) combining the beach-shoreface (onshore zone) of 5 m cell size was generated. Also, DEMs of the Nieuwpoort harbour and the offshore zone were produced with a cell size of 2 m and 10 m cell size respectively. To have a large spatial overview of the west coast, DEMs of 10 m cell size were merged to cover the area from the beach including foredunes to the offshore zone. The generated DEMs were used for two-dimensional and one-dimensional morphological analysis. DEMs of difference (DoDs) were produced between consecutive surveys and also from the reference survey corresponding to the first survey in 2000 available for the respective zones.

A morphological trend analysis on the basis of time series of topographic and bathymetric DEMs for the onshore, offshore and Nieuwpoort entrance zone was carried out in ArcGIS. It is based on a simple linear regression with least squares method performed for each DEM cell. The slope of the regression line represents the morphological trend over the considered time period for that grid cell. The coefficient of determination (R^2) can also be determined for each cell and it indicates how well the best fit line approximates the time series of depth data in the grid cell under consideration. Janssens et al. (2013) describes in more details the method. Visualization of the produced grids of morphological trend allows to delineate the spatial distribution of erosion and sedimentation zones. A threshold of 0.02 m/year of changes, based on a defined $R^2=0.5$, was applied in order to assess significant morphological changes.

A)



B)

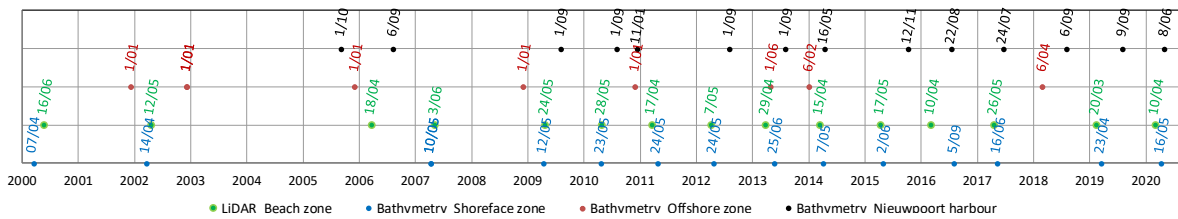


Figure 1 – A) Map indicating bathy-topographic coverage of the study zones, B) data timeline.

Location of data and analyses:

Onshore zone combining beach and shoreface zone:

P:\20_017-kstlnmdlWstKs\3_Uitvoering\Morphology\01_Data\OnshoreZone

Offshore zone:

P:\20_017-kstlnmdlWstKs\3_Uitvoering\Morphology\01_Data\OffshoreZone

Combined onshore and offshore zone:

P:\20_017-kstlnmdlWstKs\3_Uitvoering\Morphology\01_Data\OnOffZones

Nieuwpoort harbour:

P:\20_017-kstlnmdlWstKs\3_Uitvoering\Morphology\01_Data\NieuwpoortHarbour

2.2.2 Volumetric analyses of the morphological zones

The beach-shoreface (onshore zone) was split into 21 morphological zones. Of these, 10 landward morphologic zone correspond to the dune area above the fixed elevation of +5.9 m TAW, which is the lower boundary for the typical dunefoot height along the Belgian coast according to Strypsteen *et al.* (2019). These zones are numbered 1 to 11, excluding zone nr. 10 which corresponds to the access channel of Nieuwpoort harbour (Figure 2 and Table 3). For this study, the contour line of 5.9 m TAW of the LiDAR survey in 2000 was selected to delimit the study zones.

Also, 11 active morphologic zones were defined, covering the beach-shoreface between the dunefoot and a seaward boundary (i.e. depth of closure at -4 m TAW) in 2000. Appendix A further describes the characteristics of the defined morphological zones. Inside these, volumetric changes were determined over the study period from 2000 to 2020 in order to assess the sand flux from the active zone to the landward morphologic zones. The number of landward morphologic zones is lower than the active morphologic zones due to the presence of Nieuwpoort harbour along the study site. The total length of dunes is of 7.65 km, corresponding to 48% of the total length of the west coast.

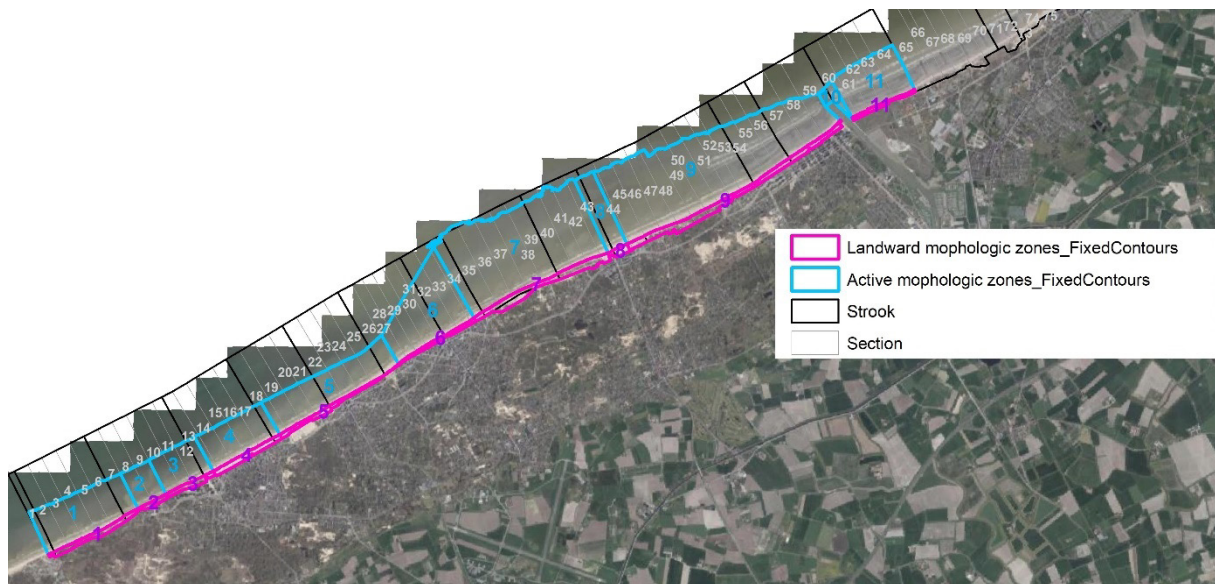


Figure 2 – Delimitation of the morphologic zones along the west Belgian coast.

Table 1 – Description of the landward and active morphologic zones.

Landward morphologic zone	Section	Location	Area of the zones (ha)
1	1-7	Natuurreserveaat Westhoek	12
2	8-9	Verkaveling Westhoek	3
3	10-13	Westhoek – De Panne Centrum	6
4	14-18	De Panne Centrum	11
5	19-26	Sint-Idesbald – Koksijde Bad	9
6	27-33	Koksijde Bad	6
7	34-43	Koksijde Bad-Oost	26
8	44	Oostduinkerke-Bad	4
9	45-59	Oostduinkerke-Oost – Nieuwpoort Bad	35
11	60-64	Lombardsijde	5

Active morphologic zone	Section	Location	Area of the zones (ha)
1	1-7	Natuurreserveaat Westhoek	110
2	8-9	Verkaveling Westhoek	31
3	10-13	Westhoek – De Panne Centrum	51
4	14-18	De Panne Centrum	72
5	19-26	Sint-Idesbald – Koksijde Bad	117
6	27-33	Koksijde Bad	128
7	34-43	Koksijde Bad-Oost	313
8	44	Oostduinkerke-Bad	42
9*	45-59	Oostduinkerke-Oost – Nieuwpoort Bad	391
10	/	Nieuwpoort harbour	10
11	60-64	Lombardsijde	83

*Section 59 does not contain the navigation channel, while it is in Houthuys et al. (2022).

Location of data and analyses:

P:\20_017-kstlnmdlWstKs\3_Uitvoering\Morphology\01_Data\StudyZone\MorphologicalZones\FixedLevels

2.3 Results

2.3.1 Morphological changes and evolution

2.3.1.1 Onshore zone (active zone and landward dune zone)

DEMs of 5 m cells covering the onshore zone combining the beach and shoreface Lidar surveys were produced for 2000, 2002, 2006, 2007, and from 2009 to 2020; also DoDs were generated. Examples of DEMs and DoDs are presented in Figure 3. A clear spatial variation of morphological changes is observed and is mainly characterized by intertidal bar migration and dune growth along the entire study site, and the shoreface connected ridge development and dynamics at Koksijde-Bad, just west of the St.-André headland (section 26-32). Opposed to other areas, either stability or erosion has dominated there in the shoreface. The beach at Lombardsijde (section 61-64) has experienced erosion, while the dunes have grown. This strong erosion is a local phenomenon, related to the fact that just before the 2010 survey, a beach nourishment had taken place there.

The linear trend analysis over 2010-2016 based on 7 surveys (a period without large nourishments was chosen) confirms a significant accretion of the dunes along the entire study site (Figure 3, Appendix B). This trend analysis shows:

- a remarkable development of the shoreface connected-ridge and channel, with erosion at the eastern end of the Potje channel and sedimentation on top of the sand ridge;
- beach and dune growth from Koksijde to Nieuwpoort;
- while significant erosion characterized the Lombarsijde shoreface (i.e. East of Nieuwpoort).

No significant trends could be observed for the rest of the study site.

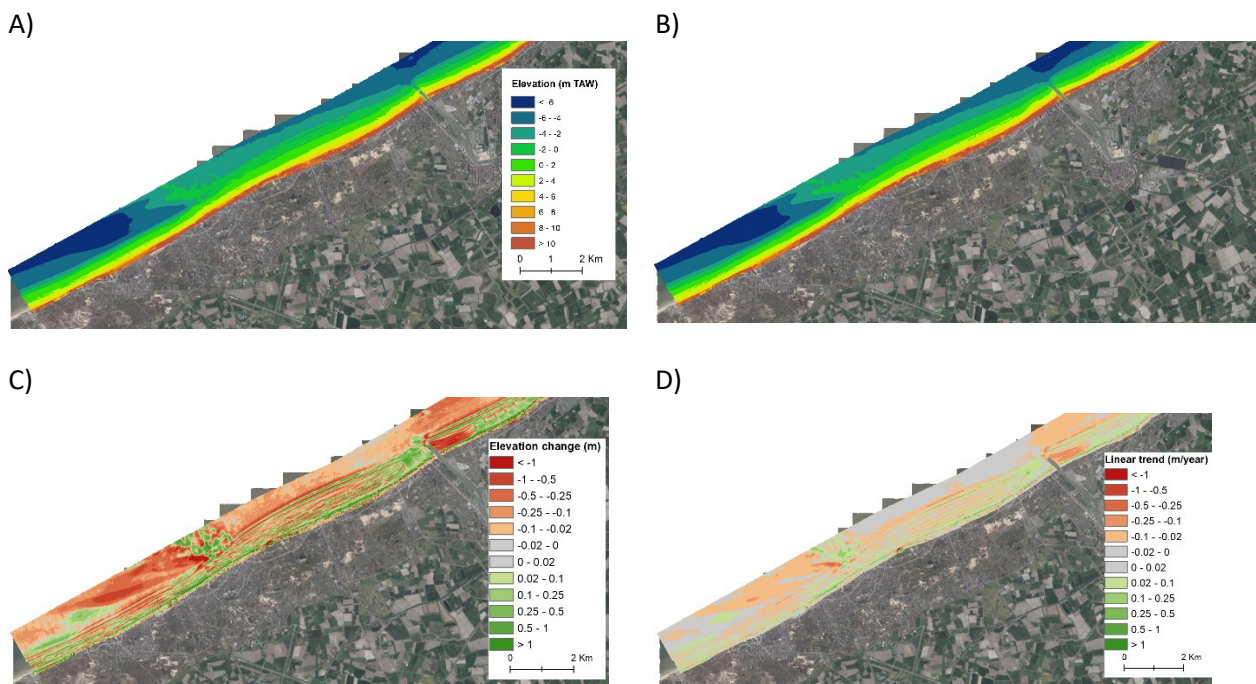


Figure 3 – A) DEM in 2010, B) 2016, C) DoD between 2010-2016 and D) linear trend between 2010-2016.

2.3.1.2 Onshore-offshore zone

2D morphology

DEMs of 10 m cells of the onshore-offshore zone were produced and DoDs were generated. DEMs in 2006 and 2014 covering the area from the coastline to 15 km offshore are presented in Figure 4. The DoD between 2006-2014 shows some spatial morphological variation, alternating between accretion, erosion and stability. The linear trend analysis over this period emphasizes that a relative stability dominates in the offshore zone (Figure 4, Appendix B). However, local erosion up to 0.17 m/year can be observed at the west side of Trapegeer sand bank, and in particular at its landward side. This might be due to an increase of tidal currents in the Potje channel. In contrast, accretion has occurred in the eastward part of the landward side of this sand bank. An antagonist trend is the seaward side of Broersbank where a small channel is present (we suggest here the name ‘Panne pas’ channel, which has no official status).

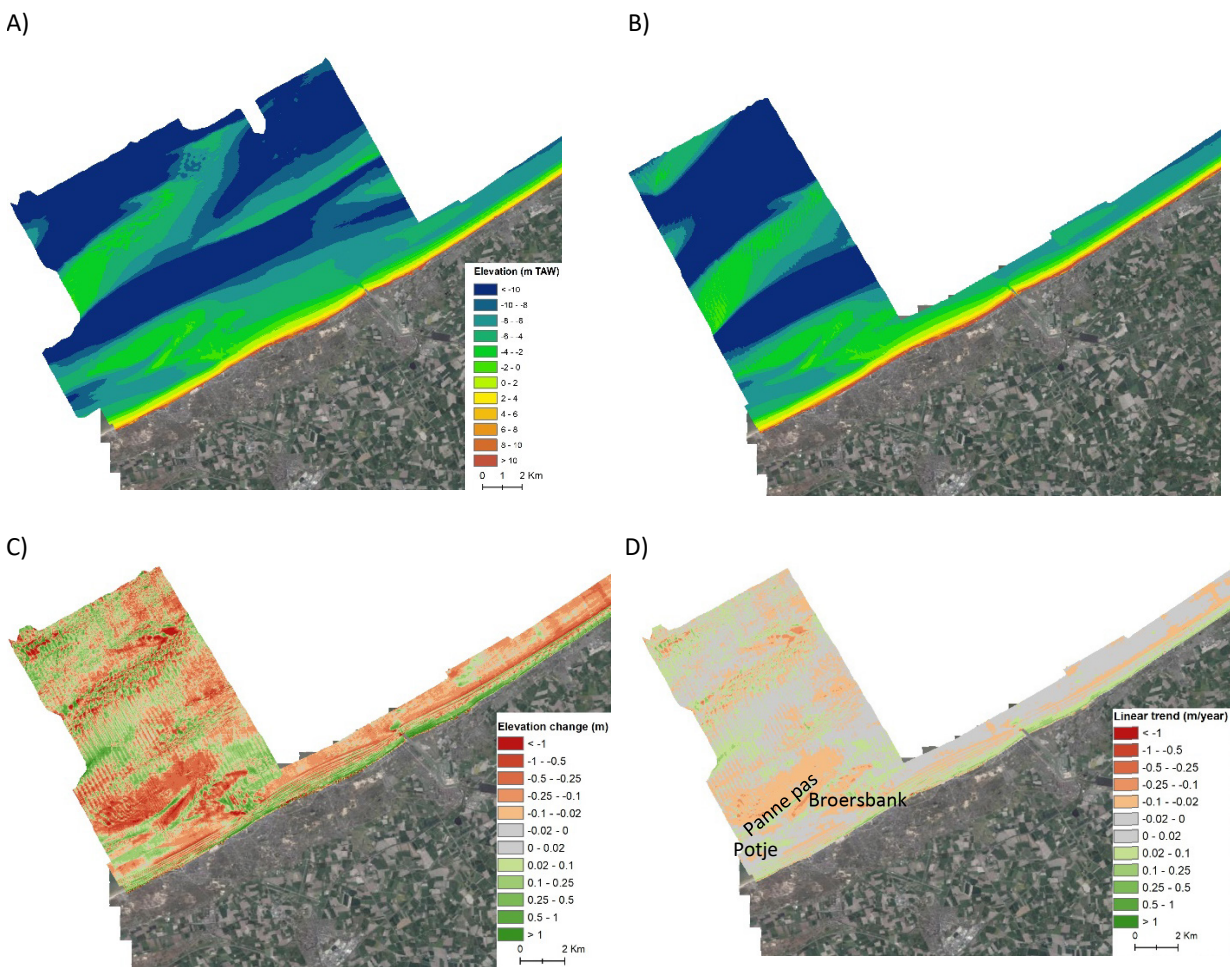
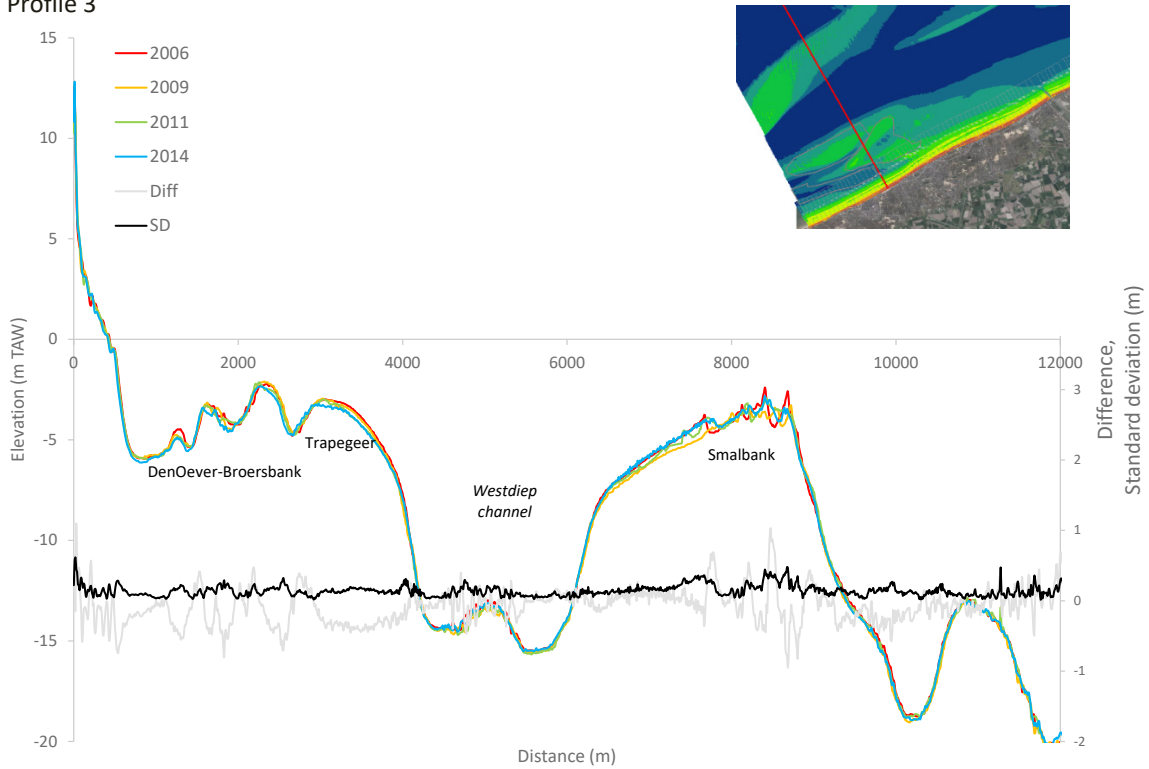


Figure 4 – A) DEM in 2006, B) 2014, C) DoD and D) linear trend between 2006-2014.

1D morphology

Several profiles were extracted from the DEMs to investigate the dynamics of the marine features (Figure 5 and Figure 6). In general, the morphological changes in the offshore zone is 0.23 m (average standard deviation of the elevation change over time). However, some parts of the profiles show consistent changes over the observation period and can therefore be interpreted as real change. These morphological trends are indicated by grey arrows in the profiles. Some areas with a decrease in height of the sea bed can be observed. The Potje channel has moved landward around 10 m between 2006-2014. Appendix C displays the migration processes observed in the Potje area. Also, the attached sand bank, Den Oever and Broersbank, is subject to a landward migration over this period. Profiles across the sand banks clearly indicate a decrease of elevation of the sand banks associated with a landward-eastward (south-eastern) movement around 10-15 m/year (Figure 6). This agrees with the observed long-term migration of the sandbanks toward the beach (Houthuys et al., 2022). Note that the shoreface in profile 3 also recedes, while the beach is stable. Profile 6 shows the attachment area of Broers Bank to the shore. Both bank top and beach show accretion.

A) Profile 3



B) Zoom Profile

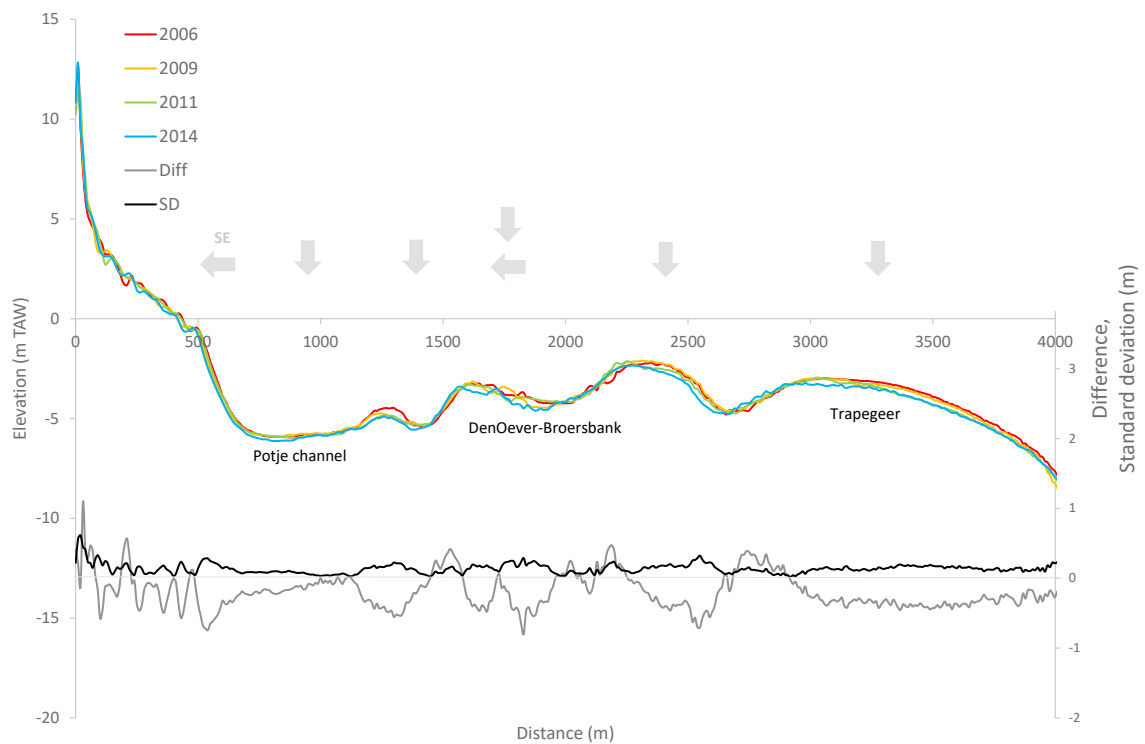


Figure 5 – A) Time series of topographic profiles in the onshore-offshore zone perpendicular to the coast from 2006-2014, B) zoom on the profile presenting the difference of elevation of the surveys between 2006 and 2014 and standard deviation over this period. Arrow indicates the observed morphological trend. Inset: location of the extracted profile.

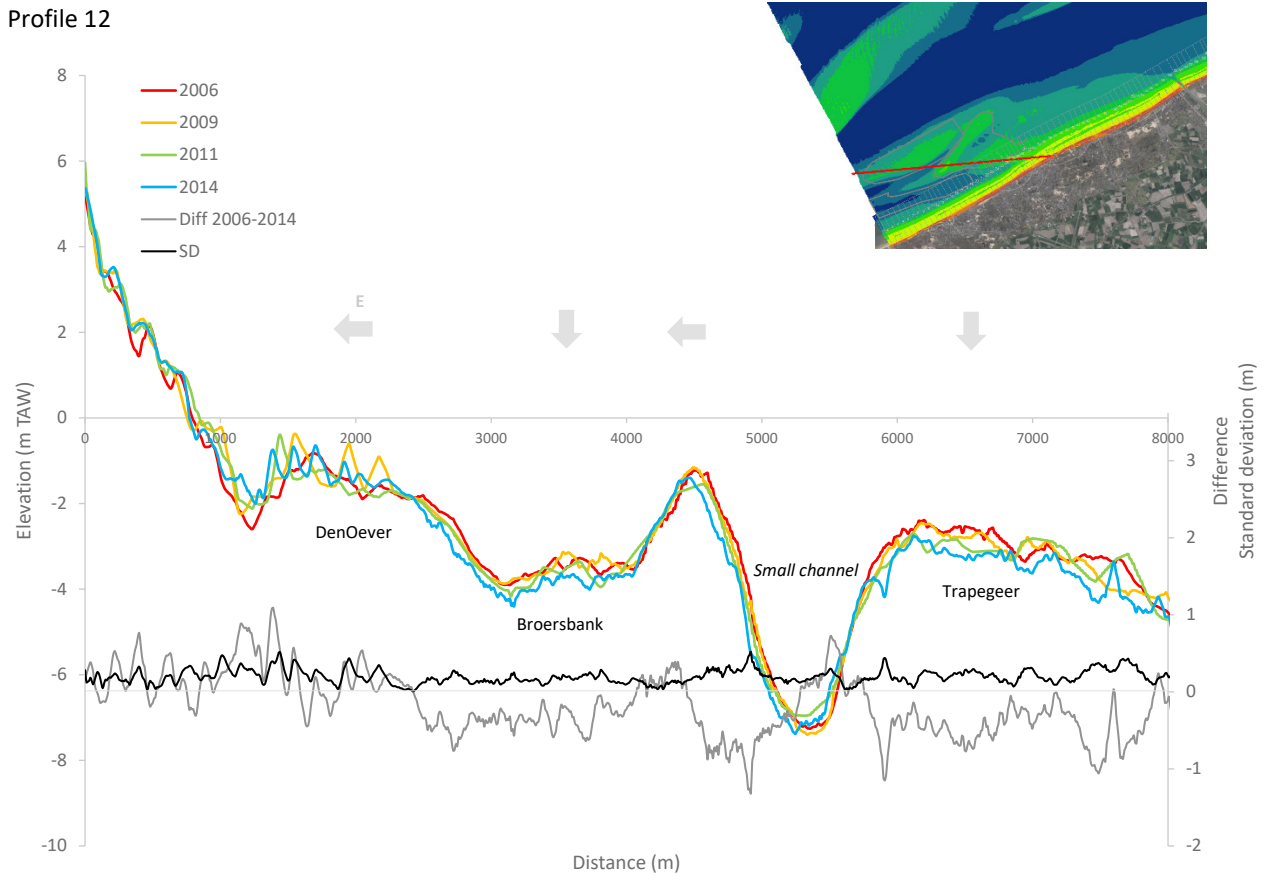


Figure 6 – Time series of topographic profiles in the onshore-offshore zone across the sand banks, presenting the difference of elevation of the surveys between 2006 and 2014 and standard deviation over this period. Arrow indicates the observed morphological trend. Inset: location of the extracted profile from east to west.

2.3.2 Comparison between Scaldis model and observed morphological changes

Introduction

A comparison between observed morphological changes and two Scaldis Coast runs was done. The purpose of this analysis is twofold:

1. In order to investigate whether a clear distinction can be made between the wave-driven onshore morphologic zone (beach-shoreface) and the tidally-driven offshore morphologic zone, a comparison was made between two model runs: one taking into account both tide and wave driven currents, one taking only into account tidal currents. If this distinction can be made based on the model runs, it would give a clear indication of the Depth of Closure, beyond which no wave driven sediment transport occurs.
2. The Scaldis Coast model has not yet been validated for the West coast. The comparison with the observed morphological changes can serve as a first qualitative validation for this area. If the model proves to be reliable, the output of Scaldis Coast can be used to estimate boundary conditions for the 1D coastline model (see §3.2.5).

Ideally, matching periods of field observation and model simulation should be used, since morphological changes can differ greatly from year to year due to inter-annual variations in wave climate. However, matching periods of model output were lacking. Therefore two different periods of field observations within two zones were used to get an estimate of this inter-annual variation in morphological changes.

The Scaldis Coast model, developed by FHR, simulates short and longer-term morphodynamics (up to 10 years) along the Belgian coast in the tidally driven offshore and wave driven nearshore zone. The computational grid consists of > 250,000 nodes with a maximum resolution of 25 m along the Belgian coastline and a minimum resolution of 750 m in the open offshore boundary. The topo-bathymetric mesh consists of a patchwork of airborne LiDAR and bathymetric survey data collected between 2004 and 2015 (Kolokythas *et al.*, 2018). Wave processes correspond to a schematisation for full wave climate of the period between June 2014 and June 2015. For the tidal forcing, a morphological representative tide has been selected. Alongshore sediment transport is based on a 10-year average. Figure 7 and Figure 8 presents the initial and end bed considered as input in Scaldis model. A comparison between Scaldis model (runs sed084 and swc005V13, see §3.2.5) and the observed bed elevation changes was carried out for a period of 1 year between 2015 – 2016 for the onshore zone and between 2013 – 2014 for the combined onshore-offshore zone (see Figure 9 to Figure 11).

Comparison

Figure 9 and Appendix D present the results of the Scaldis model of the bed evolution after 1 year by considering wave and tidal processes. Some morphological changes are modelled in the onshore zone along the entire west coast where erosion occurs on the beach around +3 and +4 m TAW. In contrast, sand accumulation dominates in the shoreface between -2 m and -4 m TAW contour line located just landward of the DoC (Depth of Closure). In contrast, the upper-beach above +5 m TAW is stable. Also the model generates a weak pattern of potential bars dynamics. Thus Scaldis model is able to simulate bar processes but not to replicate them fully due to the absence of cross-shore process in the model. Although the offshore zone is generally stable, a high spatial variability of bed evolution of the shoreface-connected sand ridge at St André and its westward side, corresponding to the landward side of the attached sand ridge, is simulated in Scaldis which reflect the complex processes-responses there. Interestingly, a morphological impact from the two long groynes located west of Koksijde is simulated in Scaldis (Kolokythas *et al.*, 2020a), while observations show relative stability. The observed morphological changes between 2015 and 2016 also indicate significant changes of the beach-shoreface with the upper-beach and dune experiencing accretion and landward migration of berms and bars. Also, the shoreface-connected sand ridge and its westward side are dynamic. The shoreface zone between -2 and -4 m TAW alternates between morphological stability and changes. A similar trend is observed over 1-year between 2013 and 2014 (onshore-offshore zone). Regarding the surrounding area of the groynes west of Koksijde, their effect on bed evolution is observed but it is lower than the simulated one. This might be attributed to an equilibrium reached by the beach. An erosion effect caused by the groynes located just west of Nieuwpoort harbour is also simulated while it does not happen in the field. This is probably an initial effect in the model which stabilizes after some time. It can be that the initial bathymetry at the tips of the groins is not well represented in the model, or that the scour effect is overestimated. A large area of negative bed evolution in Lombarsijde is modelled by Scaldis Coast which seem to overestimate the actual erosion taking place there. Noteworthy, no significant morphological changes are simulated and observed in center of Potje channel. However, it has been reported that this channel has been migrating eastward (Houthuys *et al.*, 2022). This is probably not depicted here due to the short period (1 year) of investigation. However, we can observe some negative morphological changes at its eastern tip which might suggest some migration of the channel.

The difference between the observed morphological change and the modelled one is displayed in Figure 9C. It indicates some differences in the attached sand ridge and its westward side. Also, the results show some difference of elevation above 0.5 m on the upper-beach (+4 m TAW). However, this value should be considered with care due to the difference of data type and study period. Also, alongshore processes are only considered in Scaldis so that the difference between modelled and observed could occur. For example, a bar is moving faster in the observation than in the model or visa versa, the difference will be large, but the general patterns of the bottom might be comparable.

Figure 10 and Appendix D present the results of the Scaldis model of the bed evolution after 1 year by considering only tidal processes. Significant bed evolution is simulated in the shoreface-connected sand ridge at and west of St André, while the rest of the study site is relatively stable. These are also observed on the difference of DEM between 2015 and 2016 (similar results in 2013 – 2014). The effect of the groynes located west of Koksijde is minor under the tidal process scenario of simulation. As found for the simulation with tidal and wave processes, the largest difference between the morphological observation and the Scaldis model results occurs in the shoreface of the connected ridge and at its westward side.

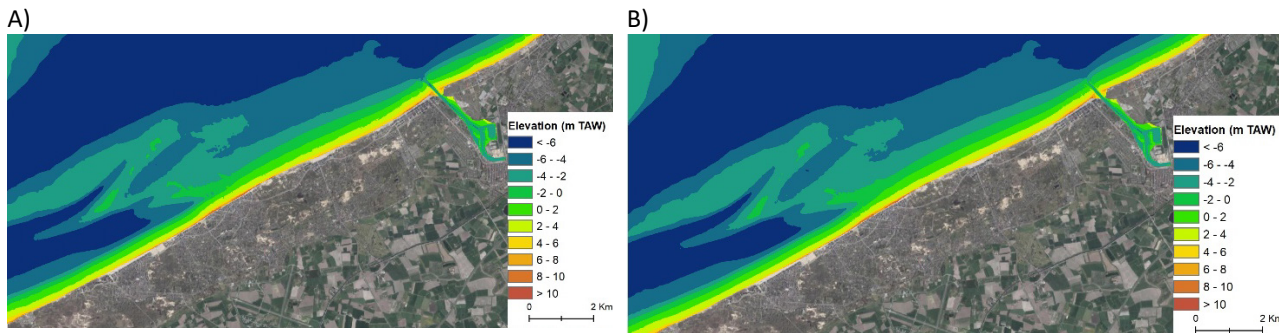


Figure 7 – A) Initial and B) final modelled bed considered in Scaldis model for only wave and tidal processes

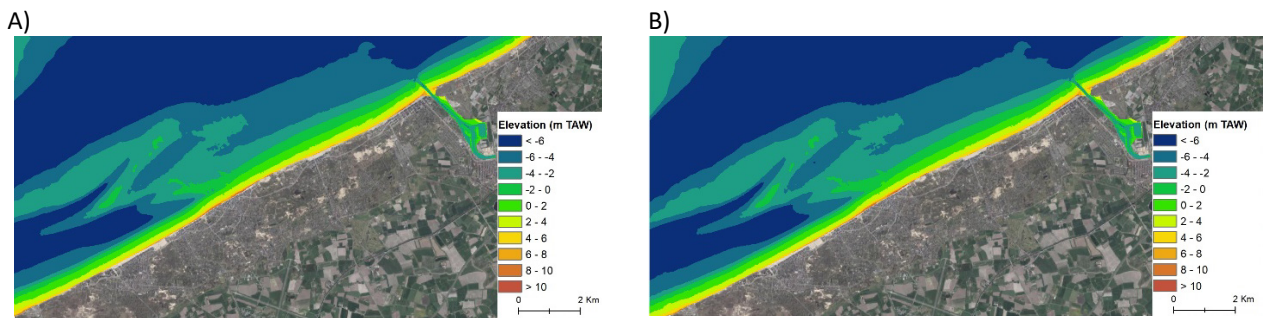


Figure 8 – A) Initial and B) final modelled bed considered in Scaldis model for only tidal processes.

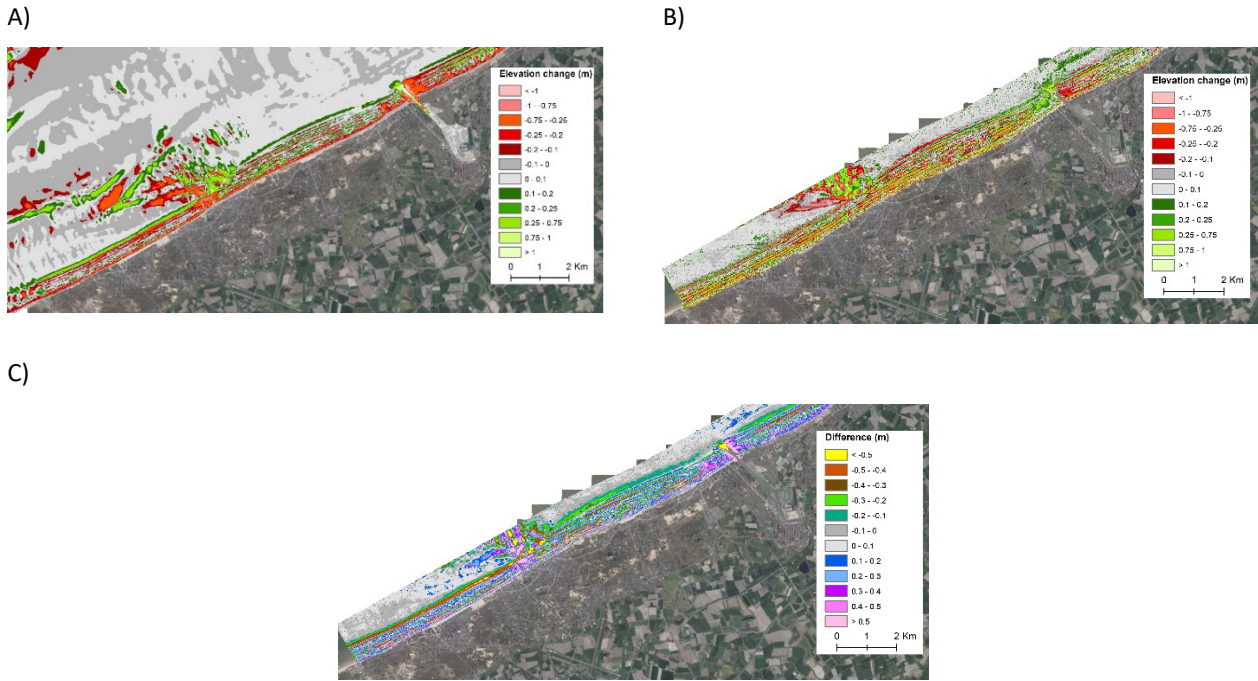


Figure 9 – A) Simulation of bed evolution results of the Scaldis model considering wave and tidal processes, B) observed morphological change between 2015-2016, C) difference between Scaldis model and observed results.

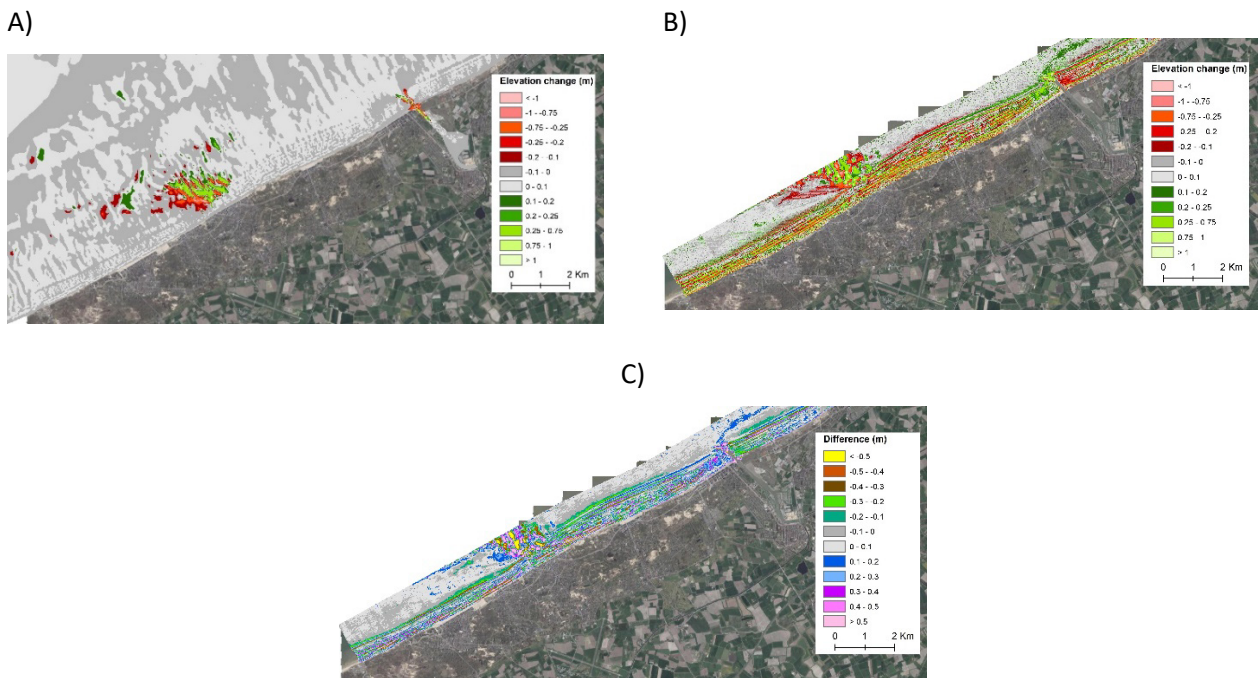


Figure 10 – A) Simulation of bed evolution results of the Scaldis model considering only tidal processes, B) observed morphological change between 2015-2016, C) difference between Scaldis model and observed results.

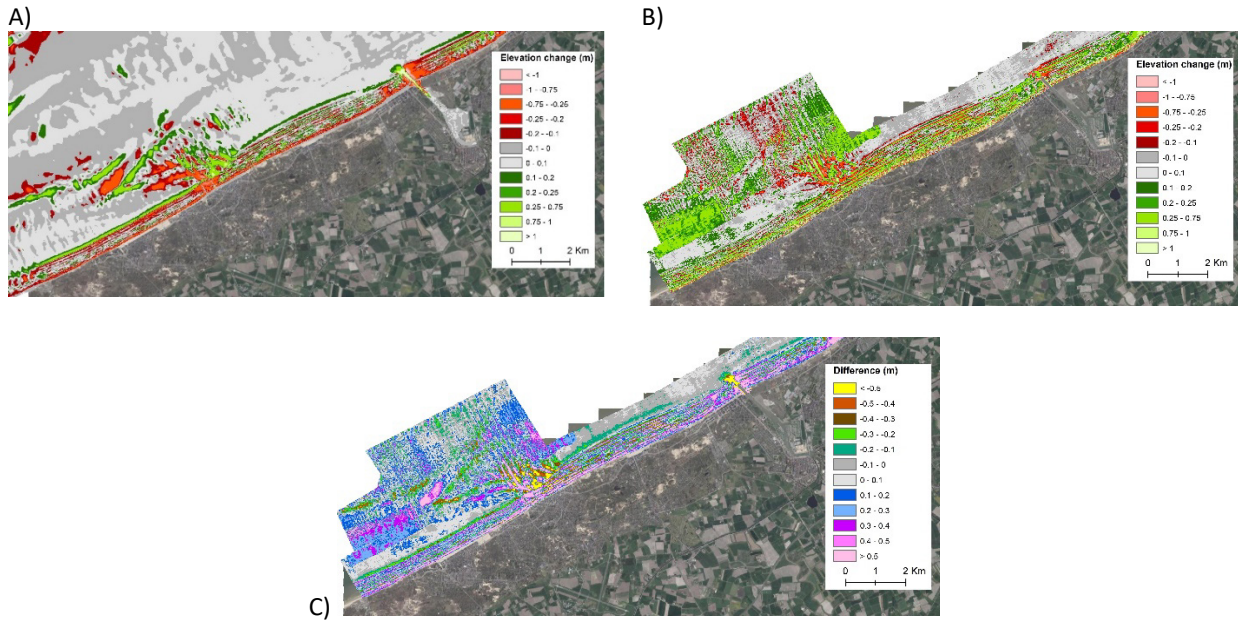


Figure 11 – A) Simulation of bed evolution results of the Scaldis model considering wave and tidal processes, B) observed morphological change for the offshore zone between 2013-2014, C) difference between Scaldis model and observed results.

Profiles were extracted to further investigate the difference between the Scaldis simulations and the observed morphological changes for the onshore and offshore zone after 1 year (Figure 12 and Figure 13). In the cross-shore profile (Figure 12), the bed evolution modelled under tidal processes only is generally much lower than the one under wave and tide processes. The same order of magnitude of morphological change is observed for the offshore zone. However, the observed bed evolution at the coast is much greater than the one simulated by the Scaldis model under both wave and tide processes. The Scaldis model under wave and tide processes presents a maximum bed evolution exceeding -0.6 m at the coast. Another peak is simulated in the onshore zone at distance 530 m, while it is observed closer to the coast (distance 450 m). This is probably due to the displacement of sand bars in cross-shore direction for which processes are not modelled in Scaldis. The oblique profile generally shows a similar pattern of morphological changes between tidal process and tidal-wave processes. The largest modelled bed evolution exceeding 1 m occurs landward of the shoreface-connected sand ridge around 1200 m along the profile. However, this change is smaller than the observed bed evolution, with a peak around 1.5 m (at 1600 m along the profile) located westward of the attached sand ridge. Both models simulated negative morphological change in the area westward of the shoreface-connected sand ridge (distance > 2000 m along the profile) while the observed bed evolution is low.

Conclusion

The Scaldis model produces similar magnitudes of bed change as the observations. The combined tidal and wave forcing produces better agreement, especially in the cross-shore direction. However, the detailed locations of change differ. This may partially be the result of a different start morphology.

Location of data and analyses:

P:\20_017-kstInmdlWstKs\3_Uitvoering\ScaldisKust

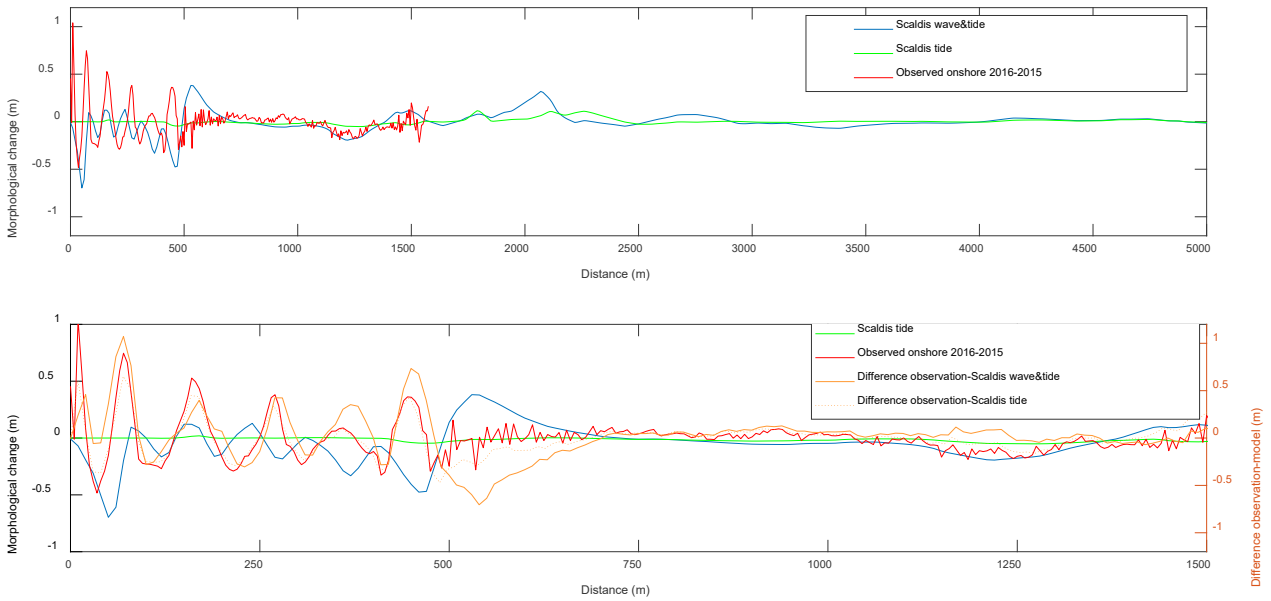


Figure 12 – Comparison between the observed bed evolution and Scaldis model after 1 year along profile 3 perpendicular to the coast. Location of the profile presented in Figure 5.

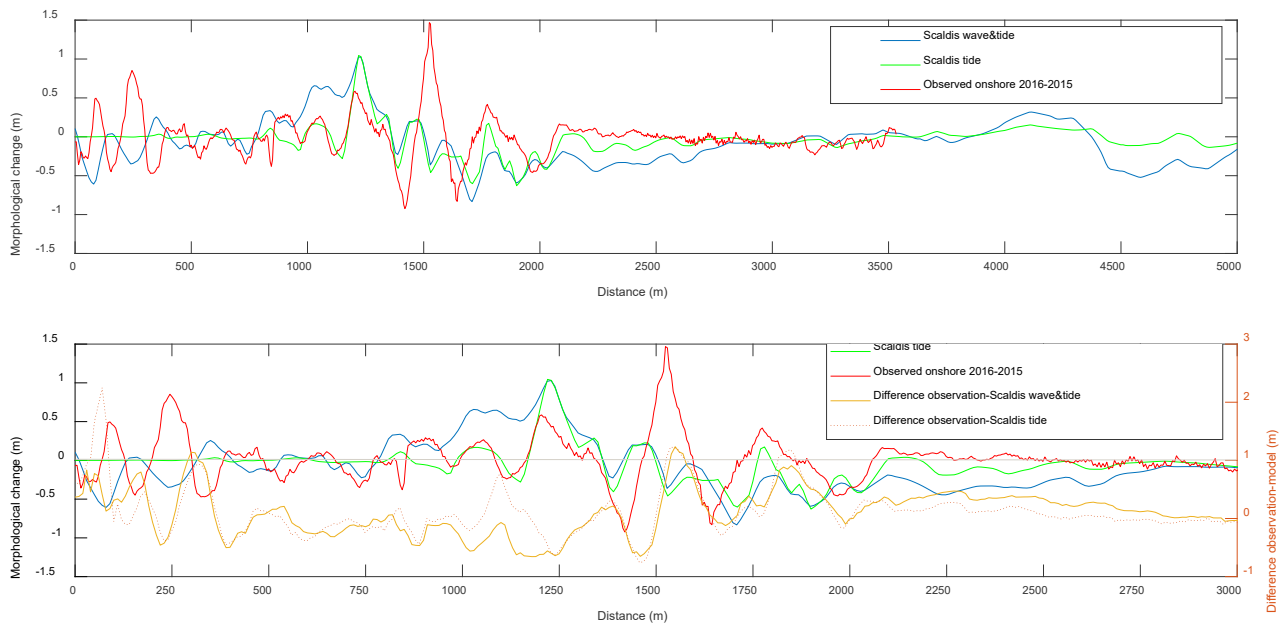


Figure 13 – Comparison between the observed bed evolution and Scaldis model after 1 year along a profile oblique to the coast. Location of the profile presented in Figure 6.

2.3.3 Nieuwpoort harbour

The DEMs of Nieuwpoort harbour entrance were generated in 2005, 2006, and yearly in the period 2009-2020 (Table 2). From these, DoDs were derived. Examples are presented in Figure 14. In general, sand accumulation is observed in the west side of the harbour entrance, while the opposite trend occurs in the east side. The linear trend applied for the period from 2009-2020 based on 12 surveys (Figure 14, Appendix B) suggests a small trend. However, sedimentation and dredging probably alternate and tend to create a long-term stable situation.

Table 2 – Surveys period.

Year	Date
2005	unknown
2006	09/2006
2009	09/2009
2010	09/2010
2011	01/2011
2012	09/2012
2013	09/2012
2014	05/2014
2015	11/2015
2016	08/2016
2017	07/2017
2018	09/2018
2019	09/2019
2020	06/2020

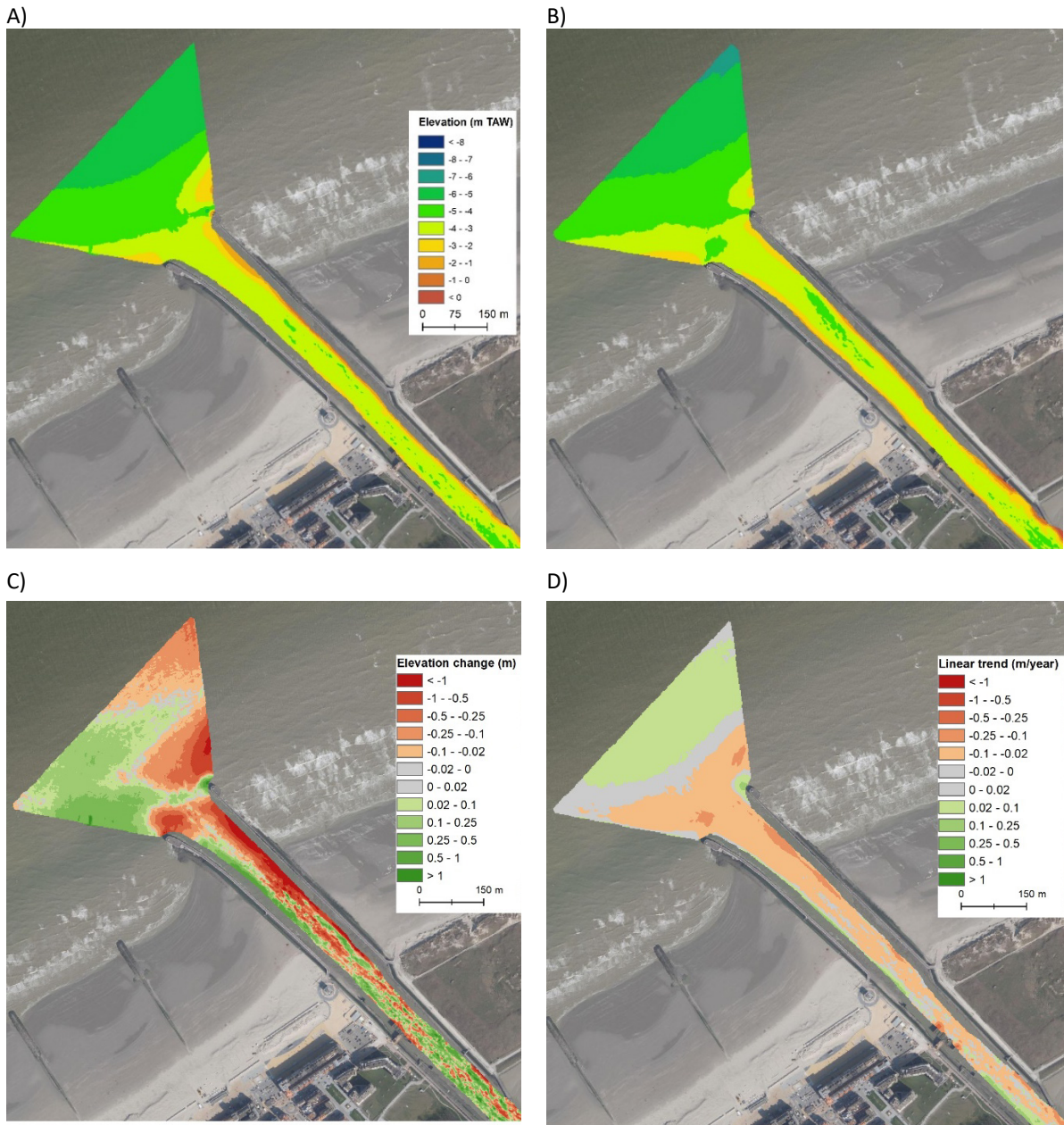


Figure 14 – A) DEM in 2010, B) 2016, C) DoD between 2010-2016 and D) linear trend between 2010-2016.
 Note: Bathymetric survey was carried out 3 months and 6 months after dredging activity in 2010 and 2016 respectively.

2.3.4 Volumetric changes of the morphological zones

Volume changes from the active zone to the landward morphologic zones were determined along the study site and were then corrected for the human interventions (small and large nourishments and beach scraping, see §2.4.1) over the last 20 years (Table 3, Appendix F). The volumetric changes between 2000-2007, 2007-2011, 2011-2015, 2015-2020, and 2000-2020 are presented in Table 4. The DoD between 2000-2020 is displayed in Figure 15. In general, the landward zones along the entire study site have gained sand. However, without the human interventions, the zones from 2 to 6 (Verkaveling Westhoek-Koksijde Bad) would have suffered erosion. The sum of the volume changes toward the dunes over all the zones between 2000-2020 is 12,000 m³/year (equivalent to 0.01 m³/m²/year for the entire landward zones system). It is however more than 3 times larger (39,000 m³/year) when incorporating the human interventions. Regarding the active morphologic zones, the volumetric trend between 2000-2020 is generally positive or stable incorporating the human interventions. However, zones 3 and 4 (from east of Westhoek to De Panne Centrum) have experienced erosion on the shoreface between +2 m and -4 m TAW. By migrating, the channel thus partly consumes the shoreface. The DoD between 2000-2020 indicates accretion in the offshore area of zone 3 and 4. This is caused by some filling-up of the center of the Potje channel after migrating. After correcting sand budgets for the carried out sand nourishments, the active zones of zones 3 and 4 have experienced natural erosion over the last 20 years. Much of the growth of the landward and active morphological zones occurs in zone 6 (Koksijde-Bad) and 9 (Oostduinkerke-Oost and Nieuwpoort Bad).

The total corrected sand volume accretion of the active morphological zones is 35,000 m³ and exceeds 241,000 m³ for the landward morphological zones. All the sand material that that contributes to dune growth is assumed to be sourced from the active zone. In accretionary dune zones, the net amount of accretion may be underestimated as the zone boundaries are fixed and based on the first survey. This amount is then contained in the volume change of the active zone. More than half of the observed and corrected observed growth occurs in Zone 9.

According to the coastal municipalities, the wind-blown sand that settles above the dyke/seawall is brought back to the beach by human interventions so that a negligible amount of sand from the system is lost inland in these sections. The landward morphologic zone 7 is characterized by the presence of a blowout (called Schipgat-Koksijde), a sandy depression connected to the beach, where sand material can escape to the inland dune system. Landward zone 7 contains 88% of the total blowout area in 2011 and 91% in 2015 and 2020 (Appendix E, top right figure presenting the covering areas). Thus, the sand volume is slightly underestimated there.

Furthermore, the sum of the observations points to a net supply from the offshore zone. This can be quantified in Table 4. The area that seems to benefit most of this source seems to be Koksijde-Bad and Oostduinkerke-Oost to Nieuwpoort. It is a bit surprising that zones 7 and 8 would not benefit from the natural supply. A temporal variation of sand budgets is observed along the study site where local erosion occurred from 2000-2015, while an overall accretion clearly dominated from 2015-2020. This trend change can be explained by the increase of human interventions with larger nourishments.

Table 3 – Sand budgets for the landward and active morphological zones between 2000 and 2020.
Erosion in red, accretion in green and no significant change in grey.

Landward morphological zones	sections	2000-2020 sand budget (m ³)	Uncertainty error (m ³)	Sand Budget (m ³ /yr)	Accumulated nourished volume (m ³)	2000-2020 corrected sand budget (m ³)	Corrected sand budget (m ³ /y)
Zone 1	1-7	51,704	+/- 5,300	2,585	0	51,704	2,585
Zone 2	8-9	-4,570	+/- 1,500	-229	0	-4,570	-229
Zone 3	10-13	4,076	+/- 2,900	204	14,227	-10,151	-508
Zone 4	14-18	42,910	+/- 4,890	2,145	72,766	-29,857	-1,493
Zone 5	19-26	83,689	+/- 3,700	4,184	232,370	-148,681	-7,434
Zone 6	27-33	55,458	+/- 2,500	2,773	141,006	-85,548	-4,277
Zone 7	34-43	62,785	+/- 12,300	3,139	12,150	50,635	2,532
Zone 8	44	11,293	+/- 1,700	565	0	11,293	565
Zone 9	45-59	426,956	+/- 16,000	21,348	67,893	359,063	17,953
Zone 11	60-64	47,891	+/- 2,050	2,395	0	47,891	2,395
Total	1-64	782,192		39,109	540412	241,779	12,089

Active morphological zones	sections	2000-2020 sand budget (m ³)	Uncertainty error (m ³)	Sand Budget (m ³ /yr)	Human intervention: accumulated nourished volume/dredging (m ³)	2000-2020 corrected sand budget (m ³)	Corrected sand budget (m ³ /y)
Zone 1	1-7	276,189	+/- 108,240	13,809	0	276,189	13,809
Zone 2	8-9	14,246	+/- 30,000	712	0	14,246	712
Zone 3	10-13	-112,553	+/- 49,800	-5,628	11,041	-123,594	-6,180
Zone 4	14-18	-154,727	+/- 70,750	-7,736	56,392	-211,120	-10,556
Zone 5	19-26	189,054	+/- 115,400	9,453	207,534	-18,480	-924
Zone 6	27-33	582,505	+/- 125,800	29,125	-113	582,618	29,131
Zone 7	34-43	-147,386	+/- 310,250	-7,369	0	-147,386	-7,369
Zone 8	44	2,847	+/- 40,700	142	0	2,847	142
Zone 9*	45-59	544,827	+/- 388,300	27,241	0	544,827	27,241
Zone 10**	/	12,630	+/- 9,350	631	57,215*	-44,586	-229
Zone 11	60-64	123,927	+/- 82,170	6,196	68,8424	-564,496	-28,225
Total	1-64	1,055,370		52,767	963,278	34,876	3,743

Note: The estimated error on volume changes for the landward morphological zones corresponds to the area multiplied by the LiDAR error of 0.05 m and for the active morphological zones is (1/2 x the LiDAR error of 0.05 m + 1/2 x bathymetric error of 0.15 m) multiplied by the area (1/2 representing the part of the active morphological zone covered by LiDAR and echosounding respectively).

* Section 59 does not contain the navigation channel, while it does in Houthuys et al. (2022).

**Dredging activity was assumed to occur only in Zone 10 where most of the sand is removed. An average of the dredged sand volumetric values from 2008-2019 reported in Houthuys et al. (2022) based on pre- and post-bathymetric surveys were used.

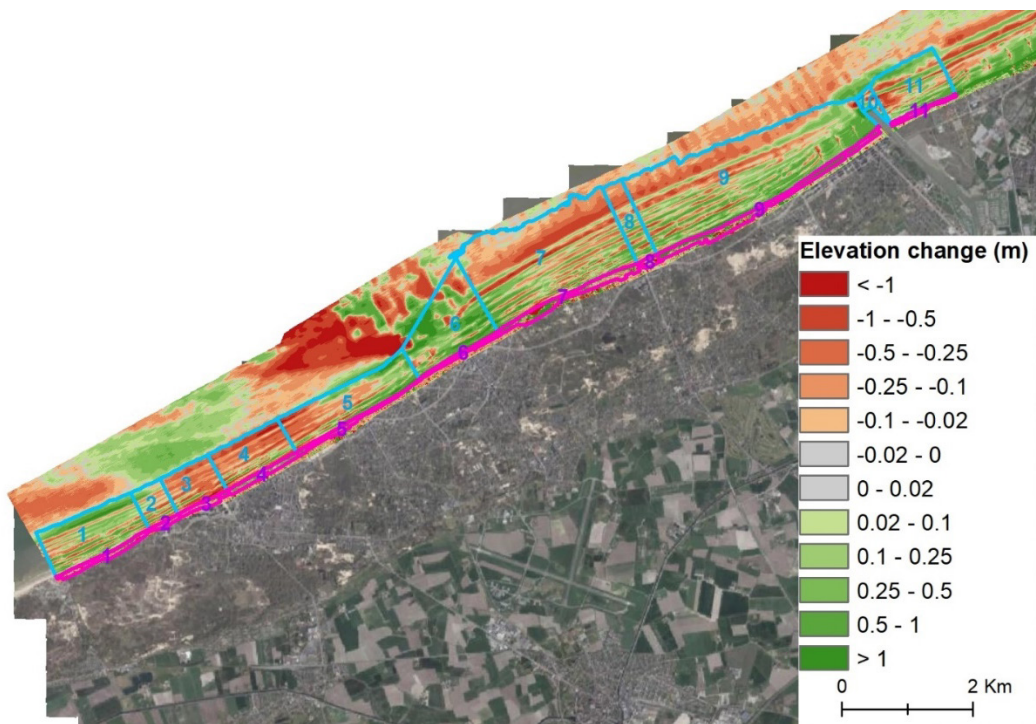


Figure 15 – DoD between 2000-2020 along the study site with the defined morphological zones.

Table 4 – The observed volumetric changes in the morphologic zones for the landward boundary and active zones. Erosion is red, accretion is green and no significant change in grey.

Landward morphological zones		Sand budget (m ³ /yr)				
Unit	sections	2000-2007	2007-2011	2011-2015	2015-2020	2000-2020
Zone 1	1-7			3,448	6,472	2,585
Zone 2	8-9	-293	-718	-771	699	-229
Zone 3	10-13	-508	-287	-291	2,019	204
Zone 4	14-18	-474	-1,072	3,825	7,086	2,145
Zone 5	19-26	1,726	3,795	4,416	7,830	4,184
Zone 6	27-33	1,846	3,549	2,412	3,784	2,773
Zone 7	34-43	458	2,048	762	9,802	3,139
Zone 8	44	471	-366	1,600	596	565
Zone 9	45-59	21,310	27,189	14,817	22,217	21,348
Zone 11	60-64	-2,888	8,531	6,100	1,967	2,395
Total	1-64	21648	42669	36318	62472	39109

Active morphological zones		Sand budget (m ³ /yr)				
Unit	sections	2000-2007	2007-2011	2011-2015	2015-2020	2000-2020
Zone 1	1-7			12,835	22,190	13,809
Zone 2	8-9	-3,463	-278	-991	8,853	712
Zone 3	10-13	-14,481	-4,702	-5,796	6,338	-5,628
Zone 4	14-18	-22,653	-12,777	-13,574	22,286	-7,736
Zone 5	19-26	-4,066	4,733	16,803	26,497	9,453
Zone 6	27-33	27,018	23,811	26,656	38,591	29,125
Zone 7	34-43	-29,604	23,699	-13,888	4,695	-7,369
Zone 8	44	2,307	-1,556	-2,186	336	142
Zone 9	45-59	24,158	7,302	21,934	52,138	27,241
Zone 10	/	371	9,234	-11,203	3,836	631
Zone 11	60-64	-16,060	111,295	-54,573	3,621	6,196
Total	1-64	-36,473	160,761	-23,983	189,381	66,576

Note: sand budgets for Zone 1 in 2007 could not be calculated due to the limitation of the bathymetric survey coverage.

Location of data and analyses:

P:\20_017-

kstlnmdlWstKs\3_Uitvoering\Morphology\01_Data\StudyZone\MorphologicalZones\FixedLevels\Volume_Zones

2.4 Human interventions

2.4.1 Beach management

Three types of human interventions have been carried out along the west coast: large nourishments in De Panne, St Idesbald and Koksijde in 2011 and 2017, local and regular small nourishments and beach scraping work (Houthuys et al., 2022). Artificial sand input per section was determined for every intervention (Figure 16).

- Large nourishments: total amounts were taken from Houthuys et al (2022). To establish the percentage of nourished sand in the different layers pre- and post-nourishment, LiDAR DEMs were used. Profiles per “strook” were extracted. It was assumed that the time lapse between pre- and post-nourishment LiDAR surveys up to 5 months from the actual nourishment did not affect the relative amounts in the different layers. The volume difference per layer (dune above the landward limit corresponding to the dunefoot (+5.9 m TAW), the dry beach between the landward limit and +4.39 m TAW and intertidal zone between +4.39 m and +1.39 m TAW) was calculated. Finally, the known values of nourished sand volume was multiplied by the length of the respective sections and divided by the total length of the “strook”.
- Small nourishments: the same method as the large nourishment was applied, but the artificial sand input was only estimated for the dry beach as this intervention type only aims at nourishing this layer.
- Beach scrapings: the principle is to remove a part of the sand in the zone around the low water line (below +2.5 m TAW) and then to deposit it on the beach above +2.5 m TAW. The assumption made is that sand comes for 50% from the shoreface and 50% from the intertidal zone below +2.5 m TAW and exported to the beach above +2.5 m TAW. The sand input of the respective section was thus determined for the dry beach and intertidal zone above +2.5 m TAW. Table 5 presents some examples of the obtained results.

Table 5 – Examples of estimated sand input per human interventions.

Koksijde-Bad, Strook 6 (section 26-32)						
Koksijde-Bad Strook 6 (section 26-31)						
Large Nourishments	Oct-nov 2011	s26				
	Dune (dynamic Ref:>9.10 m TAW)	0				
	Dry beach (dynamic Ref:9.10-4.39 m TAW)	11,221				
	Intertidal zone (dynamic Ref:4.39-1.39 m TAW)	11,679				
Scraping	2000	s29	s30	s31		
	Dry beach above 4.39 m TAW	1,488	1,645	901		
	Intertidal zone above 2.5 m TAW	369	408	223		
	Shoreface below 2.5 m TAW	-369	-408	-223		
Koksijde-Bad Strook 6 (section 26-32)						
Small Nourishments	2006	s27	s28	s29	s30	s31
	Dry beach above 4.39 m TAW	1,131	1,131	1,194	1,320	723

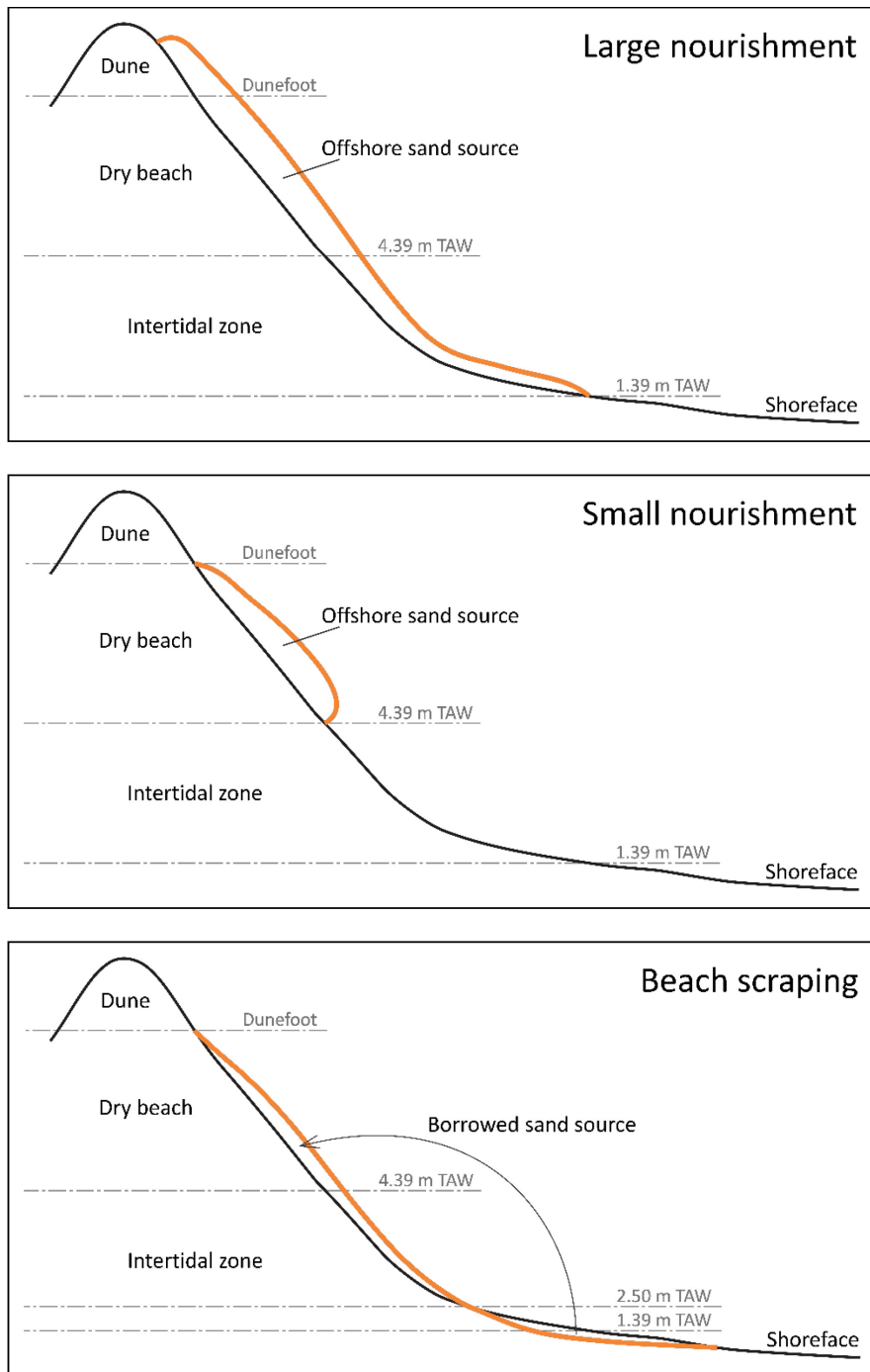


Figure 16 – Principle sketch of types of human interventions.

Location of data and analyses:

P:\20_017-kstlnmdlWstKs\3_Uitvoering\Morphology\01_Data\HumanInterventions

2.4.2 Dredging and dumping work

Figure 17 presents a timeline of dredging and dumping activities received from the BIS database (Bagger Informatie Systeem) from Maritime Access Division with bathymetric surveys at the entrance and in Nieuwpoort harbour from 2009 to 2020. In general, there are at least 2 dredging interventions per year there. The dredged material of the entrance and harbour is dumped in the nearshore of Middelkerke in the Kleine Rede channel (Loswal Nieuwpoort) and on Bruggen en Wegen Nieuwpoort (Br&W Nieuwpoort) site respectively (Figure 19). Both disposal sites are located offshore of the defined active zone and thus it is assumed that this introduces a loss of sand for the active zone.

For 2020 onboard density measurements of the dredged material were made available by Maritime Access Division. During the dredging campaigns, measurements of hopper well densimeter (HWD) – a radio-active device with U-shape, located onboard and in the centre of the dredging boat– were carried out every 10 seconds to determine the density of the dredged material. It is derived from the material volume on board and how deep the vessel sinks into the water (measure for the weight of the load). It is this number (measured moments before dumping) that is used for the official dredging/disposal statistics. Some vessels might carry a HWD that can make vertical density profiles inside the hopper well. Further description of the methodology can be found in ‘Methodology_HWD.pdf’ file (Appendix G). Figure 18 shows a vertical profile made by the HWD: density vs. depth in the well (red line).

Materials present in the entrance of Nieuwpoort harbour are mainly composed of sand: typically material with a hopper well densimeter (i.e. located in the center tank of the vessel) density higher than 1.3 t/m³ (Table 6). While inside the harbour the dredged material is mainly mud. Appendix G presents the HWD system onboard of the vessel.

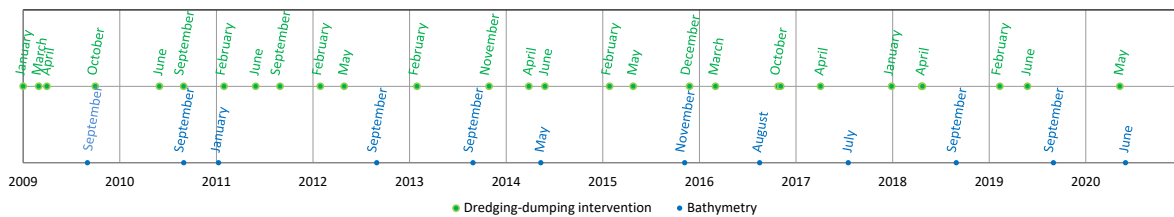


Figure 17 – Dredging timeline in Nieuwpoort harbour and entrance from 2009 to 2020.

Note: Specific dates of the interventions from 2009-2015 are unknown and dredging values were estimated from pre- and post-intervention bathymetric surveys (Houthuys et al., 2022). The focus is here on the study period from 2016-2020.

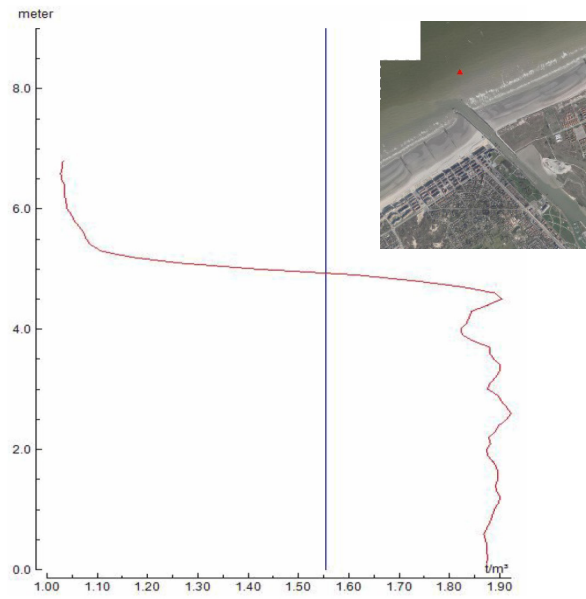


Figure 18 – Example of vertical profile of a hopper well densimeter (HWD) in the Nieuwpoort entrance, red line. The blue line corresponds to sand material threshold. Inset: location of the measurement

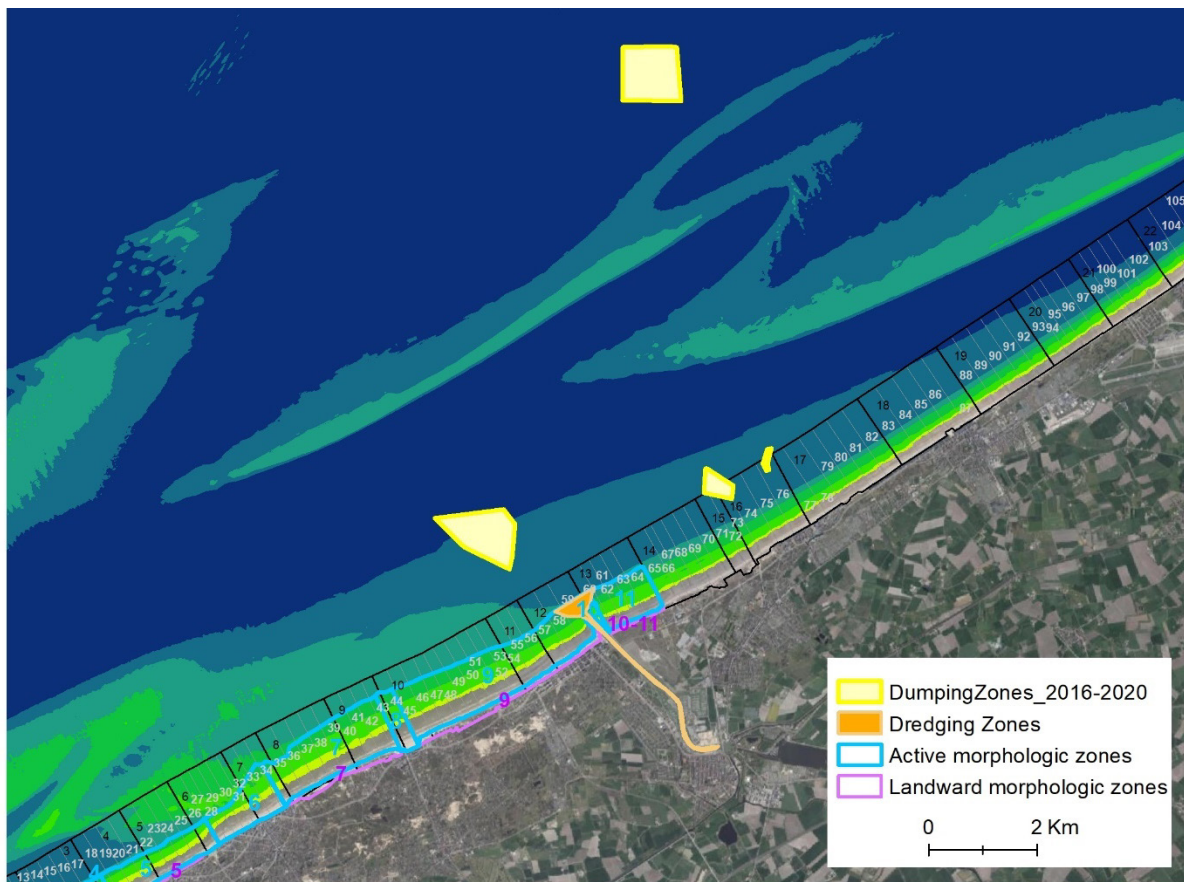


Figure 19 – Map of location of dredging and dumping zones based on common, area dredged between 2016-2020.

Based on the BIS database, the annual average of dredged volume from 2016-2020 is 79,500 m³ in the entrance of Nieuwpoort. The material is usually dumped in the nearshore of Middelkerke located 1.2 km from Sint-Laureinsstrand and Westende-Bad (sections 71-77) (Figure 19). A maximum of 105,031 m³ was dredged in 2018, while less material (42,128 m³) was dredged in 2017. For the harbour, the annual average of dredged volume load is 70,000 m³ (equivalent to 23,500 TDM). This is disposed of on Br&W Nieuwpoort located 8 km offshore from the coast.

Table 6 – Directly reported dredging activities in the entrance and harbour of Nieuwpoort from 2016-2020 from the BIS database (considering all types of material). Values averaged per year.

Annual summary	Dredging Area	Dumping Area	Weight load (t)	Volume load (m ³)	Tonnes Dry Matter (t)	Load density (t/m ³)
2016	Entrance	Vooroever Nieuwpoort	106,004	76,238	45,432	1.397
2017			57,282	42,128	22,993	1.361
2018			152,507	105,031	73,148	1.489
2019			112,308	70,698	64,964	1.475
2020			162,117	103,317	91,679	1.489
2016	Harbour	BW Nieuwpoort	168,054	139,020	41,669	1.235
2017			74,647	60,084	21,293	1.256
2018			132,891	107,233	37,469	1.239
2019			26,755	19,445	11,126	1.453
2020			26,189	21,997	5,935	1.453

Annual intensity maps of dredged volume, load density measured of matter, and determined tons dry matter (TDM) were generated from 2016 to 2020 (example in Figure 20A). Each map shows a raster of a cell size of 10 m; the cell value represents a summation over the years, except for the density load rasters which is an average per cell. Sand volume was determined by subtracting the weight load from consecutive measurements and then dividing it by the annual average of density load (reported in the BIS dredging activity characteristics in Table 7). Finally since water and gas in the pores could be present in the sand volume determined in the ships hold ($V_{in-load}$), a correction must be applied to determine the in-situ sand volume ($V_{in-situ}$). This correction factor is equivalent to a factor of 2.1 based on Dujardin *et al.* (2016):

$$V_{in-situ} = V_{in-load} \times \left(\frac{\rho_{in-situ} - \rho_{water}}{\rho_{in-load} - \rho_{water}} \right)$$

Where: $\rho_{in-situ}$, ρ_{water} , $\rho_{in-load}$ corresponds to 1.6, 1.025, and 1.3 t/m³ respectively.

Note: At the coast dredging works are always expressed as TDM. In contrast to the Western Scheldt and Lower Sea Scheldt no distinction is made based on sand/mud classification.

If the dredging reports state sand or mud, this is based on the average density.

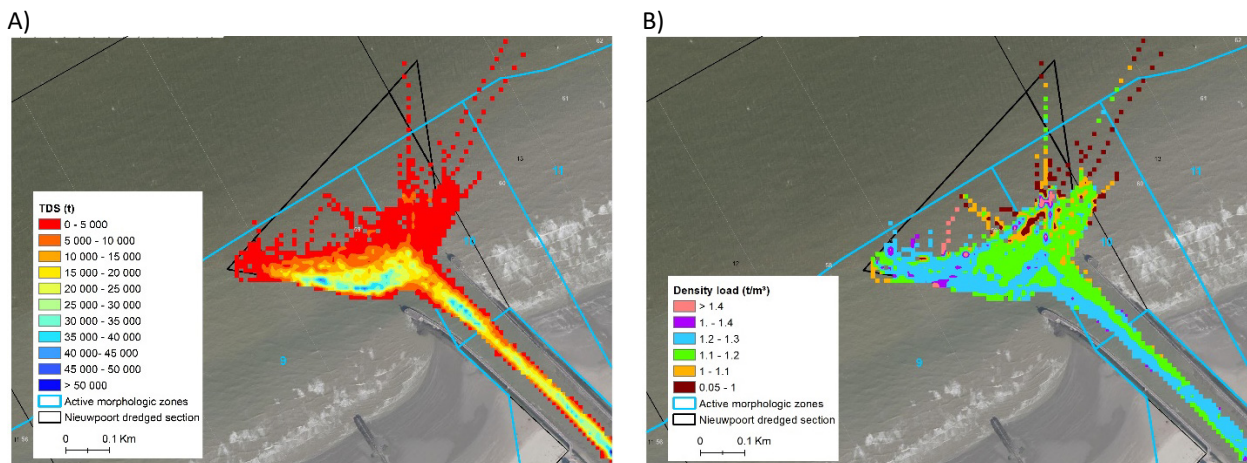


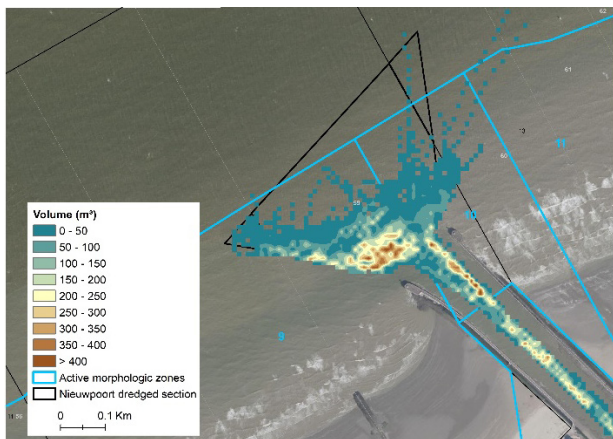
Figure 20 – Example of intensity map for the dredged sand material (excluded silt) in 2016: A) TDS, B) density load.

The dredged in-situ sand volume in the entrance of Nieuwpoort harbour (i.e. official Toegangs Geul (TG) zone) ranges from 22,341 m³ in 2017 to 32,461 m³ in 2019 with an average of 29,350 m³ (Table 7). The values only corresponds to the volume in the entrance. Thus they are lower than in Table 6. The dredged in-situ sand volumes are slightly lower than the previously reported ones from Houthuys *et al.* (2022) based on pre- and post-intervention bathymetric surveys. The disadvantage of this method is that bathymetric survey could be carried out a few days after the dredging activity. This is probably explained by the different methodologies applied. The dredged volume from the BIS database can be considered as continuous sand removal, while the methodology based on pre- and post-dredging bathymetric surveys takes only the difference in bathymetry of the zone into account and disregards any material carried in by the littoral drift during a dredging campaign lasting 2-3 weeks. Also, the dredged sand volume is here based on calendar years while Houthuys *et al.* (2022) considered survey years (i.e. the period between two consecutive nearshore bathymetric surveys). Finally, the conversion from volumes measured in the ships hold to volumes in-situ can introduce bias.

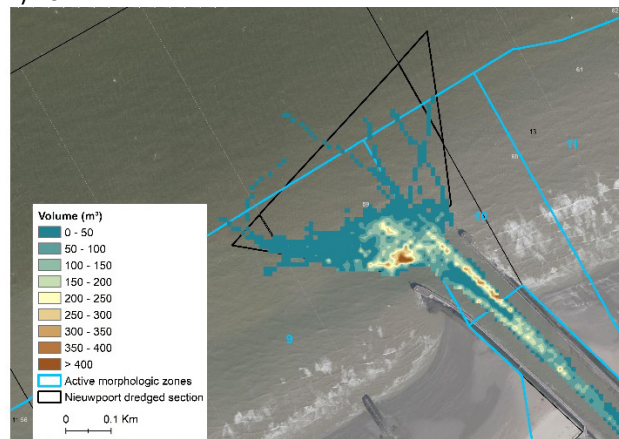
Considering the above we decided to use the volumes reported in Houthuys *et al.* (2022), averaged to 45,000 m³/year.

A time series of dredging intensity maps, derived from the BIS data, in the entrance of the harbour is presented Figure 21. Figure 22 displays a mean raster of the dredged sand volume from 2016-2020. It is clear that there are some preferential sedimentation areas. More sand is removed at the westside of the entrance (material probably brought by tidal currents from the west) and near the east pier (probably material driven by high water level combined with energetic waves or by ebb currents). This is clearly displayed on the pre-dredging bathymetric surveys of the harbour entrance from 2016 to 2021 delivered by Vlaamse Hydrografie Vlaamse overheid (Appendix H). A similar sedimentation pattern can be observed at the entrance of Blankenberge harbour (Teurlinx *et al.*, 2009). Interestingly in Nieuwpoort entrance, there is a channel-like area between these 2 zones with lower dredging intensity, which might be natural. Based on these intensity maps, it can be observed that the majority of the sand dredged in the harbour entrance and shoreface originates from the southwest side (about 20% more than the northeast side). This is visually based on the funnel shape of the pre-dredging bathymetric survey and the shape and location of the maximum sand dredging area which is attached to the southwest side of the entrance area.

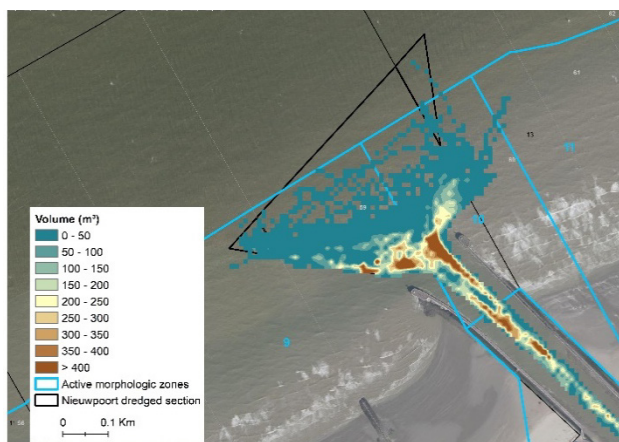
A) 2016



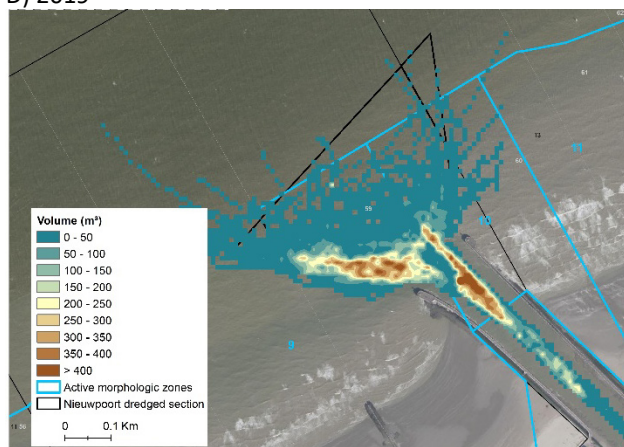
B) 2017



C) 2018



D) 2019



E) 2020

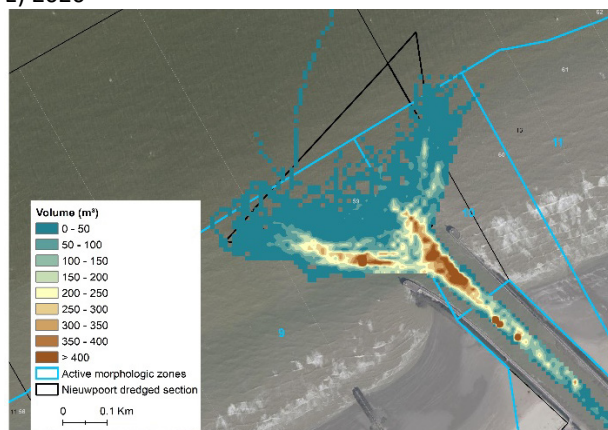


Figure 21 – Maps of determined yearly dredged sand volume from 2016 to 2020 (based on 10 sec dredging records from the BIS database).

Table 7 – Determined dredged sand volume in the entrance of Nieuwpoort from 2016-2020
 Tank volume = based on 10 second dredging records from the BIS database;
 in-situ volume is corrected for (assumed) pore volume in the seabed.

Annual summary	Tank volume (m ³)	In-situ volume (m ³)
2016	55,657	26,619
2017	46,713	22,341
2018	67,318	32,196
2019	55,911	26,740
2020	67,874	32,461

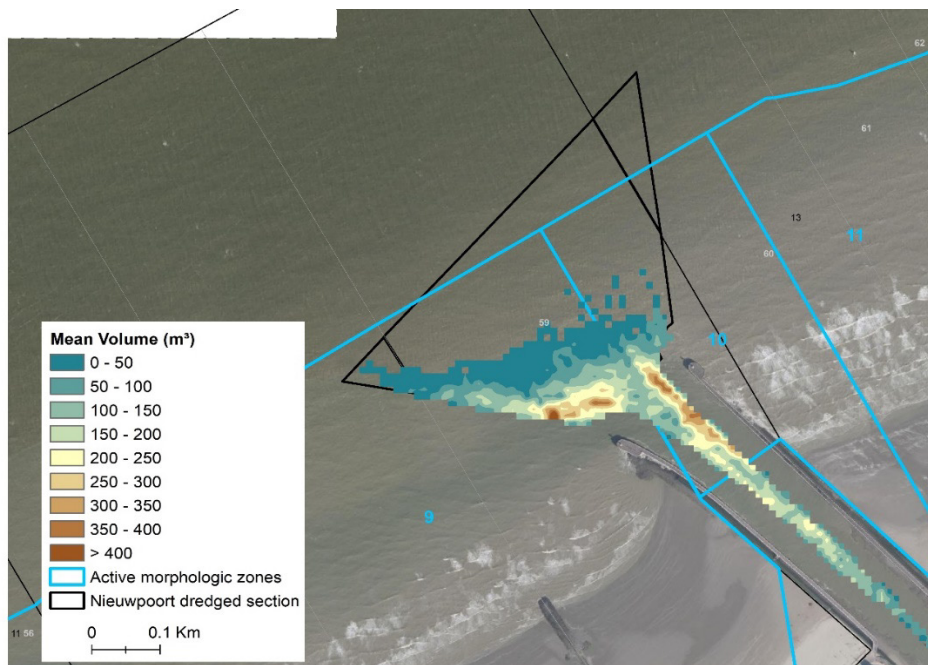


Figure 22 – Map of the determined average yearly dredged sand volume from 2016 to 2020.

Location of methodology document, data and analyses:

P:\20_017-kstlnmdlWstKs\3_Uitvoering\DredgingActivities\Nieuwpoort

3 1D Shoreline model

3.1 Introduction

For this 1D coastline model, we use Deltares software UNIBEST (**Uniform Beach Sediment Transport**: Deltares, 2020), which consists of 3 modules:

- a cross-shore model (UNIBEST-TC),
- a littoral drift model (UNIBEST-LT) and
- a coastline model (UNIBEST-CL).

The latter 2 are combined in the package UNIBEST-CL+ and are used within this project.

The littoral drift model (UNIBEST-LT) calculates the net longshore transport for a number of given cross shore profiles and schematised (yearly) climate of currents and waves conditions. The (tidal) currents can be specified for a reference depth; the currents at other locations along each profile scale with the local depth. The surfzone dynamics are derived from a built-in random wave propagation and decay model, which transforms offshore wave data to the coast taking the principal processes of linear refraction and non-linear dissipation by wave breaking and bottom friction into account. The longshore sediment transports and cross-shore distribution are evaluated according to various transport formulas, which enables a sensitivity analysis for local conditions. The output of this model is the (parameterised) relation between coastline angle and the resulting net longshore transport (S-phi curve) under the given current and wave conditions as well as the cross-shore distribution of this longshore transport at equilibrium coastline angle (the coastline angle at which no longshore transport will occur under the given current and wave conditions). An visualisation of the output of UNIBEST-LT is shown in Figure 23.

The coastline model (UNIBEST-CL) calculates the coastline changes due to longshore sediment transport gradients. Input of the coastline model are the coastline (e.g. the low water line), the transport rates obtained in the littoral drift model (for all possible coastline orientations), the sources (e.g. at Den Oever where an input flux due to transport over the shallow bank is assumed, based on the morphological observations) and a sink (dredging in the navigation channel of Nieuwpoort).

It should be noted that the concept of a 1D coastline model assumes a time independent shape of the cross shore profile so that movements of gullies/sand banks are not modelled. Also, the current velocities are modelled in a simplified way in UNIBEST (one assumes a cross-shore decrease in a profile linear with the water depth, so no dependency on the slope of the profile is taken into account).

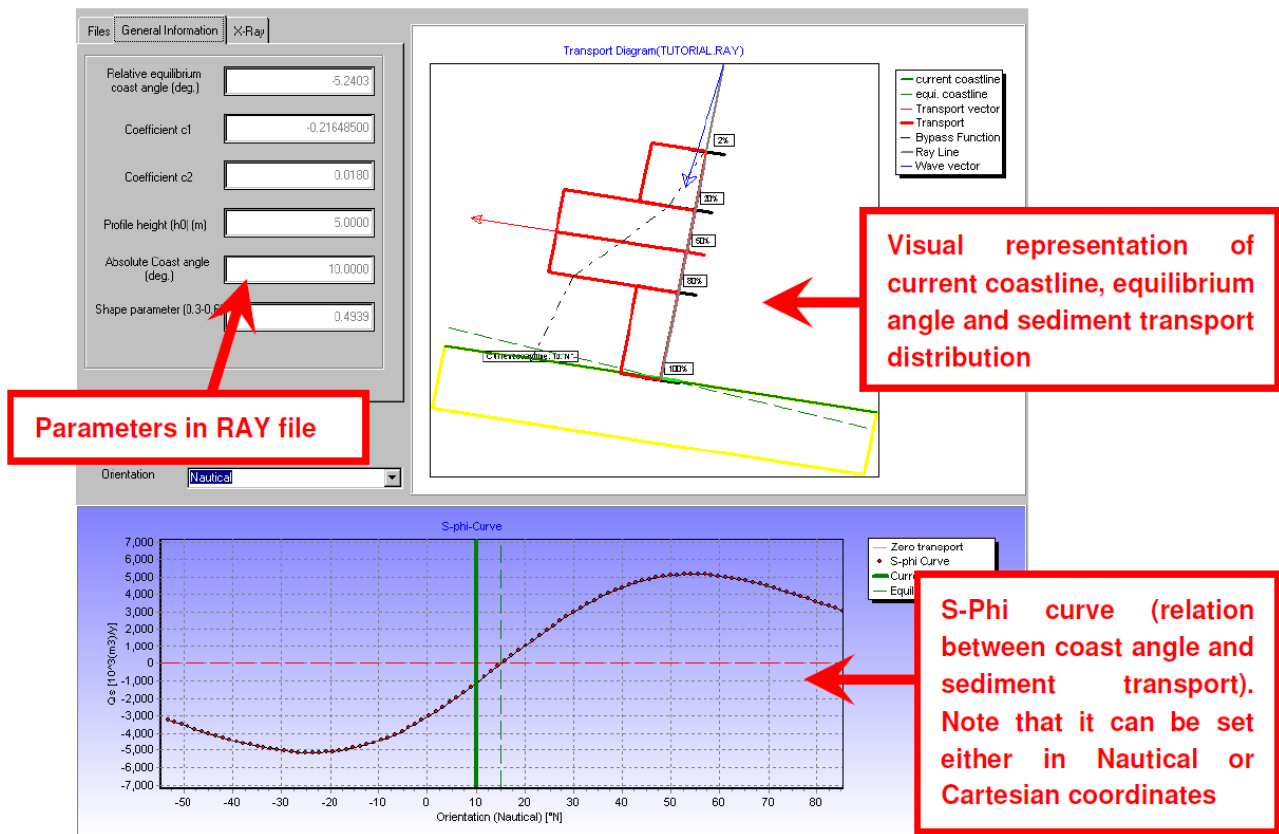


Figure 23 – Example of output generated by the UNIBEST-LT module.

3.2 Input data and boundary conditions

3.2.1 Bathymetry

For the topo-bathymetry of the model, the dataset gathered by Bart Roest within the framework of the CREST-project and his PhD-thesis is used (Roest, 2019). The dataset consist of combined height measurements, derived from topographic and bathymetric measurements of the Belgian coast. It spans a 22 year time period, from spring 1997 until spring 2019. The raw point clouds are interpolated to arrays, transverse to the coast at the theoretical positions of the single-beam soundings. This data includes the Belgian coastal zone from the dunes down to 1500 m seawards from the coastline. Coverage of the dataset is limited to the actual coverage of the raw data (no extrapolation applied). The data is based on measurements made available by the Coastal Division of the Flemish Government.

This dataset is used for several purposes:

1. Definition of the cross-shore profiles used in UNIBEST-LT
2. Definition of the depth of closure and dune foot
3. Definition of the coastline used in UNIBEST-CL

Within our study area of the Belgian West Coast, stretching from the French border till the harbour of Nieuwpoort, 160 cross-shore profiles are available.

Cross-shore profiles, depth of closure and dune foot

The first step was to analyse the morpho-dynamics in cross-shore profiles to determine the seaward and landward boundaries of the active beach and foreshore zone. Based on the 46 moments in time available,

for each profile, the average height over time was calculated. By investigating the standard deviation in the profile, as well as the change points in the slope of the profile, the depth of closure was determined at the seaward side and the dune foot at the landward side. In Figure 24, this procedure is illustrated: on the upper panel the location of the change points in the profiles slope are shown in red, and on the lower panel the cross-shore variation of the standard deviation is shown.

For many profiles coinciding change points are observed in both the slope of shoreface and the standard deviation in the profile: this location was then defined as the depth of closure (see Figure 24 as example). In other profiles no coinciding change points were found; for these profiles the depth of closure is defined as the offshore point where the shoreface reaches a slope steeper than 1/50 (Figure 25). These profiles are typically located at the eastern end of the Potje channel.

In the area where the Den Oever shoal attaches to the coast (east of Koksijde-Bad) the shoreface is very shallow and does not show a steeper part. The top of the ridge shows morpho-dynamics of equal intensity as the beach and shoreface zone (see Figure 25, compare the standard deviation at cross-shore distances 750 m till 1500 m and around 500 m). This hurdle is overcome by using interpolation: the seaward delineation in stretch 6 is the result of a spatial interpolation between the positions of the seaward boundary in the neighbouring morphologic zones 5 and 7 (see Figure 2). West of Koksijde-Bad, the depth of closure is situated at approximately -4 m TAW (Figure 26); while east of the Den Oever – Broersbank it is more shallow. At Nieuwpoort the influence of the access channel to the harbour is clearly visible. The average depth of closure for the study area is defined as -4 m TAW.

For all profiles the dune foot could be defined as the location where the slope of the profile exceeds 1/10. This location is either the foot of the dunes, or the toe of the dike in the coastal towns. Figure 26 shows the presence of elevated backshore plateaus in the coastal towns for recreational purposes. There is one location where the higher elevation of the observed dune foot has a natural cause: the dune blow-out between Koksijde-Bad and Oostduinkerke-Bad. In order not to include these artifacts in the morphological analysis (see §2.2.2), the average dune foot height of +5.9 m TAW derived by Strypsteen *et al.* (2019) was used (dashed black line in Figure 26).

Based on these observations 6 typical profiles were selected to be implemented in the UNIBEST-LT model (Figure 37):

- Transect 8, coastal section 3 & 4 – Natuureservaat Westhoek, edge of morphological zones 1 and 2: Shallow shoreface
- Transect 20, coastal section 8 – Verkaveling Westhoek, morphological zone 2: Shallow shoreface, steepening of the shoreface due to Potje channel
- Transect 34, coastal section 14 – De Panne Centrum, edge of morphological zones 3 and 4: Potje channel approaching the coast
- Transect 63, coastal section 26 – Koksijde-Bad, edge of morphological zones 5 and 6: Eastern end of the Potje channel, west of the location where Den Oever sand ridge attaches to the coast
- Transect 78, coastal section 33 – Koksijde-Bad, edge of morphological zones 6 and 7: East of the location where Den Oever sand ridge attaches to the coast, very shallow shoreface
- Transect 122, coastal section 50 – Groenendijk-Bad, morphological zone 9: Shallow shoreface

As can be seen in Figure 28 the depth of closure is located closer to the shore (dunefoot) west of Den Oever – Broersbank, while at the same time it is deeper. This leads to shorter, steeper profiles in the western part of the model and longer more gently sloping profiles in the eastern part (see Figure 37, Figure 38 and Figure 50).

Location of data and analysis:

P:\20_017-kstInmdl\WstKs\3_Uitvoering\Morphology\Ox_TopoBathy_BartRoest\define_DoC.m

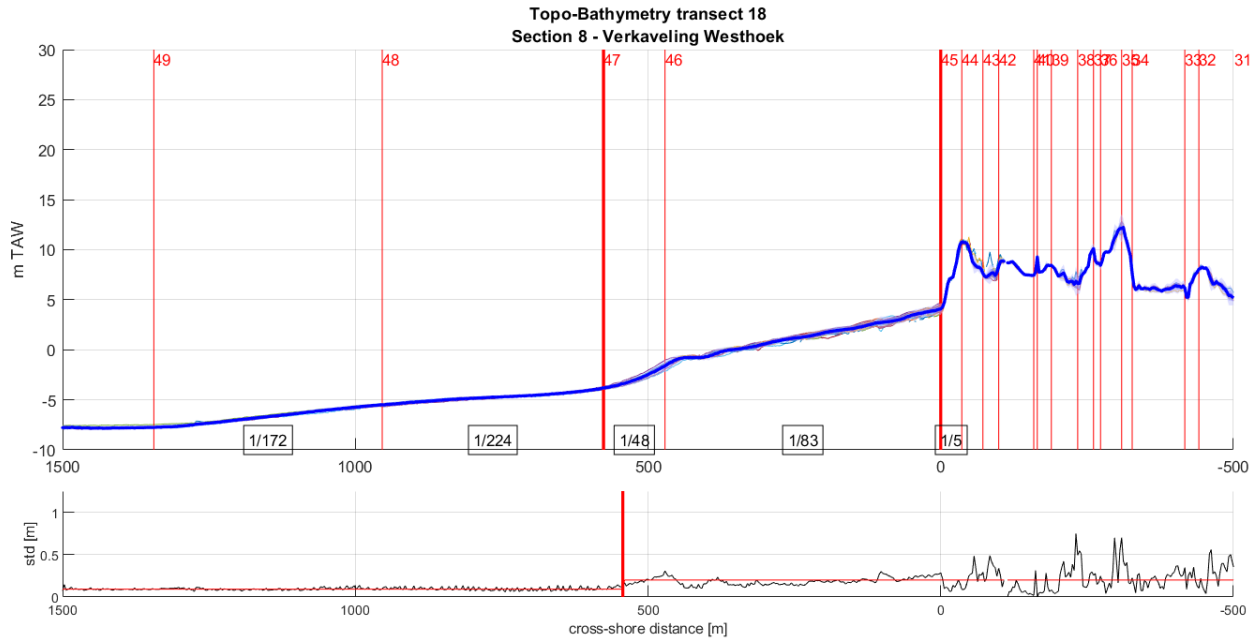


Figure 24 – Investigation of cross-shore profile dynamics using semi-annual topo-bathymetric monitoring data. Example of the cross-shore profile “transect 18”, located in coastal section 8 – “Verkaveling Westhoek”, illustrating the method used.

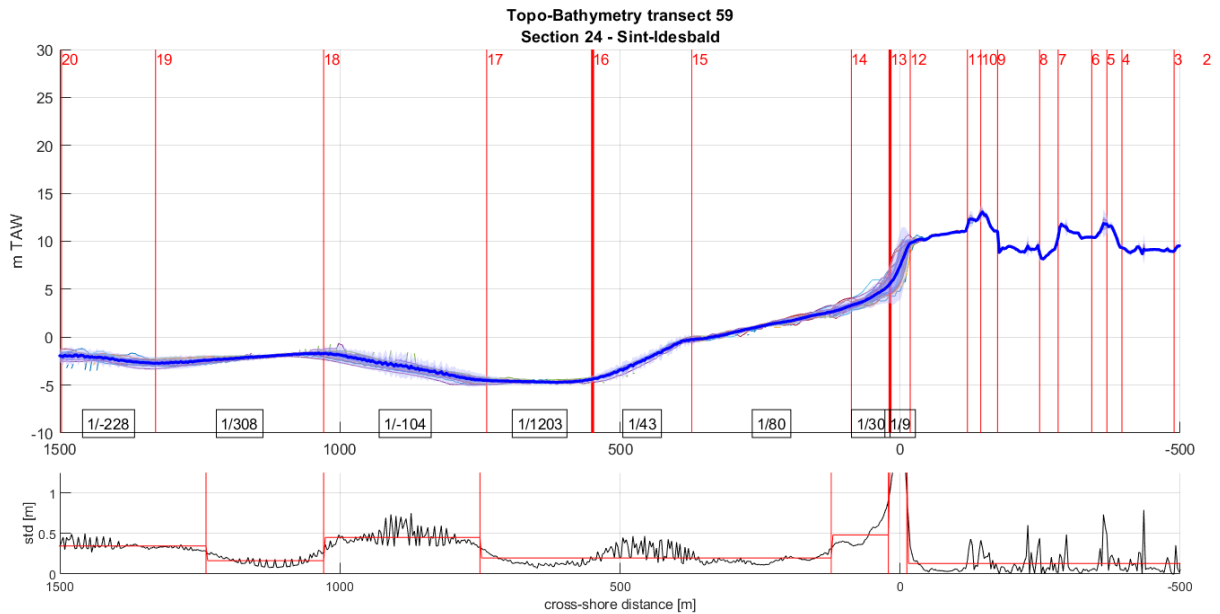


Figure 25 – Investigation of cross-shore profile dynamics using semi-annual topo-bathymetric monitoring data. Example of the cross-shore profile “transect 59”, located in coastal section 24 – “Sint-Idesbald”, illustrating the method used.

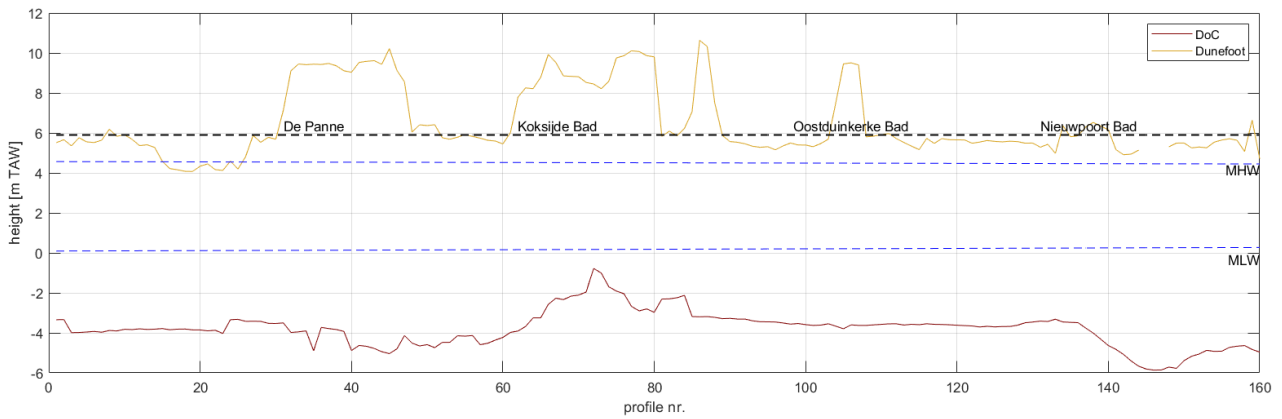


Figure 26 – Elevation of the morphological Depth of Closure and dunefoot in the study area.

MHW – Mean High Water; MLW – Mean Low Water.

The dashed black line at 5.9 m TAW shows the average dunefoot height as derived by Strypsteen *et al.* (2019).

Coastline

Several types of “coastline” can be defined: e.g. the vertical datum 0 m TAW, the local mean low or high water line, or even local observations of morphological or biological features. The first is related to mean low water in Oostende in the period 1834 – 1853 (NGI, 2021), the second are available for Nieuwpoort in the more recent period 2001 – 2010 (Afdeling Kust, 2019).

The exact x,y-position of these height levels can however change rapidly under storm conditions, which erode the upper part of the beach and deposit the entrained sediments on the shoreface. Therefore the Dutch Ministerie van Verkeer en Waterstaat (1991) developed the Momentary Coastline concept (in Dutch: Momentane Kustlijn - MKL), which takes into account the morphologically active height and width of the beach profile (Figure 27). As this concept takes into account the volume of sand in the active profile, it is less subject to the changes in pre- and/or post-storm topo-bathymetrical surveys.

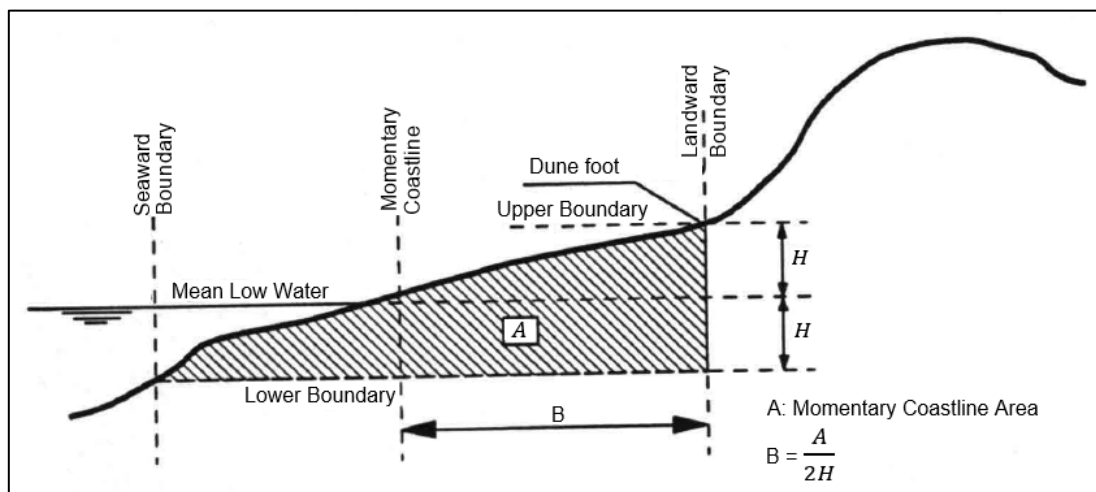


Figure 27 – Definition of Momentary Coastline (after Ministerie van verkeer en waterstaat, 1991)

The calculation of MCL for the study area was done for all 160 profiles and 16 moments in time. Albeit with a slightly different definition of the active height of the profile: instead of two times the height difference between the dune foot and the mean low water line, the height difference between the dune foot and morphological depth of closure was used. To be in line with the morphological/volumetric analysis (see §2.2) the depth of closure was kept constant at -4 m TAW and the dune foot at +5.9 m TAW.

Using the MCL concept introduces a difficulty for modelling with UNIBEST-CL, since the MCL shows an abrupt offshore shift from the coastline over the Den Oever sand ridge (Figure 28). In UNIBEST-CL this abrupt change in coastline orientation will be smoothed out over time, resulting in an exaggerated progradation of the coastline west of Den Oever, and retreat to the east of it. Therefore the preferred coastline used in the 1D modelling of this area might be the local mean low water line (between +0.09 m TAW at the French border and +0.27 m TAW at Lombardsijde) (Figure 29). A slight retreat of the mean low water line can be seen west of Den Oever, where the Potje channel approaches the shore. On top of Den Oever, and east of it, a progradation of the mean low water line can be observed.

In UNIBEST-CL, cross-shore distance 0 m in the profiles (see Figure 24 and Figure 25) is used as reference line to locate the coastline and its variation over time.

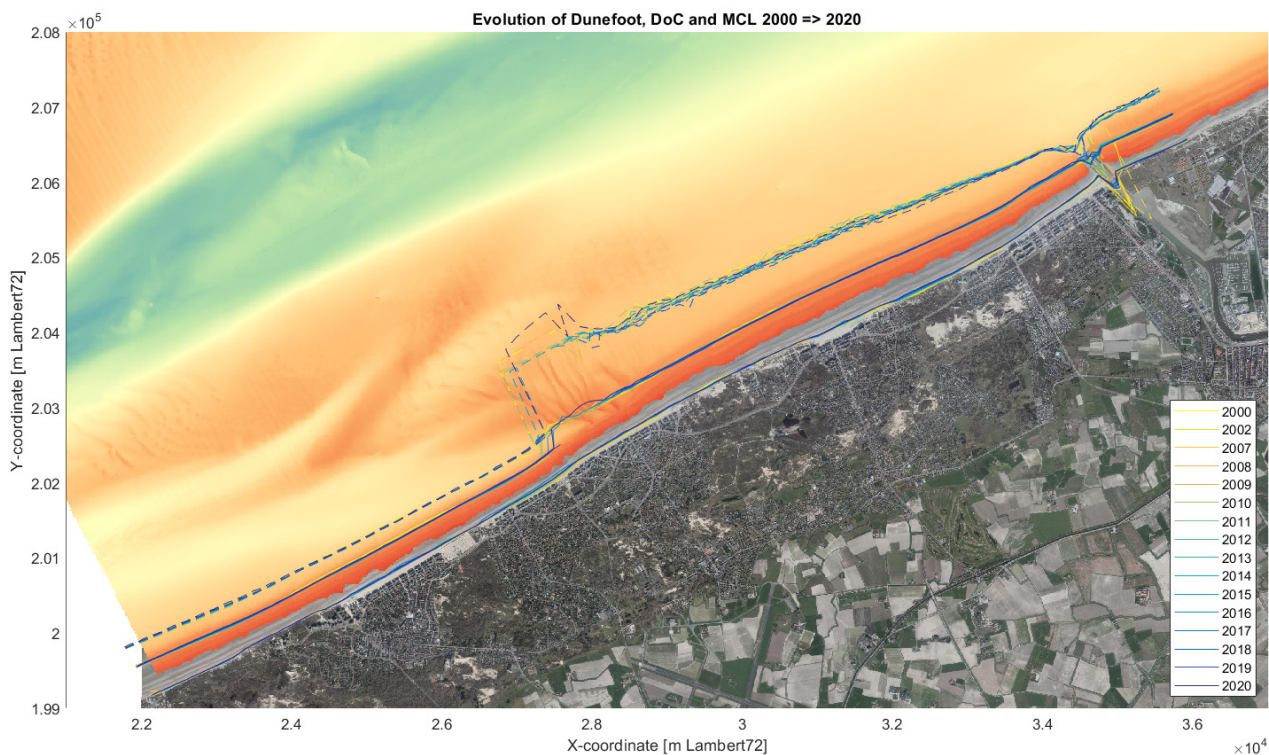


Figure 28 – Evolution of the location of the dune foot (5.9 m TAW), the depth of closure (-4 m TAW) and derived Momentary CoastLine.

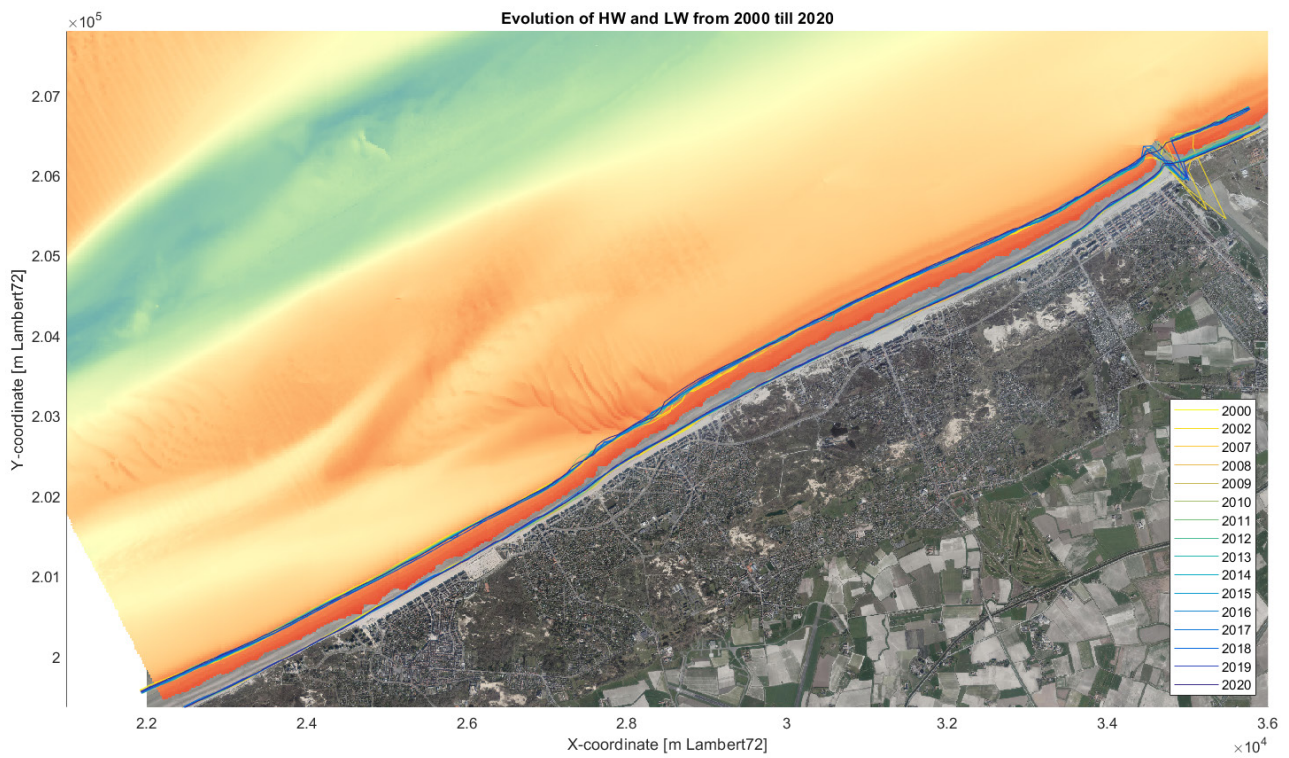


Figure 29 – Evolution of the location of the mean low water line (+0.18 m TAW) and high water line (+4.51 m TAW).

Location of data and analysis:

P:\20_017-

kstInmdlWstKs\3_Uitvoering\Morphology\0x_TopoBathy_BartRoest\define_MomentaryCoastline3.m

3.2.2 Wave climate

Within the framework of the Coastal Safety Assessment 2021, an extensive set of MetOcean data was collected; an overview of this dataset is given in Suzuki et al. (2020). Wave height data at the most offshore location (Westhinder) is available from mid-1990, but only from the year 1996 onwards, there are complete records of the wave direction.

The measured wave climate at Westhinder from September 1996 till August 2005 was used as boundary conditions for a SWAN model, to define a (modelled) wave climate at the -5 m TAW isobath along the whole Belgian Coast (International Marine and Dredging Consultants, 2009). Rather than propagating the full 10 year timeseries through the model, 9760 combinations of hydro-meteorological events (combinations of specific wave height, wave peak period, wave direction, wind speed and direction, and water level) were simulated, in order to obtain a transformation matrix between input and output wave conditions. This way, any given wave condition at the input location (Westhinder) can be transformed to any output location by interpolation on the transformation matrix.

Figure 30 shows the wave climate for both the periods 1996 – 2005 and 2006 – 2015, and for the whole dataset. The wave roses clearly show primary wave directions from the north-north-east and the south-west sectors. The period 1996 – 2005 shows a relatively higher number of occurrences in the directional bin from 5°N till 15°N (north-north-east), while the period 2006 – 2015 shows a little more spread in the range 275°N till 315°N (north-west) and a somewhat higher occurrence of wave heights in the range 2 to 3 m in the south-west sector. The period 2006 – 2015 also shows somewhat more occurrences of longer wave periods (above the upper limit of the JONSWAP spectrum), but this might be due to differences in the processing of the raw measurement data. Overall, differences between both subsets and the whole dataset are small and are here evaluated to be neglectable. Figure 31 shows that the inter-annual variation in wave conditions (occurrence of wave direction and wave height) is much bigger than the differences between the wave climates for 1996 – 2005 and 2006 – 2015. For instance the years 1999, 2000, 2008 and 2015 show the south-west sector as primary wave direction, while 1997, 2005 and 2010 show the north-north-east sector as primary wave direction. Other years have a more balanced distribution between those two primary wave directions. The year 2011 is a peculiar one, with a very pronounced occurrence of westerly waves.

From the above, we can conclude that the transformed wave climate for 1996 – 2005, as reported by International Marine and Dredging Consultants (2009), can also be used as boundary conditions for other periods in time. Suzuki et al. (2020) showed a good correspondence between measured and modelled wave height offshore Nieuwpoort at the location Trapegeer.

The wave climates are determined at 6 locations covering the study area: for each of the profiles to be implemented in the UNIBEST-LT model, the nearest output point of the SWAN model was used to define the wave climate (cfr. Figure 37 and Figure 38).

Location of data and analysis:

p:\20_017-kstlnmdlWstKs\3_Uitvoering\WaveClimate\compareWaveClimate.m

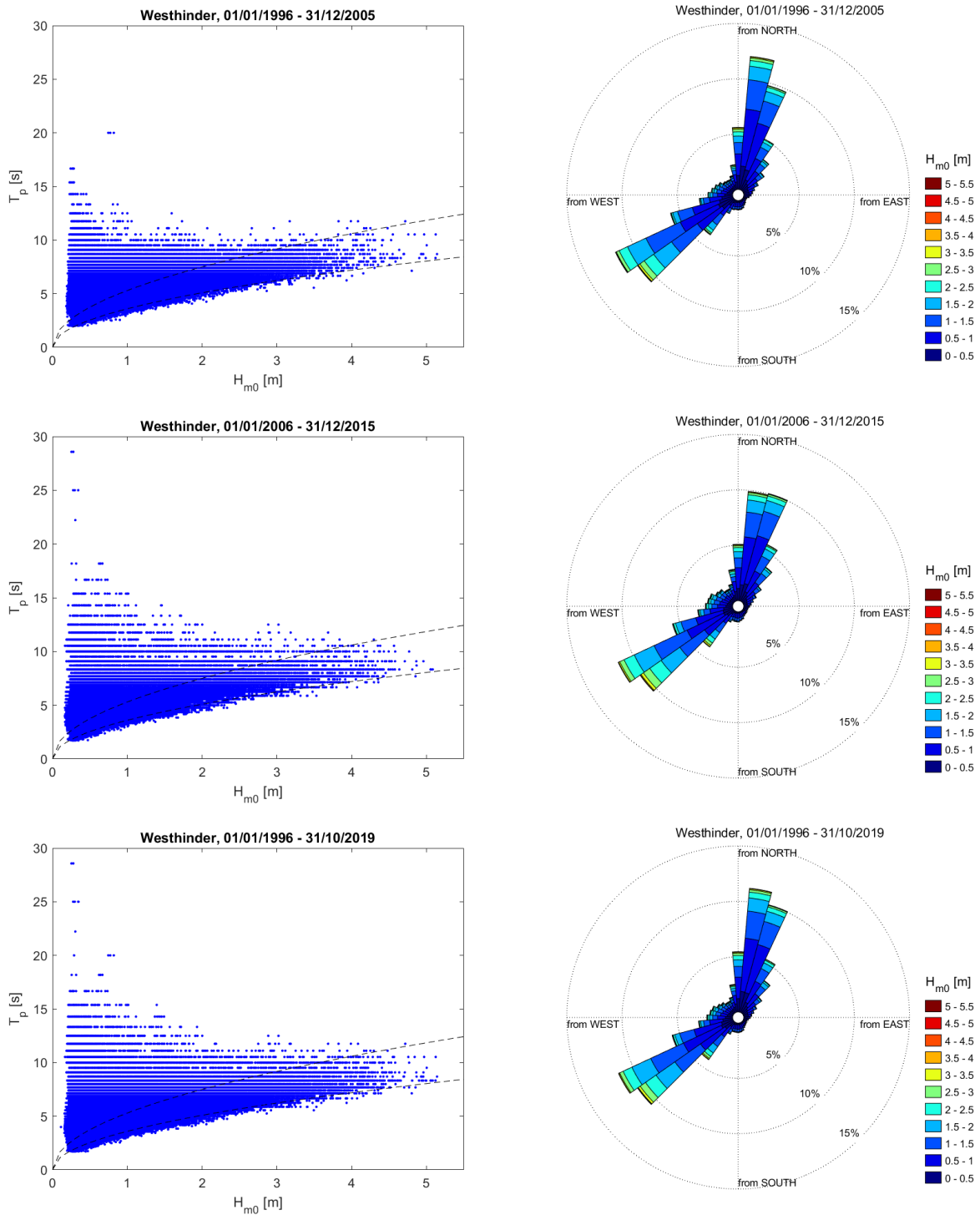
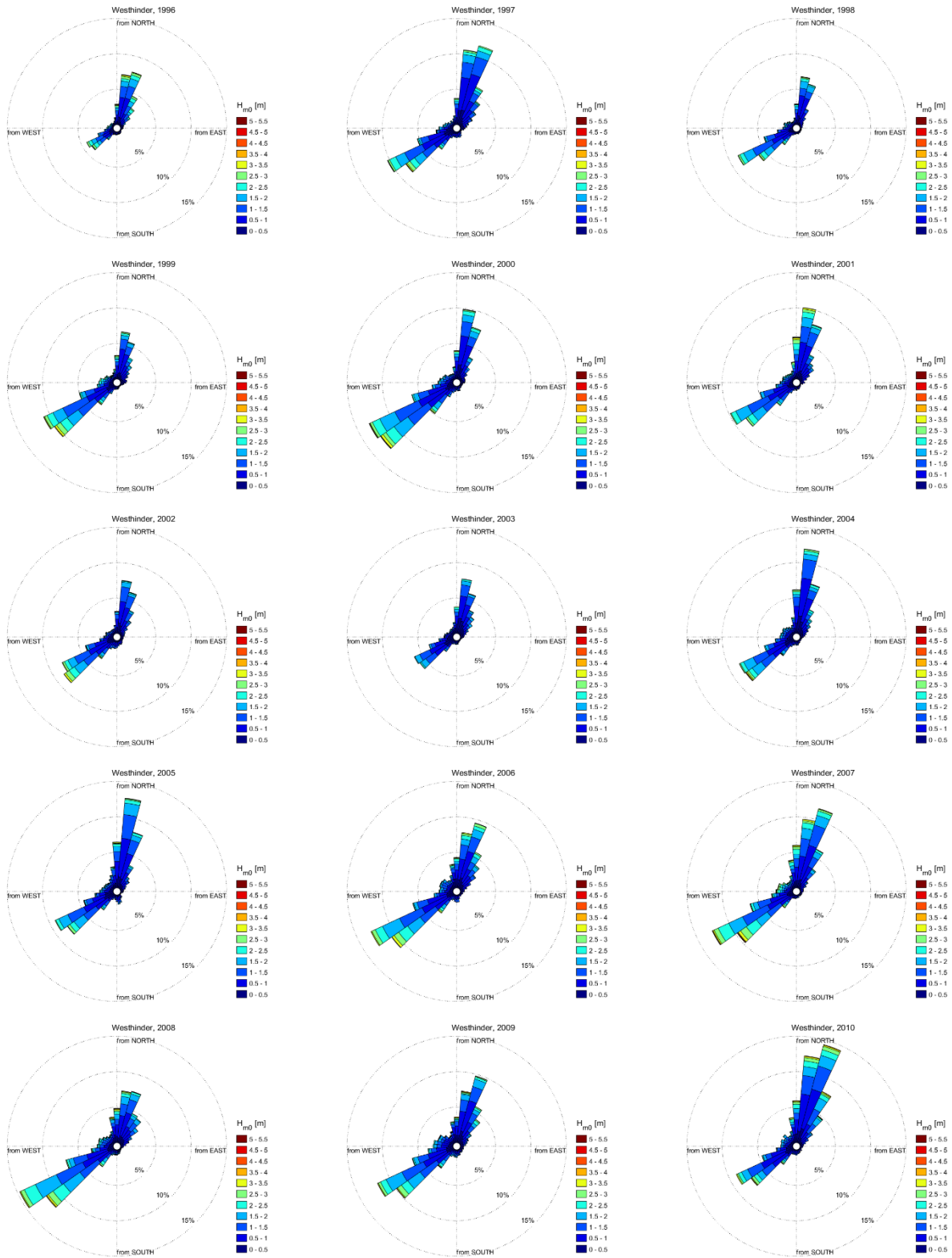


Figure 30 – Wave climate at Westhinder.

Left panels: scatterplots of measured H_{m0} vs. T_p ; the black dashed line shows the applicability range of the JONSWAP-spectrum. Right panels: measured wave roses (Nautical convention: “waves propagating from”). Missing data points are omitted from the plot; shown occurrences are thus relative to the number of valid data couples.



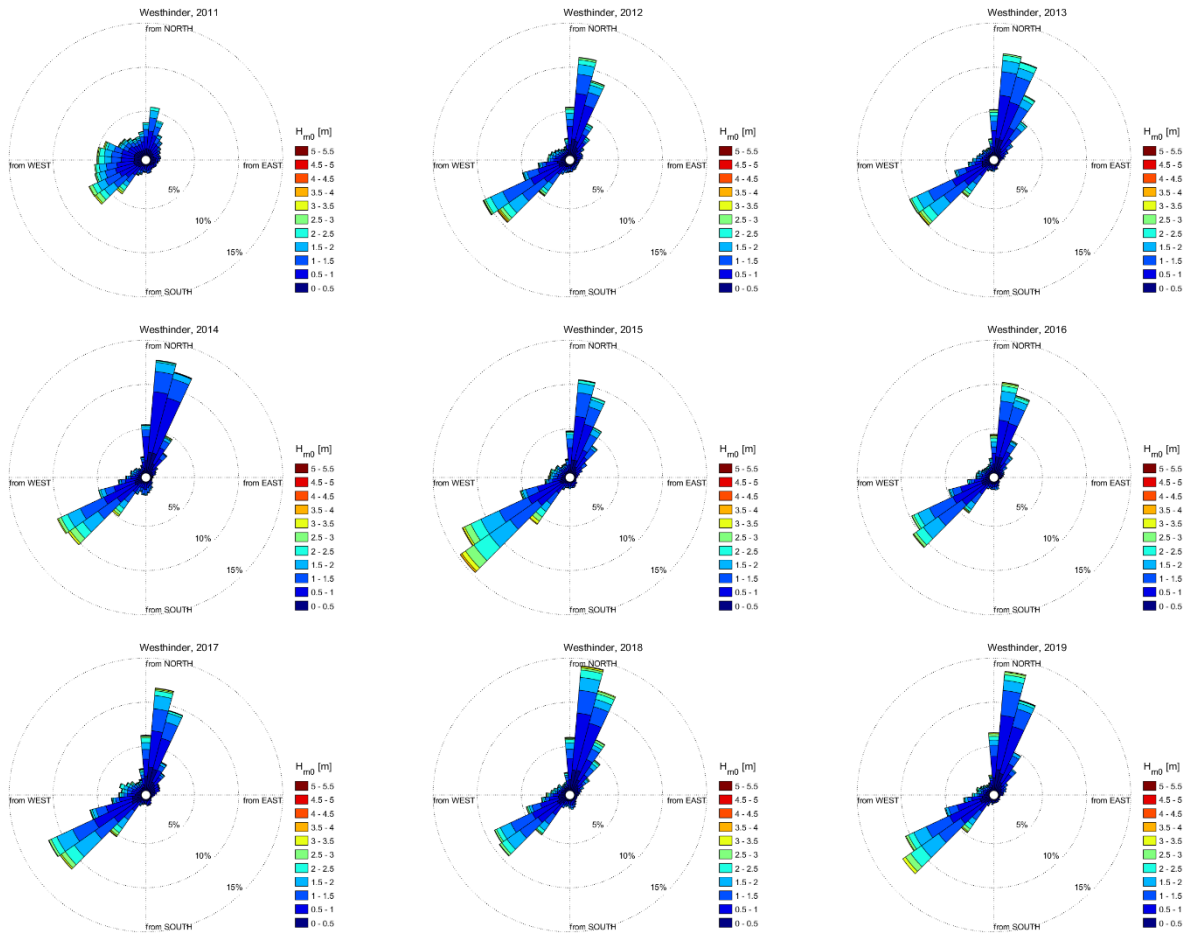


Figure 31 – Wave conditions at Westhinder per calendar year.

Missing data points are not omitted from the plots; shown occurrences are thus relative to the total number of possible data couples per year.

3.2.3 Tidal currents

Several off-shore, short to medium term, tide measurement campaigns were carried out on behalf of the Flemish Coastal Division between 2008 and 2014 ⁽¹⁾. Table 8 lists the five measurement campaigns conducted on the Belgian west coast between the French border and Nieuwpoort. Three of these campaigns include ADCP current measurements. Flanders Hydraulics Research however does not have the measurement data in the access channel to the harbour of Nieuwpoort at its disposal².

Figure 32 shows the measured tidal velocities at Oostduinkerke Bad and Potje 2. The Oostduinkerke Bad measurements were conducted on the southern flank of the Westdiep channel; the Potje 2 measurements at the southern flank of the Potje channel. At both locations, the major axis of the tidal ellipse tends to follow the local bathymetry. At Oostduinkerke Bad maximal flood velocities reach up to 0.85 m/s, and maximal ebb velocities up to 0.60 m/s. At Potje 2 the maximal flood and ebb velocities are slightly larger, reaching up to 1.00 m/s and 0.75 m/s respectively (Figure 33). When averaged according to the tidal phase (in respect to high water at Nieuwpoort), the maximal flood current reaches ca. 0.7 m/s at two hours before high water. Ebb current is more constant and reaches 0.45 m/s in the Potje channel and 0.34 m/s at Oostduinkerke Bad (Figure 34).

Table 8 – Tide measurement campaigns at the Belgian west coast.

Location	Instrument	Period	Depth	Coordinate	Reference
Oostduinkerke Bad	RDCP	12/05/2011	-4.63 m LAT	51°09.20' N 2°39.48' E	IMDC ⁽¹⁾
	Seaguard CTD	27/06/2011			IMDC ⁽²⁾
Potje	Seaguard CTD	19/05/2011	-6.16 m LAT	51°06'07" N 2°32'52" E	IMDC ⁽³⁾
		27/06/2011			
Nieuwpoort vaargeul	RDCP				IMDC ⁽⁴⁾
Potje 2	Sontek ADCP	27/03/2013	-4.80 m LAT	51°06'10.8" N 2°33'21.6" E	Antea Group ⁽⁵⁾
		10/06/2013			
Broersbank	Seaguard CTD	29/03/2013	-3.52 m LAT	51°08'12" N 2°36'51" E	IMDC ⁽⁶⁾
		20/06/2013			

⁽¹⁾ IMDC (2011). Stroommeetcampagnes in zee – Deelrapport 13: Factual datarapport stroommetingen Oostduinkerke Bad, mei tot juni 2011. IMDC NV i.s.m. Fabricom i.o.v. afdeling Kust; Bestek 16EH/07/29. Documentref. I/RA/11328/11.092/YDK.

⁽²⁾ IMDC (2011). Getijmeetcampagnes in zee – Deelrapport 19: Factual datarapport Oostduinkerke Bad, mei tot juni 2011. IMDC NV i.s.m. Fabricom i.o.v. afdeling Kust; Bestek 16EH/08/30. Documentref. I/RA/11328/11.098/BQU.

⁽³⁾ IMDC (2011). Getijmeetcampagnes in zee – Deelrapport 17: Factual datarapport Potje, mei tot juni 2011. IMDC NV i.s.m. Fabricom i.o.v. afdeling Kust; Bestek 16EH/08/30. Documentref. I/RA/11328/11.096/BQU.

⁽⁴⁾ IMDC ().

⁽⁵⁾ Antea Group (2014). Onderhoud van getij- en stroommeters voor campagnes op het BCP en de verwerking van de meetresultaten – Verwerking meetdate stroommeters Meetcampagne Potje (PT2), 27/03/2013 tot 10/06/2013. Antea Group i.o.v. afdeling Kust; Bestek 16EH/11/23. Documentref. 2232163008/lvp.

⁽⁶⁾ IMDC (2013). Getij- en stroommeters op het Belgisch Continentaal Plat – Deelrapport 20: Getijmeter op de Broersbank, maart tot juni 2013. IMDC NV i.s.m. Cofely Fabricom GDF Suez i.o.v. afdeling Kust; Bestek 16EH/11/23. Documentref. I/RA/11328/13.256/YDK.

¹ Personal communication between Hans Poppe (Coastal Division) and Toon Verwaest (Flanders Hydraulics Research), dated April 30, 2019.

² Personal communication between Toon Verwaest (Flanders Hydraulics Research) and Johan Vercruyssen (Coastal Division), dated June 2, 2020.

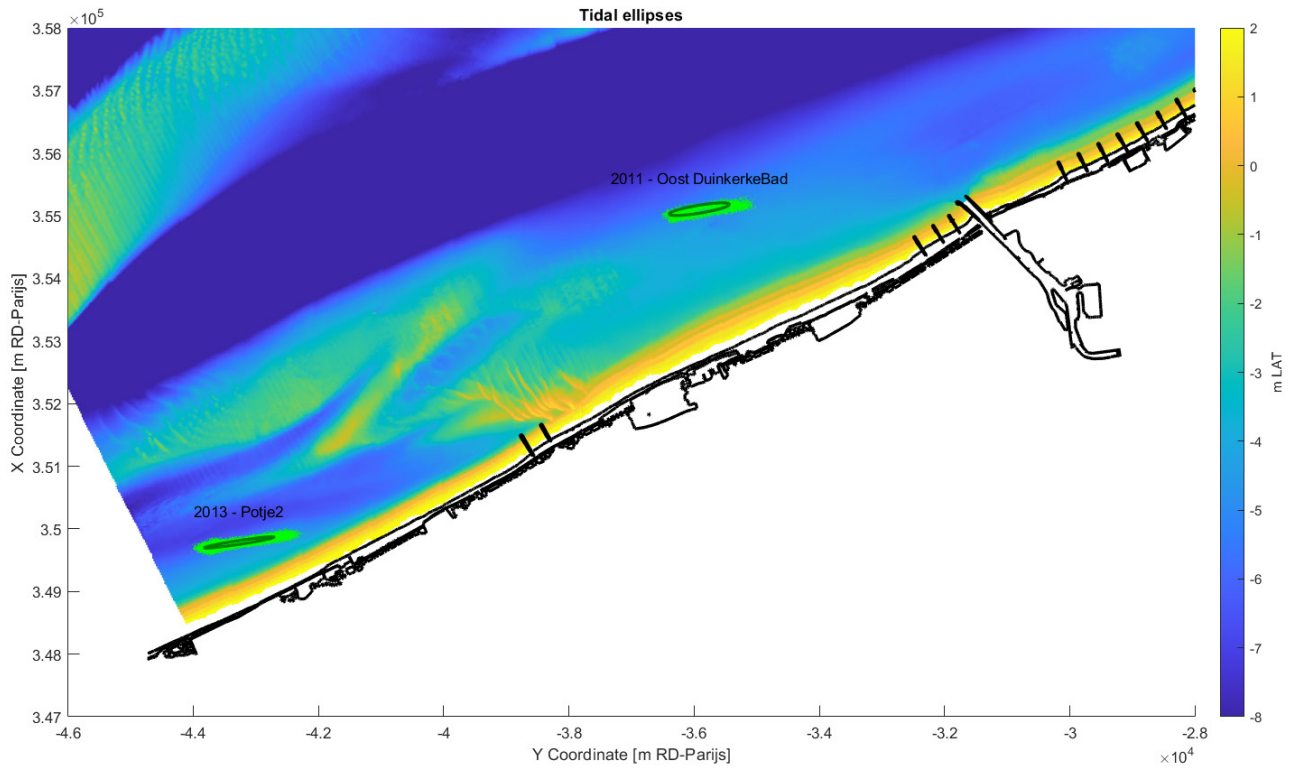


Figure 32 – Measured tidal ellipses at the West coast.

Light green: measured tidal velocities; dark green: M2 tidal ellipse, computed with t-tide (Pawlowicz *et al.*, 2002). Bathymetry source file: 200302_BELGIUM_BCP_DTM_20m_LAT, downloaded from <https://www.afdelingkust.be/en/bathymetric-database>. To enhance contrast, the bathymetry is cut-off at 8 m below LAT; therefore morphological features inside the Westdiep channel are not showing.

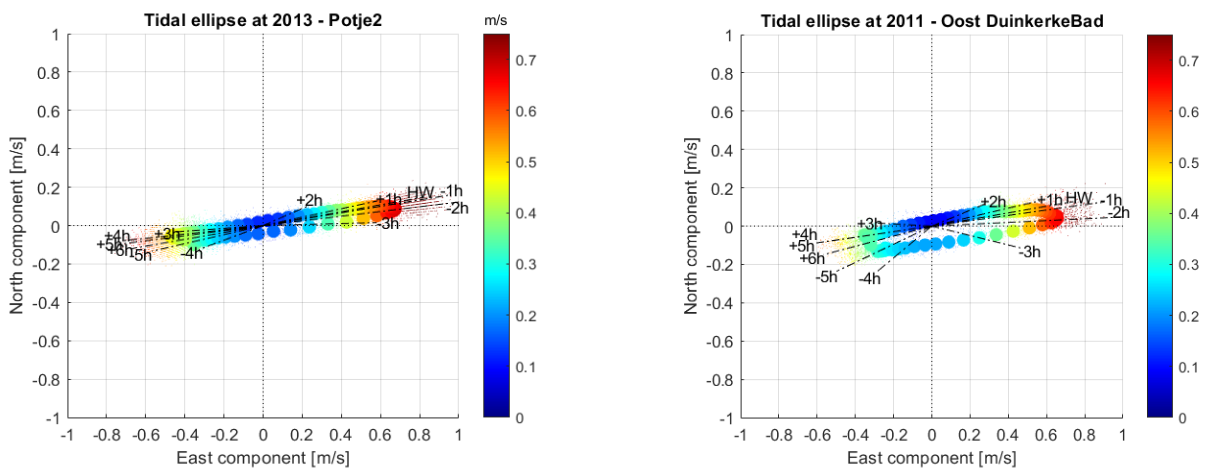


Figure 33 – Measured tidal ellipses at Potje 2 and Oostduinkerke Bad.

Small dots: measurements; big dots: average velocity, binned according to the timing in respect to high water (HW) in Nieuwpoort.

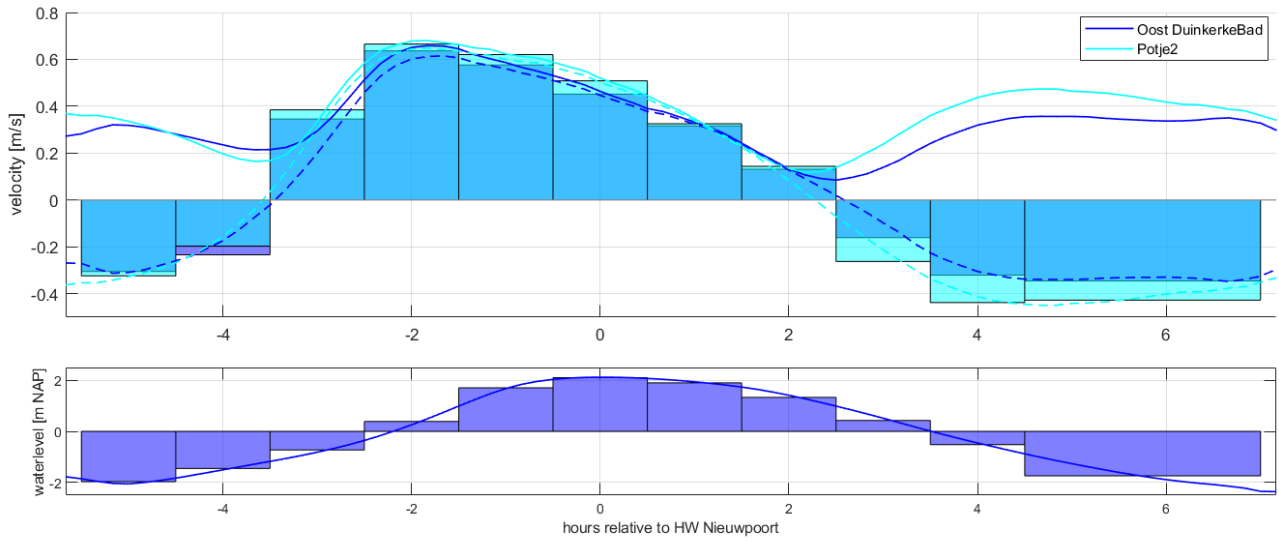


Figure 34 – Tidal currents and water levels, binned and averaged in respect to the moment of high water in Nieuwpoort.

Upper panel: full lines – current velocity magnitude; dashed lines – magnitude of the alongshore component of the current. As to be expected, maximal current and slack tide occur earlier at the Potje, due to its more westerly location. Oostduinkerke Bad measurements: 91 tidal cycles; Potje 2 measurements: 147 tidal cycles.

Lower panel: averaged water level at Nieuwpoort (147 tidal cycles from 27/03/2013 till 10/06/2013).

Bars show the hourly averages.

Location of data and analysis:

p:\20_017-kstlnmdlWstKs\3_Uitvoering\TidalVelocities\MeasurementLocations.m

3.2.4 Grain size distribution

UNIBEST-LT can use 10 different sediment transport formulas. Depending on the formula one or more parameters of the grain size distribution at the location of the profile are needed as input (D10, D50, D90).

Grain size distributions on the beach and in the dunes have been measured by VITO/Labo De Vlieger as commissioned by MDK – Afdeling Kust in 2000 – 2001. Several Excel files with the description of sediment samples in the coastal sections were provided by MDK – Afdeling Kust. Table 9 shows the derived mean grain size parameters for the different profiles used in the UNIBEST-LT model. All locations consist of fine to medium sands. At the location of Den Oever (profiles 63 and 78) the sand is slightly coarser than in the other coastal sections. This trend is confirmed by the map of Verfaillie *et al.* (2006), showing the median grain size offshore. In general the nearshore sediment median grain size between the French border and Nieuwpoort ranges from 100 to 200 μm ; only on top of the Broersbank – Trapegeer, D50 grain size can reach values up to 500 μm .

Table 9 – average grain size distributions on the beach.

UNIBEST profile	coastal section	#samples	grainsize [mm]		
			D10	D50	D90
8	3	6	0.137	0.192	0.272
20	8	6	0.138	0.196	0.289
34	14	3	0.143	0.191	0.280
63	26	8	0.151	0.208	0.326
78	34	15	0.175	0.256	0.465
120	49	6	0.128	0.182	0.254

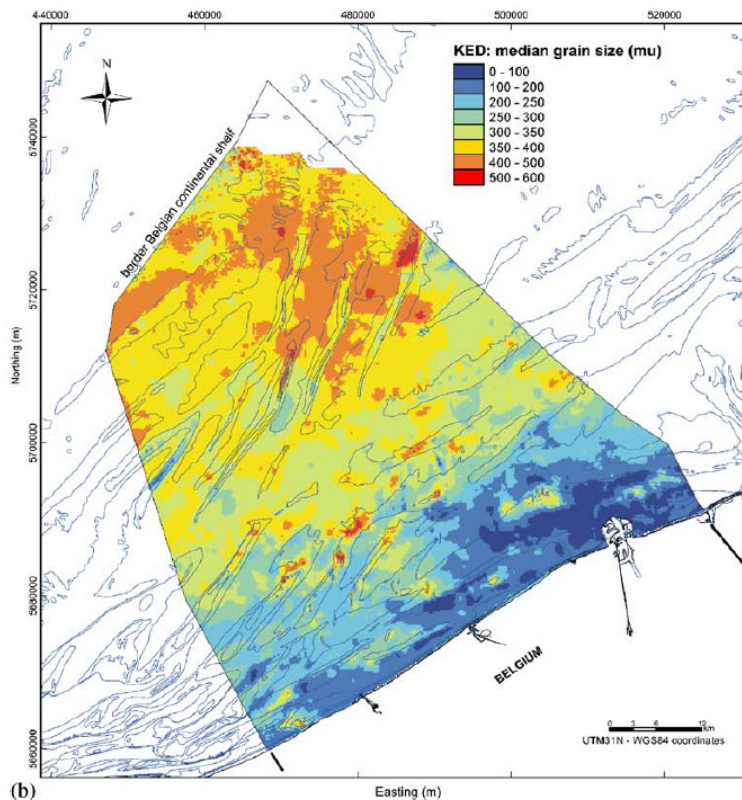


Figure 35 – Map of median grain size, on the basis of kriging interpolation with an external drift. The topography of the seabed can be recognized below the map, because this methodology uses the bathymetry to assist with the interpolation (Verfaillie *et al.*, 2006).

Location of data and analysis:

p:\20_017-kstlnmdl\WstKs\3_Uitvoering\KorrelGrootteAnalyse\processExcelFile.m

3.2.5 Sediment fluxes: Scaldis Coast

Several studies calculated longshore transport and sediment fluxes between the different coastal stretches and morphological zones of our study area (this report, §2; Houthuys *et al.*, 2022; Vandebroek *et al.*, 2017). However, none of these give an insight in the cross-shore distribution of the longshore transport or the sediment transport over the depth of closure. Therefore we analysed the results of the Scaldis Coast model (Kolokythas *et al.*, 2020b) on the lateral and offshore boundaries and typical profiles of our UNIBEST-model.

Table 10 shows the Scaldis Coast runs that were analysed for this study. The runs sed084 and swc005V13, discussed in §2.3.2, were intermediate runs in the development of Scaldis Coast (Kolokythas *et al.*, 2020a). They allowed to assess the influence of wave processes on the (longshore) sediment transport. Run HSW112 is the final, “best” run of Scaldis Coast, validated against observed morphological changes in the areas of Blankenberge and Zeebrugge, as reported in Kolokythas *et al.* (2020b).

Comparing run sed084 to swc005V13 shows the importance of the wave processes for the longshore sediment transport: without waves, the longshore sediment fluxes are an order of magnitude smaller (cfr. section 2.2.2, Table 9). Only at the location of Den Oever (transect 069) transport rates are within the same order of magnitude with or without wave processes; showing the importance of tide induced sediment transport over this sandbank. The differences between intermediate run swc005V13 and final run HW112 show the importance of the applied wave climate: the reduced, schematic wave climate of run swc005V13 yields much higher transport rates than the wave climate of December 2015 till December 2016, which was believed to be the best approach to reproduce the mean annual wave climate for the period 2009 – 2018 (Kolokythas *et al.*, 2020b).

Figure 36 shows the distribution of the sediment fluxes over the transects mentioned in Table 10 for simulation HSW112. The upper left panel in Figure 36 shows a zoom of the Broersbank – Den Oever complex and the eastern tip of the Potje channel; the densely populated cloud of model nodes between profiles 063 and 069 are representing the groynes of Koksijde-Bad. Although the overall (cross-shore) transport over the depth of closure is directed offshore (Table 10: -85,488 m³/year), the zoom of Figure 36 shows an important influx of sediment into the UNIBEST model domain over the Broersbank – Den Oever sand ridge. This influx is calculated to be +81,406 m³/year. This is for a large part the alongshore sediment flux that flows over the -4 m TAW contour line which is oblique in this zone (cf Figure 28). The active part (above -4 m TAW) of profile 63 is much shorter than the active part of profile 78. This explains partly the difference of littoral drift between these two profiles (resp. 35,000 and 180,000 m³/year). If the profile lengths are taken equal (= 1500 m long) the fluxes are respectively 125,000 and 195,000 m³/year, which is much closer together but still a considerable difference, explaining erosion offshore the -4 m TAW contour in profile 63. This sand is transported in the Potje channel. The exact (quantitative) source of this “cross shore influx” is unknown (transport from offshore, through the Potje channel or local erosion offshore the -4 m TAW contour).

Table 10 – Scaldis Coast runs.

run	MorFac	Period	Wave climate	Sediment Transport Formula	Yearly Average Transport over Transect [m ³]									
					002	008	020	034	063	069	078	120	160	DoC
sed084	10	2014	none	Bijker	3357	3222	2927	2873	6107	103999	45744	11651	6642	76902
swc005V13	10	2014	schematised/reduced	Bijker	80297	81059	71182	77131	102865	366780	279101	170361	188242	72492
HSW112	10	2015 - 2025	30/11/2015 - 29/11/2016	Bijker	45086	43109	36404	35512	34980	130849	176539	79054	69884	-85488

For the cross-shore profiles a positive value means eastward transport, for the DoC a positive value means landward transport.

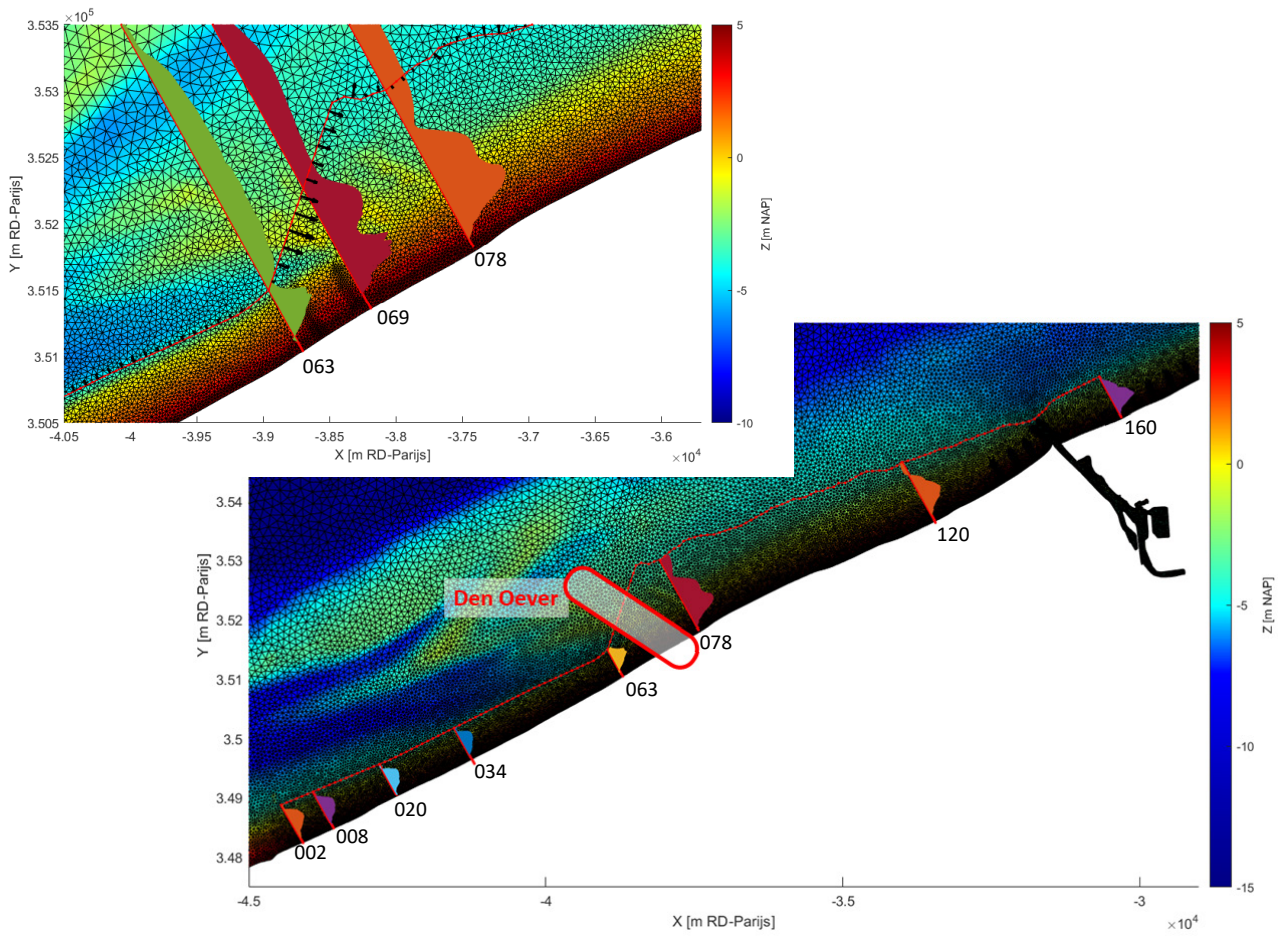


Figure 36 –Yearly averaged sediment fluxes (calculated from Scaldis Coast HSW112) on the boundaries and profiles of the UNIBEST model.

Location of data and analysis:

p:\20_017-kstInmdlWstKs\3_Uitvoering\ScaldisKust\ScaldisCoast_outputFinal.m

3.3 Model set-up

3.3.1 UNIBEST-LT

Six profiles are defined in UNIBEST-LT as illustrated in Figure 37. The littoral drift is considered between the closure depth (at -4 m TAW) and the dune foot (at 5.9 m TAW). The active height is thus 9.9 m. All parameters described in previous chapters are used as input.

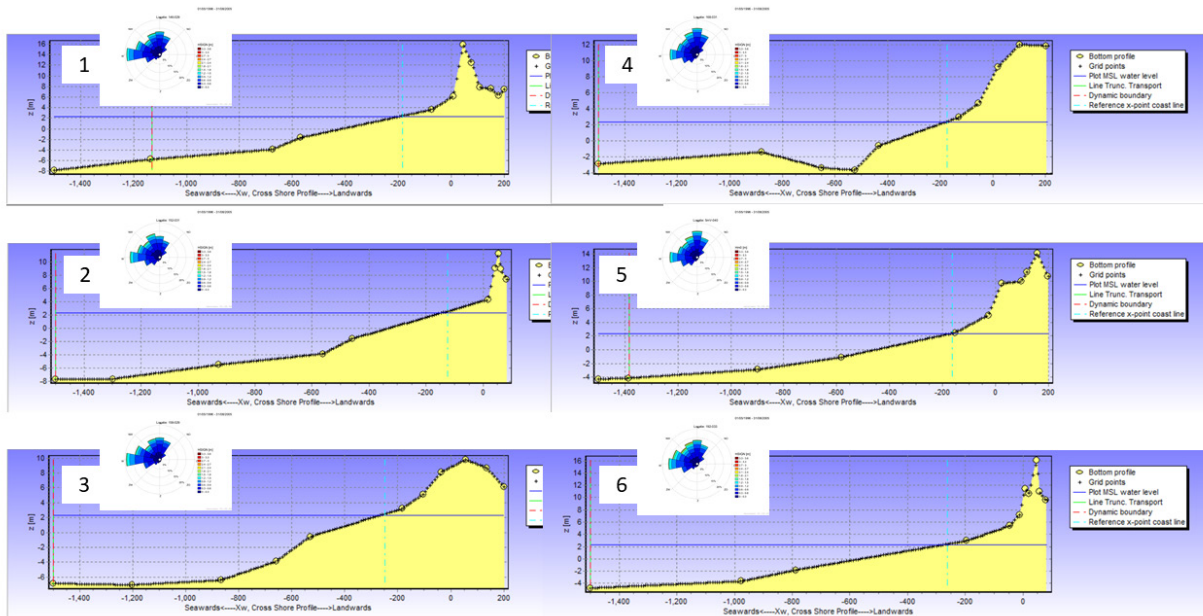


Figure 37 – Illustration of the 6 profiles implemented in UNIBEST-LT and the applied wave climate.

1 – profile 008; 2 – profile 020; 3 – profile 034; 4 – profile 063; 5 – profile 078; 6 – profile 120.

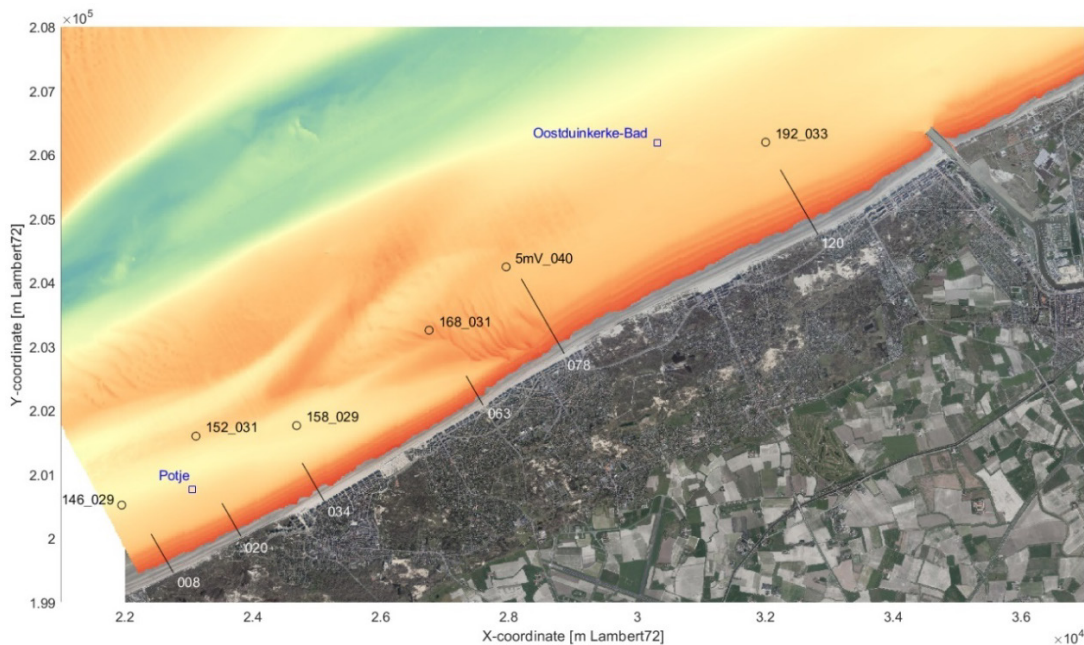


Figure 38 – Location of the 6 profiles, wave climate boundary points and two tidal boundaries implemented in UNIBEST-LT.

In the following sections the stepwise approach of the calibration process is shown. First the sensitivity to the sediment transport formulae is tested, then the hydrodynamic parameters for the selected sediment transport formula are calibrated against the Scaldis Coast results (see §3.2.5). Finally, the model is calibrated to match the resulting sediment transport fluxes to the observed volume changes (see §2.3.4).

Sediment transport formula sensitivity

Figure 39 compares the obtained sediment transport rates for different formulations of the littoral sediment transport with the results of the Scaldis-Coast model (run HSW112) for a relatively deep profile. Three formulations are used: Bijker (1971), Van Rijn (1993) and Soulsby-Van Rijn (Soulsby, 1997). Logically, the formulation of Bijker (1971) fits best in the offshore part since also in Scaldis-Coast the same formulation of Bijker (1971) is used. However, at the upper shoreface and foreshore, the LT-model with Bijker (1971) overestimates the sediment transport compared to the Scaldis-Coast model, which might be explained by an underestimation of the wave dissipation or an overestimation of the current velocities. Van Rijn (1993) and Soulsby-Van Rijn (1997) give much higher sediment transport rates in the offshore end of the profile. In the breaker zone Van Rijn (1993) results in relatively high transport rates and Soulsby-Van Rijn (1997) in relatively low transport rates.

Figure 40 shows the results for a relatively shallow profile. In this case, the current velocities at the offshore end of the profile are much smaller. Also now, the Bijker (1971) results for both numerical models correspond better over the whole profile.

Calibration of the hydrodynamic parameters

The simplified UNIBEST model cannot capture all complex wave and current processes. Given the complex area, with a high variation in shape of cross shore profiles and length of the profiles, it is necessary that for each type of profile a detailed analysis and calibration is performed, using different boundary conditions for each type of profile. In this area especially the tidal current velocities have to be determined with care, as both the model stability and the resulting sediment transport rates have shown to be sensitive to the current velocity.

For all profiles, the sediment transport formulae and its parameters are kept constant (Bijker):

- Bottom roughness: 2 cm
- Critical deep water Hm_0/h : 0.07
- Critical shallow water Hm_0/h : 0.6
- The calibration (scaling) coefficient at deep water: 2
- The calibration (scaling) coefficient at shallow water water: 4

Calibration of the hydrodynamic parameters is done by varying:

- the current velocity: the current velocity is calculated in UNIBEST by scaling the reference velocity at a reference depth using the water depth. The smaller the water depth, the smaller the current velocities. However, this is not realistic. E.g. over the shallow Broersbank, higher velocities can be expected. For this reason, the current velocities as defined in §3.2.3 are increased for profiles with a shallow shoreface. Also a small (up to 3 cm/s) increase/decrease of the velocities is applied (constant reduction/increase over the tidal cycle)
- The wave height: the wave height at the offshore boundary is varied up to 15%
- Wave direction: as the wave direction is given with 22.5° bins, a small rotation (up to 12°) is sometimes used.

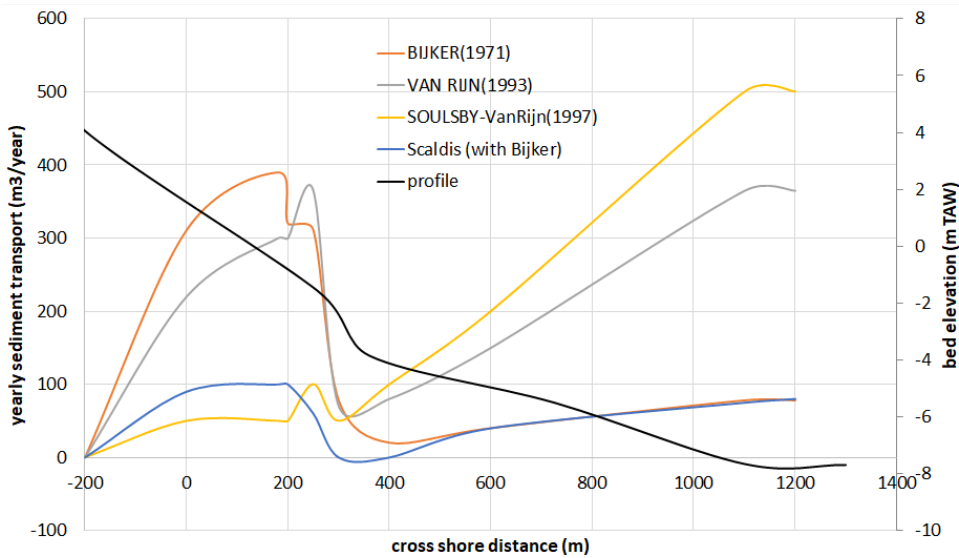


Figure 39 – Comparison of the sediment transport rates using different formulations in Unibest with the results of Scaldis-Coast (HSW112), for a relatively deep profile.

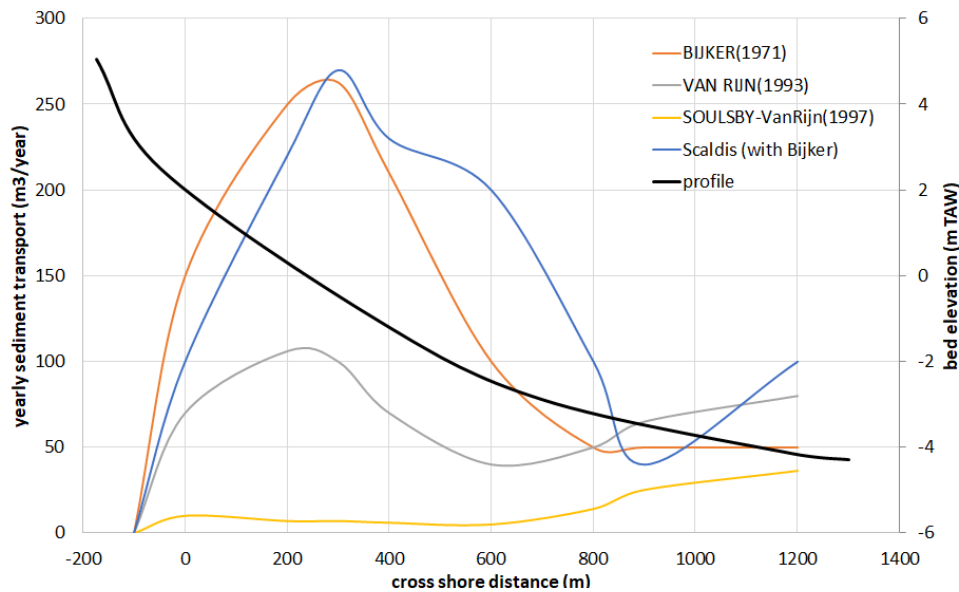


Figure 40 – Comparison of the sediment transport rates using different formulations in Unibest with the results of Scaldis-Coast, for a relatively shallow profile.

Calibration of the sediment transport

For each of the 6 profiles, the local coastline orientation was looked up. For this orientation, the parameter settings are calibrated in order to obtain the target littoral drift. The target littoral drift is set to the result of the Scaldis model (§3.2.5). For the Broersbank (coastal cell 6 as defined in §2.2.1) these transports, together with the cross shore input (between profile 63 and 78) of 80,000 m³/year (Table 10) would result in loss of sediment of $(35+80-180) 10^3 = -65,000 \text{ m}^3/\text{year}$, while in reality, a gain of about 30,000 m³/year is observed (Table 4, active morphological zone, cell 6). For this reason, the transport values are corrected as presented

in Table 11. At the model boundaries, Scaldis gives a transport of 45,000 m³/year (influx from the West, profile 2) and 70,000 m³/year (outflux to the East, profile 160). The cross shore influx is increased to 110,000 instead of 80,000 m³/year.

Table 11 – Target littoral drift

profile	Littoral drift as derived from Scaldis Coast (m ³ /year *1000)	Corrected littoral drift (m ³ /year *1000)
West boundary	45	
008	43	43
020	36	36
034	35	35
063	35	56
078	180	140
120	79	79
East boundary	70	
Offshore boundary	80	110

With these corrected values, the modelled fluxes match with the observed erosion/sedimentation volumes of Table 3:

- For morphological zones 1 to 5 a loss of 9,000 m³/year is obtained (losses in dunes are incorporated since this sand is part of the morphological system, losses in the dunes feed the beach and vice versa). With the corrected values for the littoral drift, a value of 45-56 = -11,000 m³/year is obtained.
- For morphological zone 6 the influx is 56,000 m³/year (littoral drift) +110,000 m³/year (cross shore input) = 166,000 m³/year. The output is 140,000 m³/year, the net result 26,000 m³/year which is equal to the observations.
- Since the harbour groins are difficult to model correctly in both the Scaldis and the UNIBEST model (due to the 3D flow over the groins), the fluxes over these groins are unknown. For this reason, the area east of profile 78 (Broersbank) stretches up to morphological zone 11, east of the harbour. The dredged volumes between the groins (50,000 m³/year) are incorporated. The influx is 140,000 m³/year, the outflux 50,000 m³/year (dredging) + 70,000 m³/year (east boundary), so the net influx is 20,000 m³/year. In this area the volume in morphological zones 7 up to 9 (west of the harbour) is 41,000 m³/year, while east of the harbour the erosion is 26,000 m³/year, in total 15,000 m³/year (comparable with the modelled influx of 20,000 m³/year).

Results and discussion

The calibration of the UNIBEST-LT model has led to acceptable results for each of the 6 profiles:

- In a first step the calibration of the hydrodynamic parameters for each profile have led to result that agree with the transport rates obtained in the Scaldis Coast model
- In a second step the transport rates themselves were calibrated to obtain the observed volume changes (§2.3.4)

All obtained calibration parameters are presented in Table 12.

The output of the UNIBEST-LT calculations are a parametrisation of the littoral drift:

- Parameters describing the dependency of the net littoral drift as a function of the coastline orientation
- A distribution of the littoral drift over the cross shore section.

In reality, this cross shore distribution depends strongly on the coastline orientation. The distribution in the UNIBEST-LT model output however only corresponds to a coastline orientation that is in equilibrium (no net transport) (personal communication, Deltares). The modelled distribution differs strongly from the real distribution for the actual coastline orientation (in the schematisation most of the transport is situated at the offshore end of the profile because there the current is dominant). This gives problems for the modelling of groins, since the relatively short groins do not block much of the transport if UNIBEST indicates (wrongly) that most of the transport is situated offshore the tip of the groin.

Table 12 – Calibration parameters

profile	coastal orientation (°)	increase of tidal velocities (m/s)	amplification of tidal velocities	rotation (clockwise) of wave direction (°)	amplification of wave height	littoral drift (x1000 m ³ /year) for a coast line at 330°	littoral drift (x1000 m ³ /year) at actual coastline orientation	target littoral drift (x1000 m ³ /year)
8	323	-0.03	0.9	12	0.9	19	45	43
20	328	-0.03	0.9	13	0.85	32	39	36
34	333	-0.03	0.9	13.5	0.87	49	40	35
63	323	0	1.2	12	0.95	33	38	35
63-corrected	323	0	1.37	12	1	51	57	56
78	330	0	1.44	12	0.95	177	177	179
78-corrected	330	0	1.35	12	0.9	133	133	140
122	324	0	1	12	0.88	57	85	79

3.3.2 UNIBEST-CL

The UNIBEST-CL model consists of following elements:

- **Reference line:** (along-shore) reference for all cross-shore distances
- **Coastline:** the +1.39 m TAW isohypse of 2002 is used as initial coastline. In the model the location of the coastline is expressed as its cross-shore distance to the reference line
- **Littoral drift** at 6 locations giving the sediment transport as a function of the instantaneous coastline orientation and a distribution over the cross shore profile (generated with UNIBEST-LT). In between these 6 locations, UNIBEST-CL interpolates the littoral drift
- **Groins:** the length of the groin (relative to the reference line) determines which part of the littoral drift (cf. cross shore distribution) is blocked. Also the percentage of blocking can be specified. As explained in §3.3.1 the cross shore distribution of the littoral drift output from UNIBEST-LT intended as input for UNIBEST-CL is not realistic (too much situated in the offshore part). Therefore, using the real length of the groin does not block enough of the littoral drift. Since the groins of Koksijde are situated in an area with net sedimentation and the fact that the height difference between the groins and the neighbouring beach is less than 1 m the blocking due to these groins is neglected in the model set up. This is an assumption that will have to be taken into consideration when interpreting the UNIBEST-CL model results. The groins of Nieuwpoort and the harbour entrance are incorporated in the model
- **Sources and sinks:** in Koksijde (morphological zone 6) 3 sources are defined (at profiles 63, “Den Oever” and 78), with a total input of sediment of 110,000 m³/year. In the harbour entrance of Nieuwpoort a (negative) source of 50,000 m³/year is implemented to incorporate the dredging of the channel

Using this inputs the coastline model (UNIBEST-CL) calculates the changes in coastline location (and orientation) due to longshore sediment transport gradients.

Discussion: calibration of the influence of groines/harbour entrance of Nieuwpoort

The UNIBEST concept using only 1 value for the net littoral drift (instead of using a littoral drift climate considering the occurrence of conditions of littoral drift from SW to NE as well as conditions of littoral drift from NE to SW) does not work well in cases of sharp changes in bathymetry due to the presence of a harbour entrance with groins. Let us consider e.g. the western groin of the harbour of Nieuwpoort. In reality, the transport from west to east is not much reduced due to the limited height of the groin (measured as the vertical distance between the beach and the groin crest). However, for transport from east to west, the groin + harbour channel blocks almost all transport. Suppose the brutto transport from west to east amounts 180,000 m³/year (unknown number, not calculated) and the brutto transport from east to west 130,000 m³/year. Suppose half of this transport is situated along the groin and the other half more offshore, then the transport from west to east is 180,000 m³/year (no blocking) and from east to west 65,000 m³ (half of the 130,000 m³/year). The net transport is thus 115,000 m³/year. Without groin/harbour channel, the net transport would be 180,000 - 130,000 m³/year (no blocking for both components) thus 50,000 m³/year. So, the harbour groin/channel does not reduce the net littoral drift at the upstream end, but on the contrary, it increases it!

This might also explain the increase in net littoral drift as seen in Figure 41 between km 13 and 14. Using a groin to block sediment transport does not work in this case. For that reason, near the harbour an additional profile is defined and the transport components giving transport from east to west are reduced (all negative current velocities are set at 0 m/s and all waves with a direction of 345° or more (including e.g. NE) are set at 0 m wave height. The goal was to have an influx of 100,000 m³/year in the navigation channel. Since 30,000 m³/year is eroding east of the harbour and at the eastern boundary of the model the littoral drift is 80,000 m³/year, this means that 50,000 m³/year is passing at the eastern groin of the harbour (mainly at the part of the profile offshore the groin). This gives: 100,000 influx, 50,000 outflux, thus net influx 50,000 m³/year, which is dredged (sink term in the model). A drawback of this method is that beach erosion

does not influence the blocking of the littoral drift (as long as the coastline orientation remains the same) contrary to the use of a groin, where the groin becomes relatively longer when the coastline retreats and resulting in extra blocking.

For the eastern groin, there is an effective reduction of the littoral drift, which is achieved in the model by making a long groin and applying 100% blocking over the groin, in order to obtain that about 50,000 m³/year is transported over the groin.

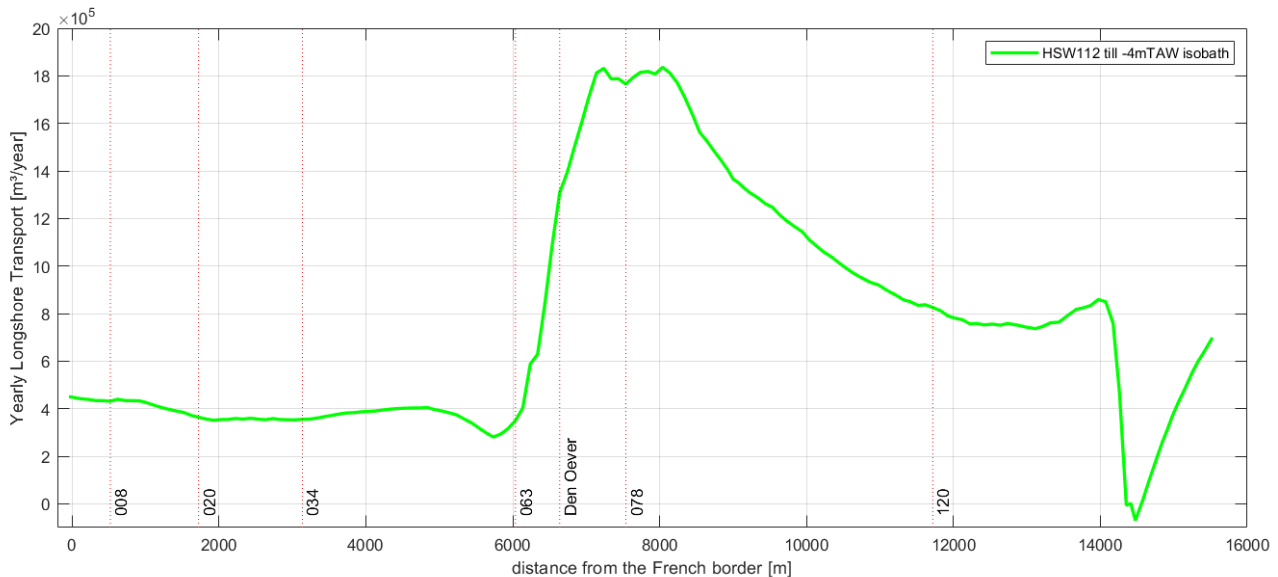


Figure 41 – Net alongshore transport (Scaldis Coast model)

Results

A UNIBEST-CL simulation was done for a period of 5 years. Output is analysed after 1, 2 and 5 years.

The results of the littoral drift over this period are shown in Table 13 and Figure 42. As can be seen, due to changes in the coastline orientation, the littoral drift also changes (slightly) in time. Not everywhere the target is achieved perfectly, but given the uncertainties on all modelling (and measurements), the correspondence is reasonable. Figure 42 (UNIBEST-CL+) matches well with Figure 41 (Scaldis Coast):

- Between km 5 and 6 a decrease in sediment transport is visible due to the change in coastline orientation.
- The increase around km 7 is comparable (taking into account that the littoral drift profile 78 is reduced in order to match with the measured erosion/sedimentation). The 2 kinks in the curve are due to the sediment sources at the profiles 63, “Den Oever” and 78. In total 110,000 m³/year is added in this section.
- Also the increase of sediment transport just west of the harbour entrance is visible.
- Just east of the harbour the littoral drift has to increase again due to the blocking of the groins/harbour channel.

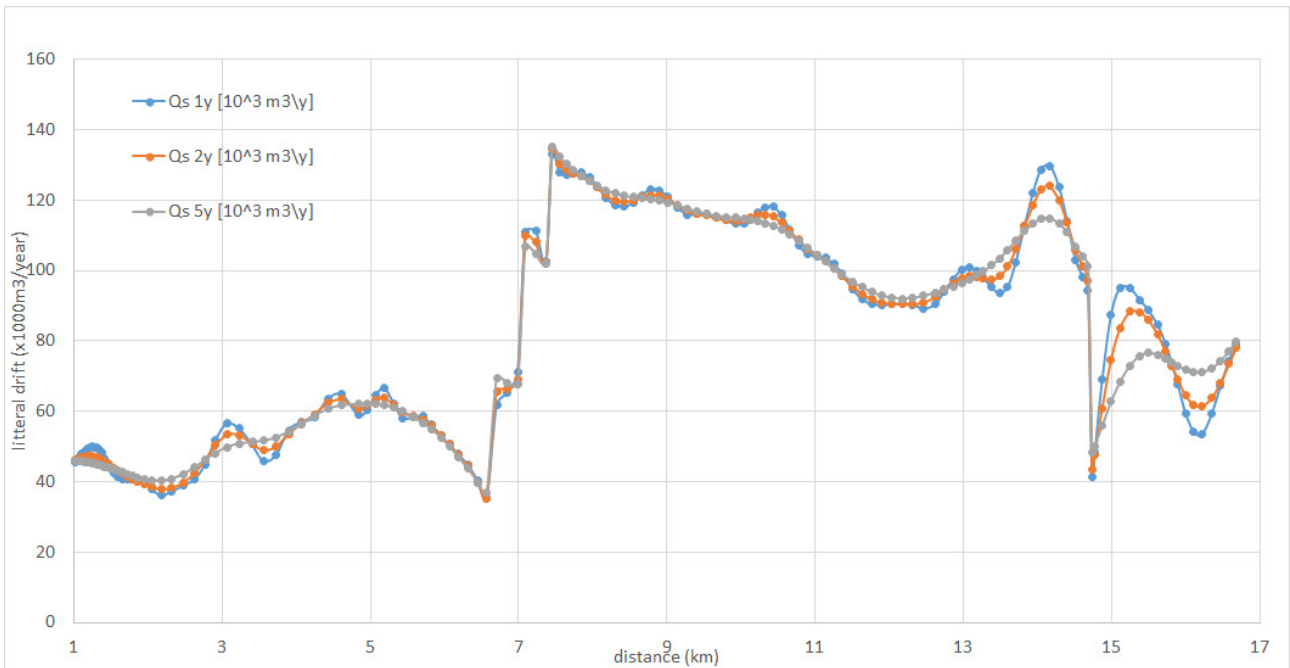


Figure 42 – Littoral drift after 1,2 and 5 years

Table 13 – Littoral drift (x1000 m³/year)

	target	1y	2y	5y
profile 8	45	44.2	45.4	47.2
profile 63	56	53.3	53.2	52.5
profile 78	140	127.8	126.7	127.0
profile 145 (harbour W)	100	98.1	101.3	104.1
profile 148 (harbour E)	50	41.4	43.5	48.3
profile 160	80	79.1	78.1	79.9

Table 14 – and sedimentation volumes (x1000 m³/year)

	first year	second year	average next 3 years	measured
cell 1 to 5	-7.9	-6.5	-4.0	-9
cell 6	40.5	34.0	33.6	26
cell 7 to 10	32.4	25.1	22.6	41
harbour	0.3	5.7	5.2	0
cell 11	-35.9	-35.8	-34.3	-28

Table 14 shows the obtained erosion and sedimentation volumes. Again, the correspondence with the measurements is reasonable. Further fine tuning would be possible, but it has less added value for the general purposes of this project.

The model is calibrated to obtain the measured erosion/sedimentation volumes for 4 areas (west of Broersbank, Broersbank, east of Broersbank, Lombardsijde). It was not the intention of the project to have detailed results per coastal stretch. However, Figure 43 gives a comparison between the modelled and measured propagation of the coastline for 1 year (first year, second year and average of years 3 to 5 of the 5 year-simulation). The values for the “measured trend” are obtained by adding up the trends of the “shoreface” and volume above LW (see §2.3.4) and dividing this by the active height (9.9 m). So this is not the real movement of a contour but makes results comparable to the modelled movement of the coastline. Near the harbor, the trend of section 59 is strongly positive due to the sedimentation in the navigation channel which is taken into account. The measurements are averaged values over a coastal stretch of about 1 km, which is a coarser resolution as in the model (+/- 100 m). In the model, this area west of the harbor, is not influenced by the navigation channel, so the difference between measured and modelled is a (strong) overestimation. The modelled trends are shown after 1 year (thin line, strongly influenced by very local fluctuations in the coastline), between year 1 and 2 and the averaged propagation over the next 3 years. The largest difference between modelled and measured values occurs between km 5 and 6 (Koksijde, sections 22-25). The strong measured erosion is mainly at the shoreface, due to the movement of the Potje channel and due to cross shore transport. As stated in the introduction (§3.1) both phenomena cannot be incorporated in a one-line model.

Possible application of the model

Above results give an indication for the nourishment strategy needed to maintain the current coastline (based on the 2000 DEM) in 2020 – 2050 (however not considering the possible need to strengthen sea defences at some locations for safety against a 1000y storm). Two regions are in need to be nourished to maintain the position of the coastline:

- the beach of Lombardsijde, due to its location downdrift of the harbour entrance of Nieuwpoort
- De Panne coastal town

The erosion at the Panne-city (km 2 to 4) is visible in the model. A simulation is done with a yearly input of sand in this area of 32,000 m³ (nourishments). As can be seen, this amount is enough to compensate the erosion. The groins in Nieuwpoort-Bad cause a complex pattern in coastline change due to the limited possibilities to model groins correctly. It should be repeated that the model is not calibrated for local phenomena and that the groins are modelled inaccurately.

Another possible application is to assess the impact of sea level rise (§3.4)

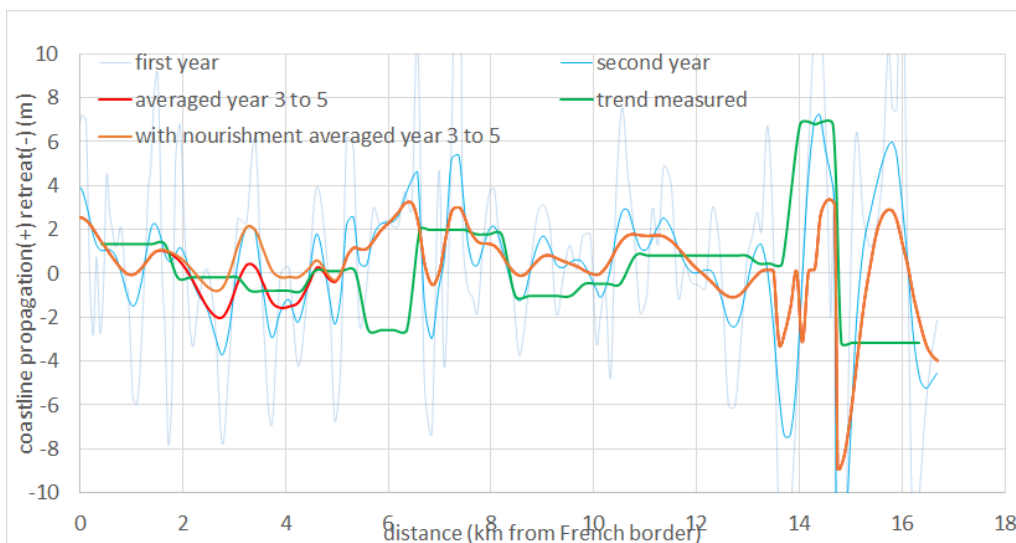


Figure 43 – Coastline propagation/retreat with and without nourishments

3.4 Sea level rise

To examine the effects of sea level rise, both the change in littoral drift and the coastal retreat due to the higher water levels (Bruun-effect) are examined separately.

3.4.1 Effect of SLR on the littoral drift

In order to perform a sensitivity analysis on the effect of SLR on littoral drift, all water levels in the model were increased with 1 meter and the littoral drift was recalculated. The truncated calculation for the harbour groin of Nieuwpoort was not changed since the effect of sea level rise on the blocking by the groin cannot be expressed by only increasing the water levels. The depth of closure was changed to -3 m TAW (to get the same water depth at the location of the depth of closure).

The results of the calculations are shown in Table 15.

Table 15 – Littoral drift without and after 1 m SLR

profile	Without SLR Qs (x1000 m ³ /y)	1 m SLR Qs (x1000 m ³ /y)
8	45	43
20	39	36
34	40	37
63	56	65
78	133	89/158
122	85	134

For the short profiles (8, 20 and 34) the littoral drift decreases slightly. Although the current velocity increases slightly (as it scales with the depth in UNIBEST), the littoral drift is smaller due to the smaller width of the area where most of the littoral drift occurs. Due to the higher water level, the sediment transport is partly situated above the actual HW level, where the profile is steeper. This gives a different cross shore distribution (as illustrated in Figure 44) of the littoral drift (higher peak, but over a much smaller cross shore distance). However, in reality, due to cross shore transport, the profile would become less steep around HW and probably, the littoral drift would remain almost the same as in the actual situation.

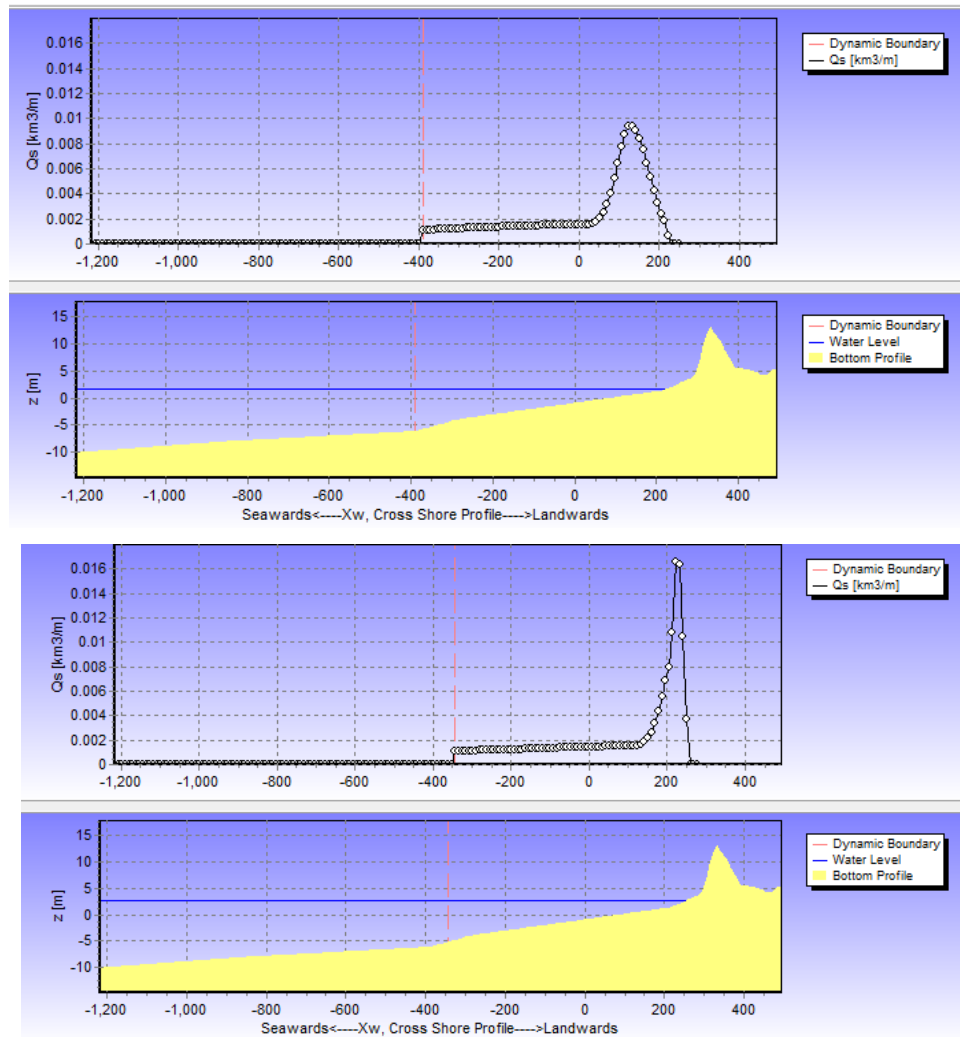


Figure 44 – Littoral drift for profile 8 for a climate condition with high waves (top: without SLR, down: with SLR)

For profile 63 the littoral drift increases: the shallow sand bank in front of the profile reduces the wave height. At higher water levels (SLR) this reduction is smaller, giving more sediment transport. However, in reality, this sandbank might adjust to SLR by vertical growth.

Profile 78 is the longest profile and the bottom slope between -3 and -4 m TAW is very gentle. Reducing the depth of closure from -4 to -3 m TAW has a large impact on the littoral drift (decreases from 133 to 89 x10³m³/year, cf. Figure 45). But in that case, also the influx (“cross shore”) over the depth of closure line would decrease. Without this shift in depth of closure (keeping it at -4 m TAW), the littoral drift increases.

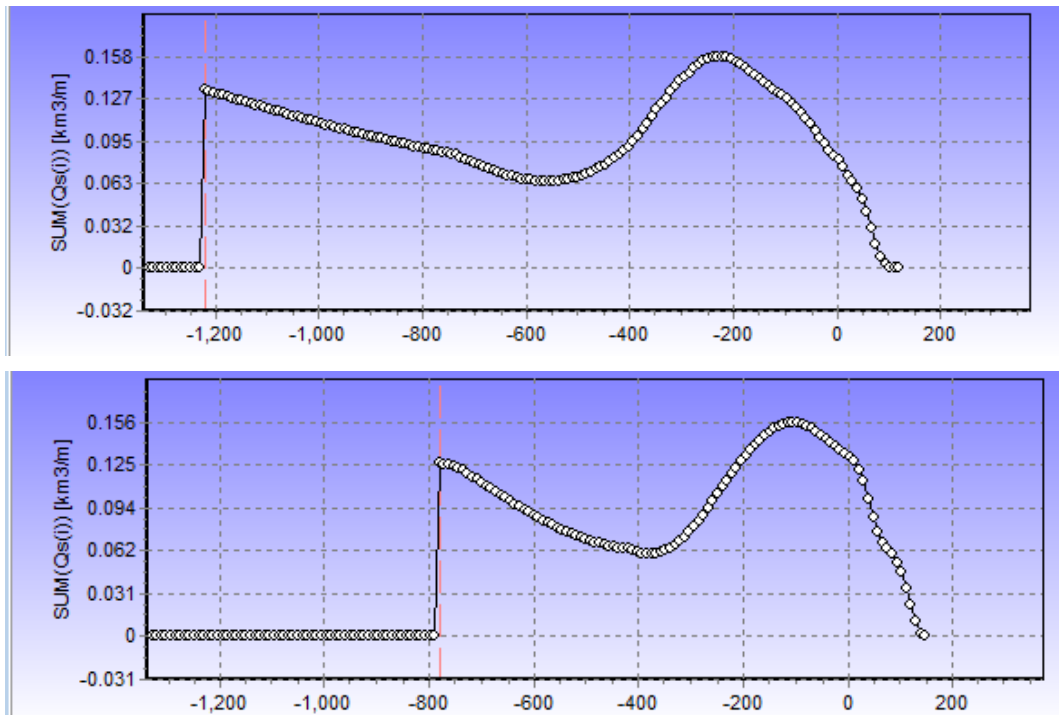


Figure 45 – Yearly total littoral drift for profile 78 (top: without SLR, down: with SLR)

For profile 122 the higher current velocities seem to be dominant, leading to an increase in littoral drift with about 50%. It is at present not clear how the currents are impacted by sea level rise, and this effect is not incorporated in the simulation.

It must be concluded that the change of behavior of the sediment transport in the Potje channel and on the Broersbank due to SLR on the longer term needs to be studied with different types of models (less process-based). Also the current velocities will behave differently than modelled in UNIBEST (e.g. if the tidal range remains constant, higher water levels would lead to a reduction of the tidal velocities, contrary to the result in UNIBEST). The observations above (UNIBEST simulations of Table 15) can only give a rough indication of possible effects of SLR.

The effect of the groin is not recalculated: beach accretion/erosion and higher water levels lead to an unknown effect on the blocking of littoral drift.

The results of the coastline model are shown in Figure 46 and Figure 47 for the case in which for profile 78 the littoral drift is calculated down to -4 m TAW and the cross shore influx is kept constant (and without groins in Nieuwpoort, these have only a local effect). As can be seen, more accretion occurs near Nieuwpoort and less accretion near Koksijde.

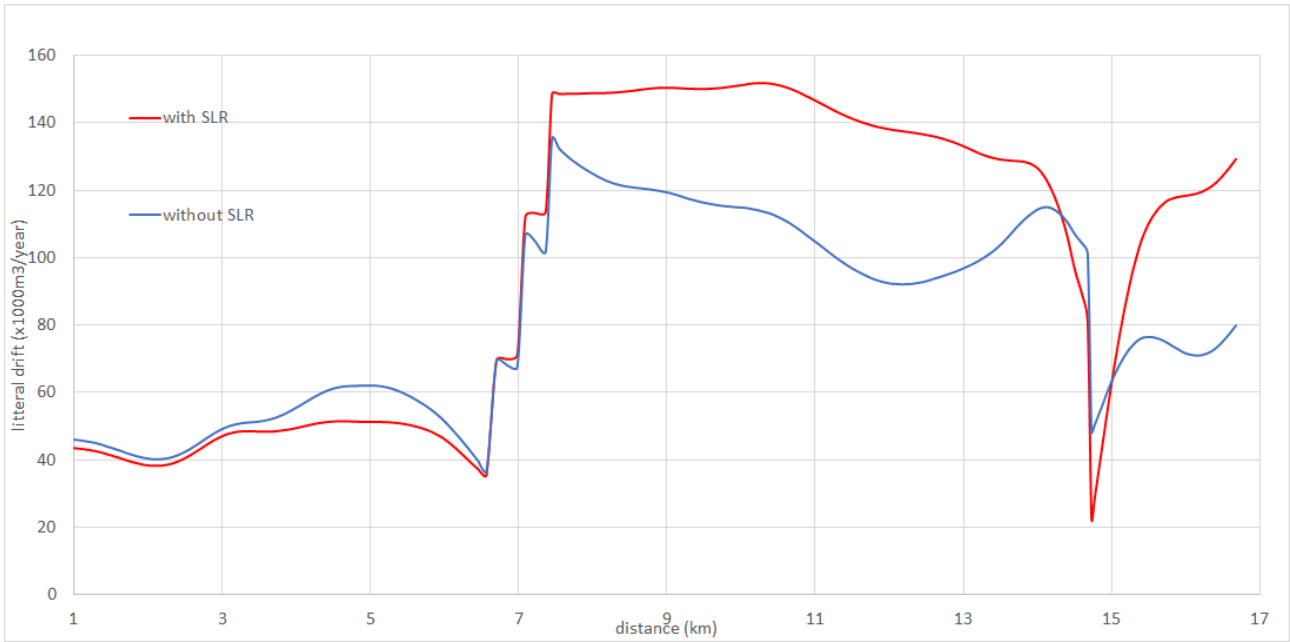


Figure 46 – Littoral drift along the coast after 5 years without and with SLR

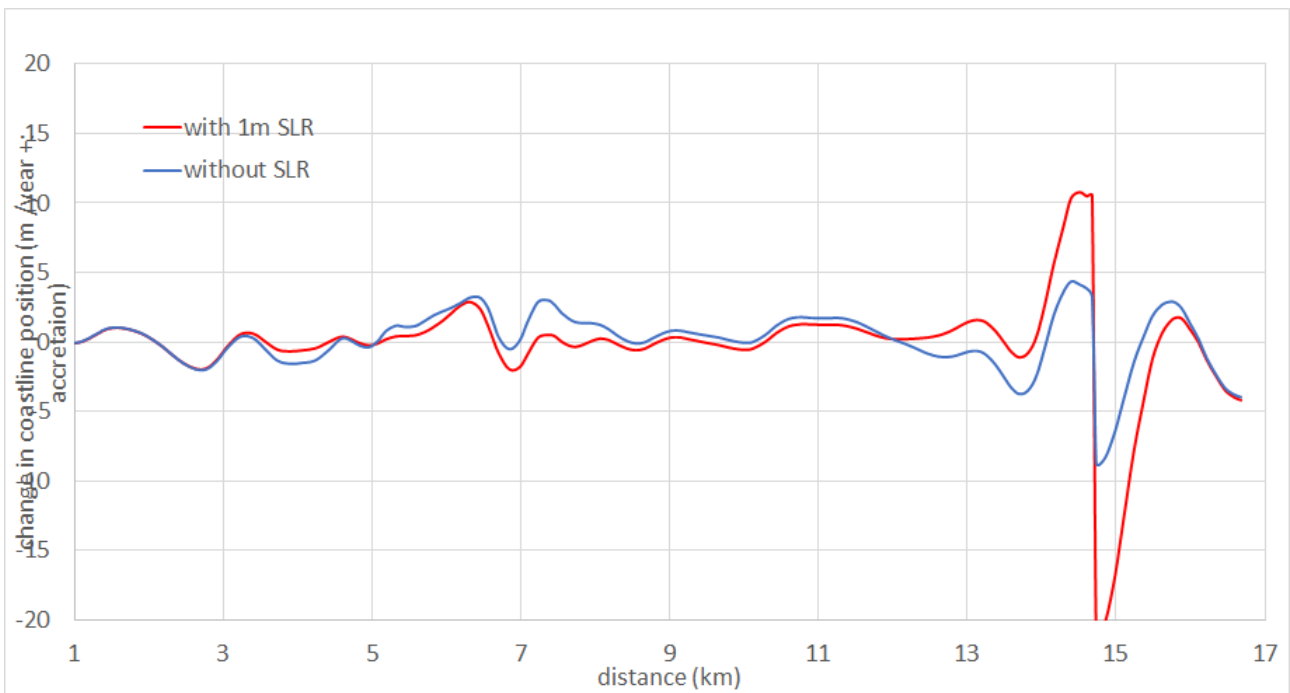


Figure 47 – Coastline accretion/erosion per year between the 2nd and 5th year without and with SLR

3.4.2 Application of the Bruun-rule

The effect of the retreat of the coastline due to SLR is modelled by incorporating a sink term as defined by Bruun (1962):

$$Q_{\text{sink}} = \text{SLR}_y \times L$$

With:

- Q_{sink} : the applied sink (per m stretch)
- SLR_y : rate of SLR per year (= 80 cm/100 y = 0.008 m/year). This sea level rise rate of 8 mm/year is based on projections for the Belgian coast for the period 2020 – 2050. So, for this period of 30 years the total sea level rise amounts to 0.24 m
- L: length of the active zone (= averaged slope x active height)

Q_{sink} varies along the project area due to the variation of the width of the active profile. The sink terms are applied as point sinks (1 point every +/- 200 m)

Following data (Table 16) are input to the model per morphological zone. The last column gives the theoretical retreat of the coastline, according to Bruun-rule, after 30 years.

Table 16 – Model input according to Bruun-rule.

profile start	profile end	L	sink (m ³ /year/m)	Distance (m)	total sink (m ³ /year)	number of sources	sink per source	theoretical retreat after 30 years
0	8	706	5.648	800	4,518.4	5	-904	-17.1
8	20	660	5.28	1,200	6,336	8	-792	-16.0
20	34	600	4.8	1,400	6,720	7	-960	-14.5
34	63	540	4.32	2,900	12,528	10	-1,253	-13.1
63	78	600	4.8	1,500	7,200	6	-1,200	-14.5
78	90	850	6.8	1,200	8,160	6	-1,360	-20.6
90	122	1,089	8.712	3,200	27,878.4	11	-2,534	-26.4
122	140	891	7.128	1,800	12,830.4	9	-1,426	-21.6

(no retreat is applied east of the harbor since it is not realistic that erosion progresses without compensation by nourishments to prevent the destruction of the dunes)

The model was applied for a period of 30 years. The progress/retreat is shown in Figure 48. As can be seen, the modelled retreat is close to the theoretical retreat. This indicates no significant differences in coastline orientation between a run with and without SLR occur. Such a differences would lead to differences in littoral drift and thus changes in erosion/sedimentation patterns. The harbor of Nieuwpoort is an exception, but as mentioned before, the groin is not modelled correctly. Also simulations are done with the same nourishment strategy. The results show that generally, this nourishment rate (32,000 m³/year) is sufficient (while without SLR generally the coastline would be moving seaward).

The more general policy question that can be addressed using a coastline model such as UNIBEST-CL is how a target coastline (not necessarily the current coastline) has to be maintained by a nourishment strategy on a time scale of decades.

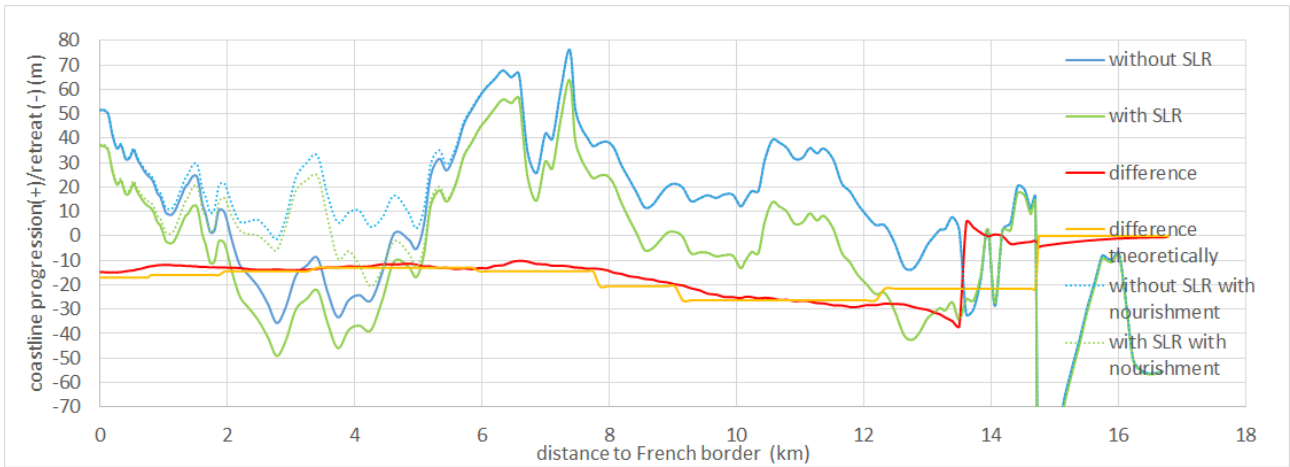


Figure 48 – Total accretion/sedimentation over the next 30 years without SLR and by applying the Bruun rule for SLR of 8 mm/year

4 Discussion and Conclusions

4.1 Discussion

Overall, one can distinguish between three sections of the study area (Figure 49).

In the first section, west of Den Oever, stretching over the coastal towns of De Panne and Sint-Idesbald in the westernmost part of the study area, the corrected volumetric trend in the active zone for the period 2000 – 2020 is mildly erosive: $-2 \text{ m}^3/\text{m}/\text{year}$. In the second (middle) section -stretching over the coastal towns of Koksijde, Oostduinkerke and Nieuwpoort- there is a significant accretion trend: namely $+8 \text{ m}^3/\text{m}/\text{year}$. In the third section, located at Lombardsijde at the eastern side of the harbour of Nieuwpoort, a strong, erosive trend of $-23 \text{ m}^3/\text{m}/\text{year}$ is observed. The sand balances were presented in Table 3 and summarised for each of these three sections in Table 17.



Figure 49 – Distinguishing three sections in the study area based on sand balances.

Table 17 – Results from volumetric analysis. Sand balances for three sections (shown on Figure 49).

	De Panne and Sint-Idesbald (west of Den Oever)	Koksijde and Nieuwpoort (between Den Oever and the harbour)	Lombardsijde (east of the harbour)	Total study area
Observed growth	20,000 m^3/yr	77,000 m^3/yr	9,000 m^3/yr	ca. 105,000 m^3/yr
Nourished	30,000 m^3/yr	11,000 m^3/yr	37,000 m^3/yr	ca. 80,000 m^3/yr
Corrected growth	-10,000 m^3/yr	66,000 m^3/yr	-28,000 m^3/yr	ca. 25,000 m^3/yr
Coastal length	6.3 km	8.1 km	1.2 km	15.6 km
Nourishment intensity	5 $\text{m}^3/\text{m}/\text{yr}$	1 $\text{m}^3/\text{m}/\text{yr}$	31 $\text{m}^3/\text{m}/\text{yr}$	ca. 5 $\text{m}^3/\text{m}/\text{yr}$
Corrected growth intensity	-2 $\text{m}^3/\text{m}/\text{yr}$	+8 $\text{m}^3/\text{m}/\text{yr}$	-23 $\text{m}^3/\text{m}/\text{yr}$	ca. 1.5 $\text{m}^3/\text{m}/\text{yr}$

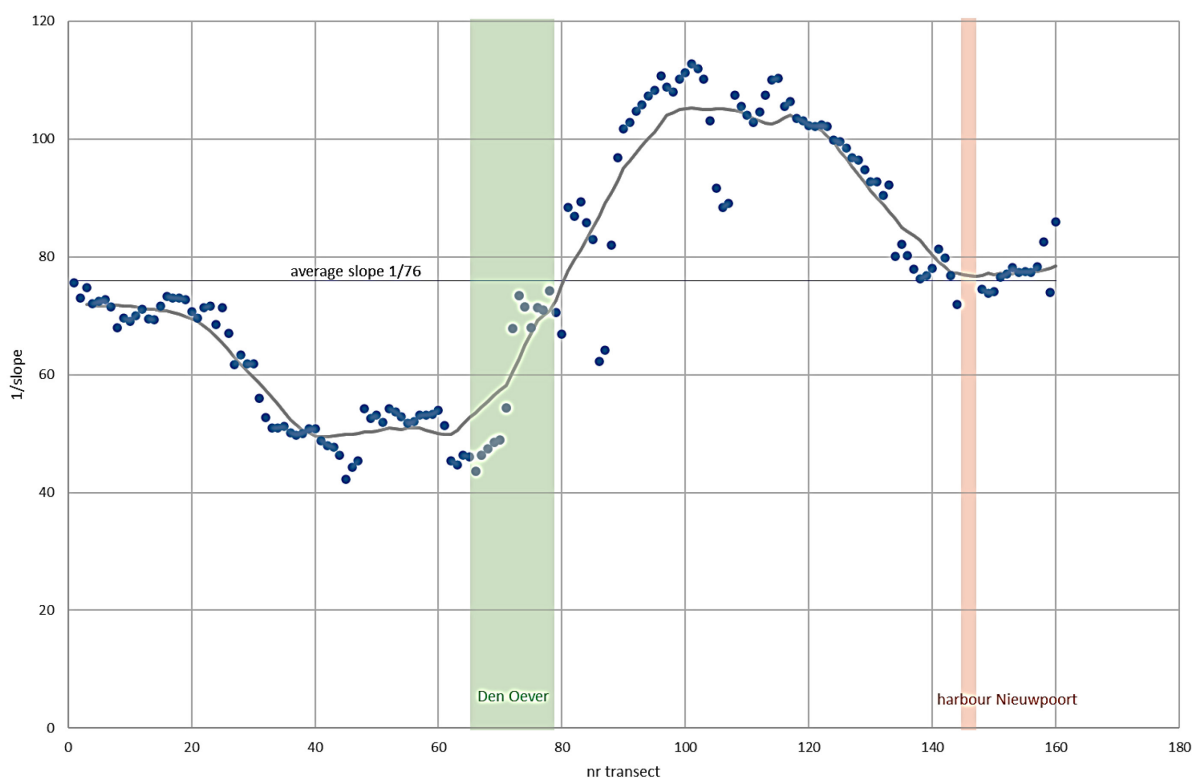


Figure 50 – Variability of the slope of the active beach and shoreface zone in the study area.
Blue dots – value per profile; grey line – moving average

The variability of the averaged slope of the active beach and the shoreface zone in the study area is in agreement with this distinction between three sections in the study area (Figure 50). One can observe that the average slope of 1/76 is influenced by the presence of the channel – sand bank system in the whole study area. The slope is steeper where the channel is present, while it is milder where the sand bank is present.

Considering the sand balance of the study area, a growth rate of 105,000 m³/year is observed (Table 17). Sand works contribute for 35,000 m³/year of this (net result of the nourishments in the three sections and dredging in Nieuwpoort access channel). This suggests that the remaining 70,000 m³/year has to come from natural feeding, alongshore and/or cross-shore. The estimates for the littoral drift (as derived from the Scaldis-Coast model, §3.2.5) are considered reliable, resulting in a net loss from the study area of 25,000 m³/year. Consequently, cross-shore feeding has to be as large as 95,000 m³/year. The hypothesis is that this cross-shore feeding consists of two components. A first component at location Den Oever comes from (or over) the crest of the shoreface connected ridge, for which the estimate from the Scaldis-Coast model is 85,000 m³/year (which is rounded from +81,406 m³/year calculated in §3.2.5). A second component of 10,000 m³/year is needed to close the volume balance. It is distributed over the central part of the study area (the coastal towns of Koksijde, Oostduinkerke and Nieuwpoort) which coincides with the location of the base of the shoreface connected ridge and further to the east.

The knowledge on the large scale sand transports components in the study area can be summarized in the conceptual model presented in Figure 51.

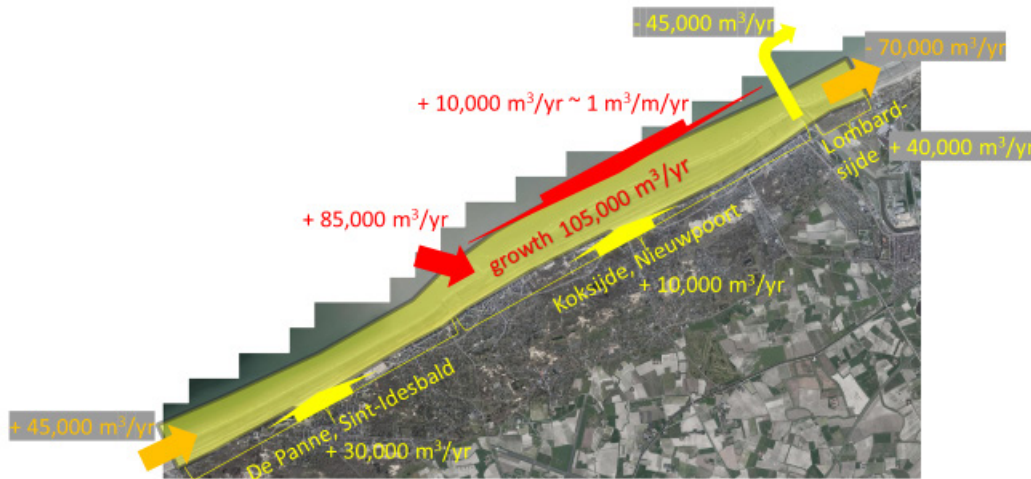


Figure 51 – Conceptual model for the large scale sand exchanges in the study area.

The most important component is the cross-shore natural feeding indicated by the two red arrows. It is the source for both the increase of the littoral drift from the southwest to the northeast part, as well as the progradation of the coastline between the coastal towns of Koksijde and Nieuwpoort. On Figure 51 the yellow arrows represent sand works resulting in gains (nourishments) or losses (dumping of dredged sand outside the active beach and shoreface zone), and the orange arrows represent the littoral drift at the western and at the eastern boundary.

This case study on the Belgian West Coast illustrates the morphological interaction between the coastline and the channel-sandbank system off-shore. Overall a cross-shore natural feeding of 95,000 m³/year is estimated for this study area in the period 2000-2020. A quantification of the natural feeding was possible due to the availability of topo-bathymetric monitoring data spanning several decades. Processes driving this natural feeding are related to the existence of a shoreface-connected ridge:

- a first component is related to sand transport by combined action of tidal currents and wave action near the crest of the ridge. Using the Scaldis-Coast model developed for the Belgian coast we were able to obtain a more detailed in-sight in the spatial distribution of this transport. Additional simulations would result in more insight on the temporal distribution;
- a second component is supposed to be related to a net wave-driven cross-shore transport over the relatively shallow base of the ridge. More research into this process is needed in order to better understand the physics and to be able to reproduce it in a numerical model that would allow more detailed knowledge of the spatial and temporal distribution of this transport.

It would be interesting to compare the results on cross-shore natural feeding for the Belgian West Coast to other sites with a similar setting. In literature, morphological descriptions are given of sites with shoreface-connected ridges present, e.g. in northern France, between Calais and Dunkerque (Héquette et al, 2010), in central Holland in the Netherlands (Van de Meene et al, 2000) and Fire Island, New York (Kana et al, 2011). However, quantifications of cross-shore natural feeding are rare and with a very wide uncertainty band e.g. a range between 0 and 370,000 m³/year is given for Fire Island (Kana et al, 2011).

This must be related to difficulties to measure in the field. In our study the transports were estimated by closing a sand balance for a 20 year period for an area with a coastal length of 16 km. Another method would be to have field campaigns with a duration of typically some weeks, deploying instruments to measure sand transport on representative locations. Such measuring techniques are notoriously difficult and expensive. They are never covering the entire spatial area and temporal range. Prior to a deployment instruments to measure sand transport in the field should be thoroughly validated in laboratory conditions. Nevertheless,

the basic problem remains that it is almost impossible to measure very close (cm) to the bottom, where most sand transport takes place.

The processes of cross-shore natural feeding explain why this coastal area has shown resilience against sea level rise in the past decades. What will happen when sea level rise will accelerate? The answer must be found in the large scale morphological behaviour of the channel – sand bank system. In Nnafie (2014) it is stated that a critical sea level rise rate exists above which the sand bank crest height will no longer be able to grow at a pace high enough to follow sea level rise. This hypothesis is based on non-linear stability analyses using a specific morphodynamic model. In this context, the sand bank would drown. Then the consequence might well be that natural feeding to the coastline would stop, resulting in drowning of the beach as well. Therefore, the coastal resilience would be lost. A challenge for future research is to quantify the critical sea level rise rate for the Belgian West Coast. This should be done by developing a specific morphodynamic model for the channel – sand bank system as well as the neighbouring coastline that focuses on decadal/centennial time scales.

What about the interaction of the channel – sand bank system with the coastline on these time scales? Apart from the active profile adjusting to sea level rise according to the Bruun rule, also the relation to the dunes is an essential element. Two basic situations have to be distinguished:

- in case of progradation or stability of the coastline, foredune building occurs, meaning a sand transport occurs from the active beach and shoreface towards the dunes;
- in case of retreat of the coastline, foredune erosion occurs, providing sand to the active beach and shoreface as well as to the inland (e.g. via blow-outs).

4.2 Conclusion

Based on volumetric observations, and insights gained from both an existing 2D model -namely Scaldis-Coast (Telemac-2D software)- and a newly setup 1D coastline model (UNIBEST-CL+ software), a conceptual model for the large scale sand fluxes at the Belgian West Coast is presented (Figure 51). From this conceptual model it was concluded that the shoreface-connected ridge acts as a natural sand motor for the Belgian West Coast. Where the crest of the ridge connects to the coastline a local protrusion in the coast-line is created due to an accumulation of sand originating from off-shore. Like in the case of an artificial sand motor alongshore transport distributes sand to the neighbouring coastal areas stimulating coastal protection in a wider coastal zone.

More knowledge on the cross-shore natural feeding will be crucially important for coastal protection because in the coming decades more sand will be needed to maintain the sandy coastal defences (beaches, dunes, shorefaces) under the expected climate change. A better nourishment strategy will be found if one can take into account the natural processes of cross-shore feeding from off-shore to the coastline.

Furthermore this study showed some limitations of the UNIBEST-CL+ software:

- In a UNIBEST-CL model the interaction with the dunes can only be schematized by a constant sink or source. So, model software development is needed to be able to describe the more complex interaction between the active beach and shoreface zone on the one hand and the dunes on the other hand. Qualitative indications are given by the Psuty-diagram (Psuty, 2004). According to this theory coastline progradation results in foredune growth, but coastline retreat can result in either foredune growth or foredune loss depending on the rate of coastline retreat. In case of foredune loss sand transfer is partly towards the inland dunes (e.g. blowouts) and partly towards the beach.
- The schematization of (tidal) currents over a profile in UNIBEST-LT should be improved. For the Belgian coast the tidal currents are a major forcing apart from the waves.
- The coupling of UNIBEST-LT and UNIBEST-CL only takes into account the net longshore transport, neglecting the gross; and also only takes into account the cross-shore distribution of the litoral drift at equilibrium coastline angle (coastline angle at which no net longshore transport occurs). This leads to unexpected behaviour (net longshore transport higher with groins than without) when the

coastline hasn't reached the equilibrium angle yet, the hydrodynamics are mainly tidally driven and the blockage of the groin is highly asymmetric (e.g. groin adjacent to harbour entrance channel). In this study, at the location of the western harbour jetty of Nieuwpoort, this problem was solved by adding an extra profile to the UNIBEST-LT module for which all hydrodynamic boundary conditions resulting in transport from east to west were set to zero (ebb current and waves coming from N to NE).

5 References

- Afdeling Kust - Vlaamse Hydrografie** (2019). Getijtafels voor Nieuwpoort, Oostende, Blankenberge, Zeebrugge, Vlissingen, Prosperpolder, Antwerpen en Wintam 2020 T.A.W.; Getijtafels voor Nieuwpoort, Oostende, Blankenberge, Zeebrugge, Vlissingen, Prosperpolder, Antwerpen en Wintam 2020 L.A.T. IVA Maritieme Dienstverlening en Kust: Brussel. 142 (T.A.W.);136 (L.A.T.) pp.
- Bijker, E.W.** (1971). Longshore transport computations. Proc. ASCE, Journal of the Waterways, Harbours and Coastal Engineering Division, WW4, November 1971.
- Bruun, P.** (1962) Sea-level Rise as a Cause of Shore Erosion, Journal of Waterways Harbors Division, 88, 117–130, 1962, American Society of Civil Engineers.
- Deltares** (2020). UNIBEST user manual. 17 February 2020.
- Dujardin, A., Vanlede, J., Van Hoestenbergh, T., Verwaest, T., Mostaert, F.** (2016) Invloedsfactoren op de ligging van de top van de sliblaag in het CDNB: Deelrapport 2 – Analyse periode 1999-2011. Versie 5.0. WL Rapporten, 00_078. Waterbouwkundig Laboratorium & Antea Group: Antwerpen, België.
- Héquette, A.; Aernouts, D.** (2010) The influence of nearshore sand bank dynamics on shoreline evolution in a macrotidal coastal environment, Calais, Northern France. Continental Shelf Research, 30, 12, p 1349-1361, 2010.
- Houthuys, R., Verwaest, T., Dan, S., Mostaert, F.** (2022) Morfologische evolutie van de Vlaamse kust tot 2019. Versie 0.1. WL rapporten, 18_142. Waterbouwkundig Laboratorium, Antwerpen. 225p.
- International Marine and Dredging Consultants.** (2009). Afstemming Vlaamse en Nederlandse voorspelling golfklimaat op ondiep water: deelrapport 5. Rapportage jaargemiddelde golfklimaat. Waterbouwkundig Laboratorium: Antwerpen.
- Janssens, J., Delgado, R., Verwaest, T., Mostaert, F.** (2013) Morfologische trends op middellange termijn van strand, vooroever en kustnabije zone langsheen de Belgische kust: Deelrapport in het kader van het Quest4D-project. Versie 2_0. WL rapporten, 814_02. Waterbouwkundig Laboratorium, Antwerpen. 88p.
- Kana, T.W.; Rosati, J.D.; Traynum, S.B.** (2011) Lack of evidence for onshore sediment transport from deep water at decadal time scales: Fire Island, New York. Journal of Coastal Research, Special Issue, No. 59, pp. 61-75, 2011.
- Kolokythas, G., Fonias, S., Wang, L., De Maerschack, B., Vanlede, J., Mostaert, F.** (2018) Modelling Belgian Coastal zone and Scheldt mouth area. Sub report 7: Progress report 3 – Model developments: Hydrodynamics, waves and idealized modelling. Version 2.0. FHR Reports, 15_068_7. Flanders Hydraulics Research: Antwerp
- Kolokythas, G., Fonias, S., Wang, L., De Maerschack, B., Vanlede, J., Mostaert, F.** (2020a) Modelling Belgian Coastal zone and Scheldt mouth area. Sub report 11: Progress report 6-Model developments: Grid optimization, Morphodynamics, Dredging/dumping subroutines, Wave conditions. Version 0.1. FHR reports, 15_068_11. Flanders Hydraulics Research: Antwerp.

- Kolokythas, G.; Fonias, S.; Wang, L.; De Maerschack, B.; Vanlede, J.; Mostaert, F.** (2020b). Modelling Belgian Coastal zone and Scheldt mouth area: Sub report 14: Scaldis-Coast model – Model setup and validation of the morphodynamic model. Version 0.1. FHR Reports, 15_068_14. Flanders Hydraulics Research: Antwerp.
- Ministerie van verkeer en waterstaat** (1991). "De basiskustlijn, een technisch / morfologische uitwerking" (in Dutch).
- Monbaliu, J.; Mertens, T.; Bolle, A.; Verwaest, T.; Rauwoens, P.; Toorman, E.; Troch, P.; Gruwez, V. (eds.).** (2020) CREST Final scientific report: Take home messages and project results. VLIZ Special Publication, 85. 145 pp. Flanders Marine Institute (VLIZ): Oostende, 2020. ISBN 978-94-920439-0-0
- Nationaal Geografisch Instituut (2021).** <https://www.ngi.be/website/tweede-algemene-waterpassing/> consulted on 25/01/2021.
- Nnafie, A.** (2014) Formation and long-term evolution of shoreface-connected sand ridges: modeling the effects of sand extraction and sea level rise. PhD thesis. 142 pp. Utrecht University, Institute for Marine and Atmospheric research Utrecht, 2014. ISBN 978-90-393-6258-7
- Psuty, N.P.** (2004) The coastal foredune: a morphological basis for regional coastal dune development. In Coastal Dunes: Ecology and Conservation. Ecological Studies, Martinez M.L., Psuty N.P. (eds.), Vol. 171. Springer-Verlag: Berlin; 11-28.
- Roest, B.** (2019). Gecombineerde topografie en bathymetrie van de Belgische kust, geïnterpoleerd naar kustdwarse raaien (1997-2019). Available at: <http://vliz.be/nl/imis?module=dataset&david=6366>.
- Soulsby, R.** (1997). Dynamics of Marine Sands, American Society of Civil Engineers, Thomas Telford, Ltd., London.
- Stive, M.** (2004) How important is global warming for coastal erosion?, an Editorial Comment, Climatic Change 64: 27-39, 2004; DOI:10.1023/B:CLIM.0000024785.91858.1d
- Strypsteen, G., Houthuys, R., Rauwoens, P.** (2019) Dune volume changes at decadal timescales and its relation with potential aeolian transport. Journal of Marine Science and Engineering, 7, 357.
- Suzuki, T.; Trouw, K.; De Roo, S.; Mostaert, F.** (2020). Methodology for Hydraulic Boundary Conditions and Safety Assessment 2021: SWAN v41.20 validation report for a higher wave climate. FHR Reports, 18_037. Flanders Hydraulics Research: Antwerp: Antwerp.
- Teurlincx, R.; Van der Biest, K.; Reyns, J.; Verwaest, T.; Mostaert, F.** (2009). Haven Van Blankenberge - Verminderen van de aanzanding van de havengeul en het voorplein: Eindrapport. Versie 2_0. WL Rapporten, 643_12. Waterbouwkundig Laboratorium: Antwerpen, België.
- Van de Meene, J.W.H.; Van Rijn, L.C.** (2000) The shoreface-connected ridges along the central Dutch coast, part 2: morphological modelling. Continental Shelf Research, 20, 2325-2345, 2000.
- Van Rijn, L.C.** (1993). Principles of Sediment Transport in Rivers, Estuaries and Coastal Seas. Aqua Publications, The Netherlands.
- Vandebroek, E.; Dan S.; Vanlede, J.; Verwaest, T.; Mostaert, F.** (2017). Sediment Budget for the Belgian Coast: Final report. Version 2.0. FHR Reports, 12_155_1. Flanders Hydraulics Research: Antwerp & Antea Group.
- Verfaillie, E.; Van Lancker, V.; Van Meirvenne, M.** (2006). Multivariate geostatistics for the predictive modelling of the surficial sand distribution in shelf seas. Continental Shelf Research 26 (2006) 2454-2468. doi:10.1016/j.csr.2006.07.028

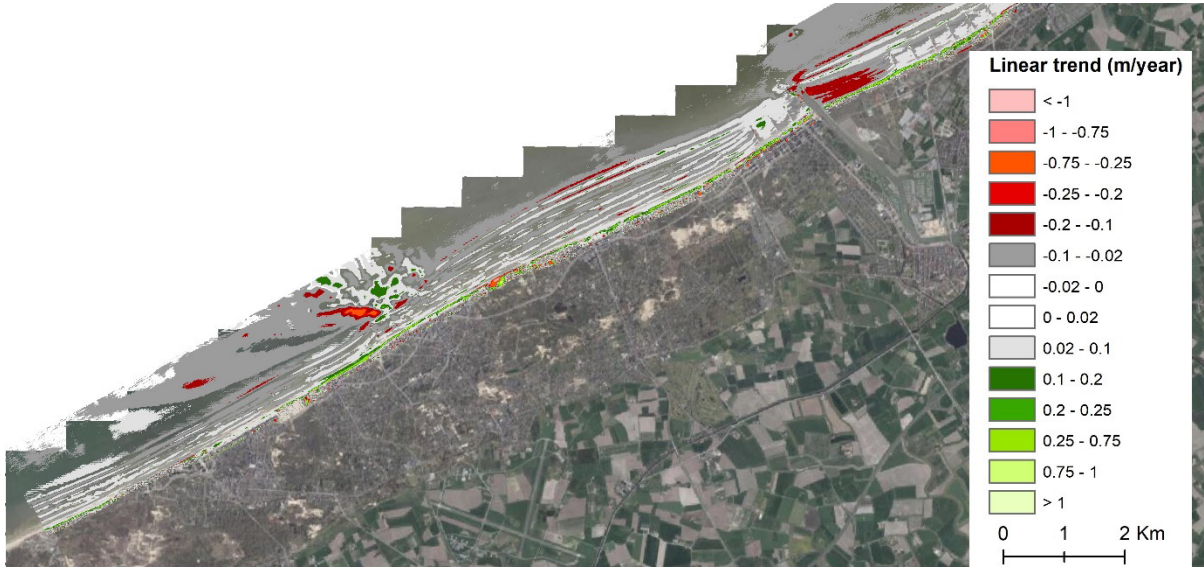
Appendix A

Active morphologic zone	Section	Location	Description of zone characteristics
1	1-7	Natuurreservaat Westhoek	change points in mean beach profile slope (breaker zone) and altitudes standard deviation coincide somehow
2	8-9	Verkaveling Westhoek	only change point in mean beach profile slope (breaker zone) and no significant change points in altitudes standard deviation (offshore, nearshore, breaker zone, beach)
3	10-13	Westhoek - De Panne Centrum	higher variation in altitudes standard deviation in nearshore zone than in breaker zone with east De Panne structure
4	14-18	De Panne Centrum	higher variation in altitudes standard deviation in nearshore zone than in breaker zone with west De Panne structure
5	19-26	Sint-Idesbald - Koksijde Bad	higher variation in altitudes standard deviation in offshore zone => Broersbank attaching to coast
6	27-33	Koksijde Bad	very shallow foreshore with eastside SCHIPGAT blowout
7	34-43	Koksijde Bad-Oost	change points in mean beach profile slope (breaker zone) and altitudes standard deviation coincide with westside SCHIPGAT blowout
8	44	Oostduinkerke-Bad	change points in mean beach profile slope (breaker zone) and altitudes standard deviation coincide along urbanized beach
9	45-59	Koksijde Oost-Nieuwpoort Bad	change points in mean beach profile slope (breaker zone) and altitudes standard deviation coincide along coastal dunes
10	60	Nieuwpoort harbour	Harbour
11	61-64	Lombardsijde	change points in mean beach profile slope (breaker zone) and altitudes standard deviation coincide along nourished beach with influence of the Nieuwpoort harbour

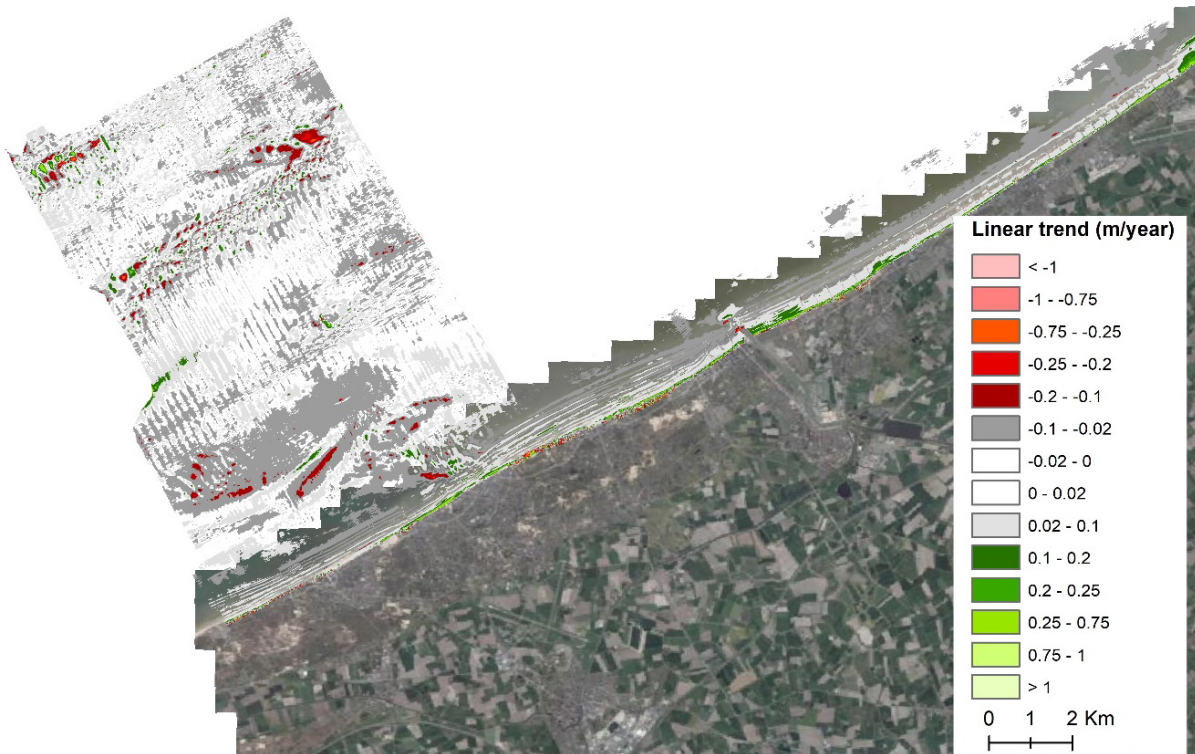
Appendix B

Linear trend analysis with threshold of 0.02 m/year (equivalent $R^2=0.05$).

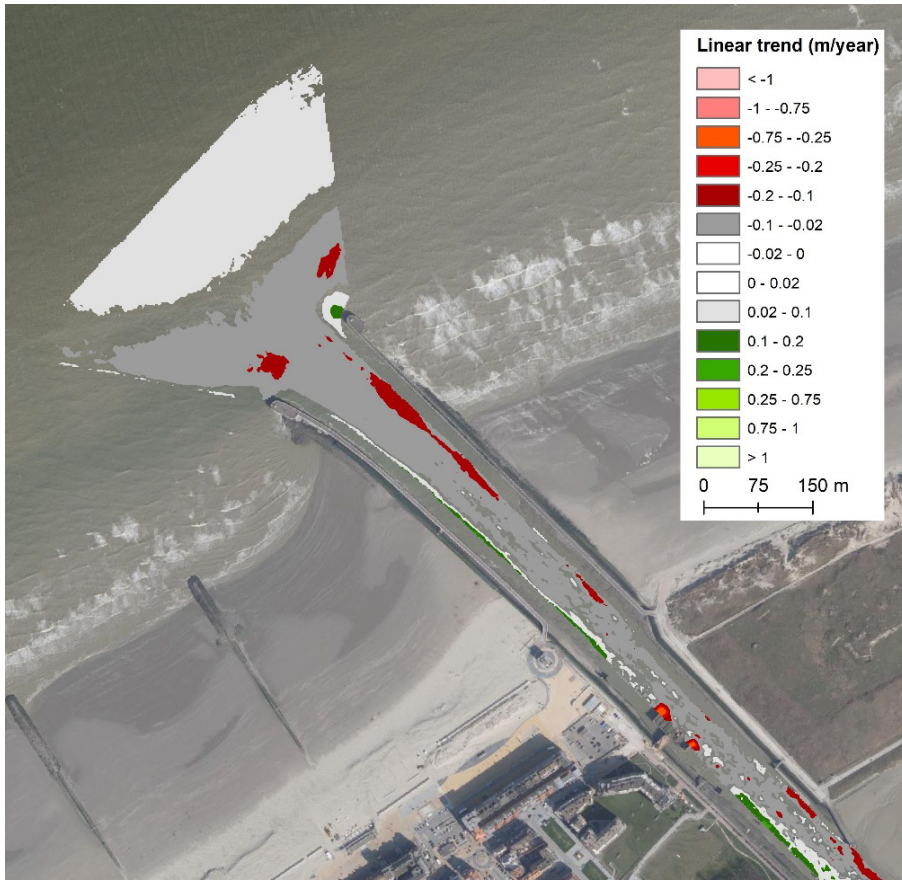
Onshore zone over the period from 2010-2016 based on 7 surveys



Onshore-Offshore zone over the period from 2006-2014 based on 4 surveys



Nieuwpoort harbour entrance over the period from 2009-2020 based on 12 surveys



Appendix C

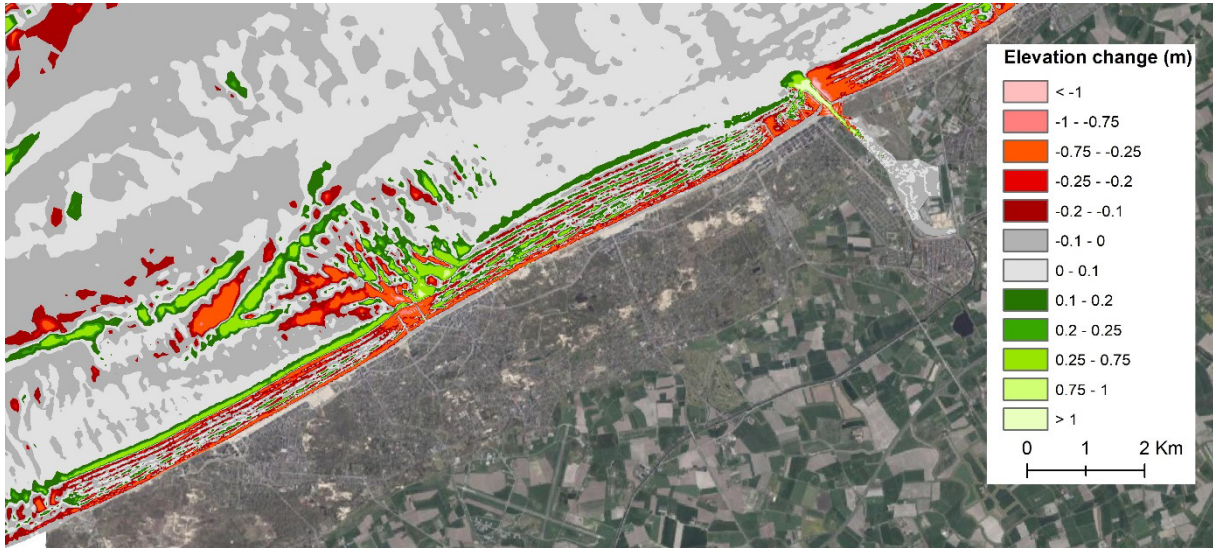
Maps of contour lines from the coast to the offshore zone between 2006 and 2014 indicating the migration of the Potje channel (grey arrow). Orange and blue contour lines in 2006 and 2014 respectively. Contour lines above 0 m TAW every 4 m; below 0 m TAW every 2 m.



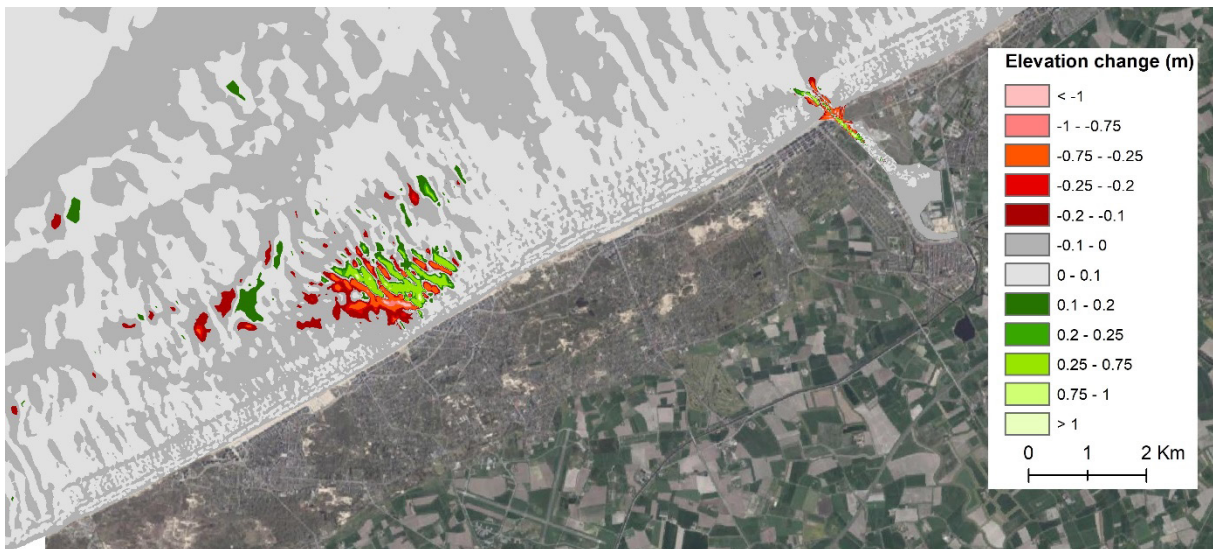
Appendix D

Results of Scaldis model of bed evolution of 373 days (1.02 year) between 2015 and 2016

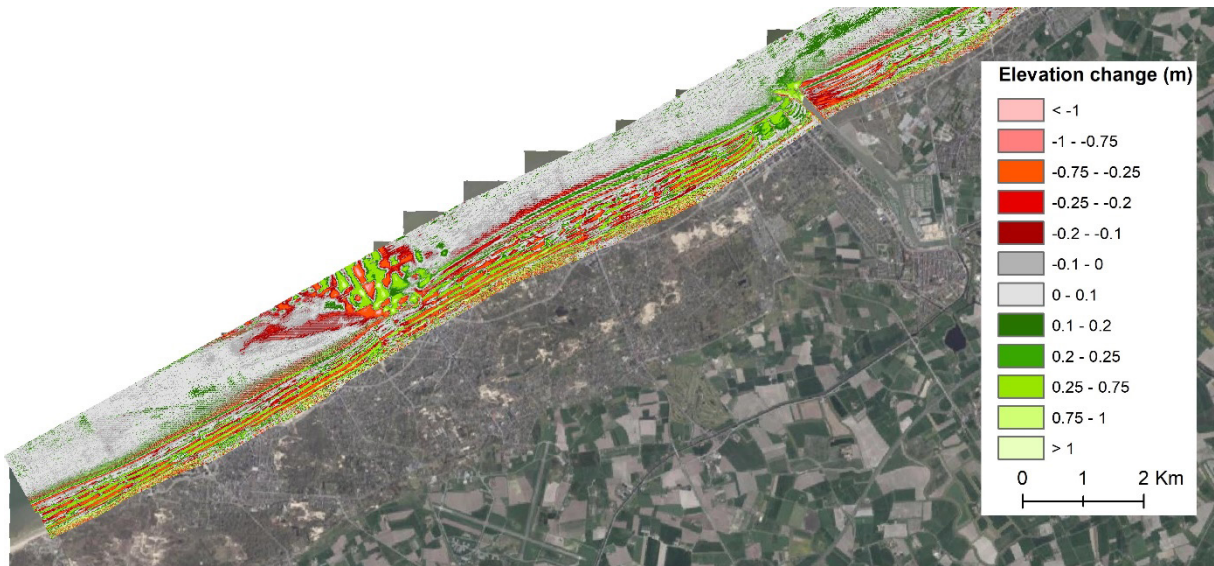
Wave and tidal processes (swc005V13a)



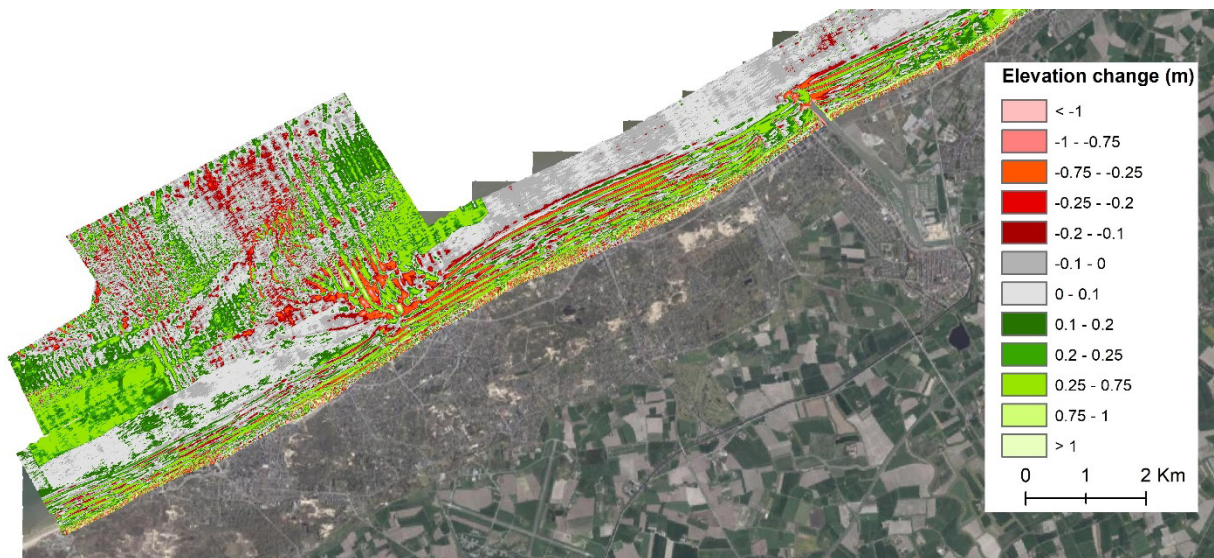
Tidal processes (sed084)



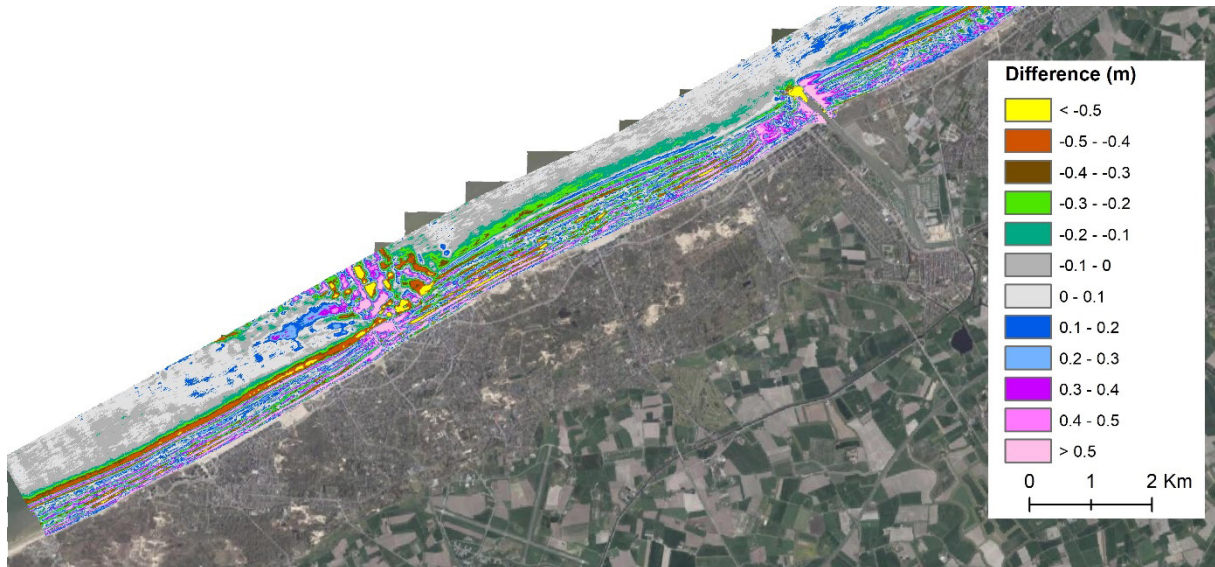
Results of the observed bed evolution of 1.13 year between 2015-2016 covering the onshore zone



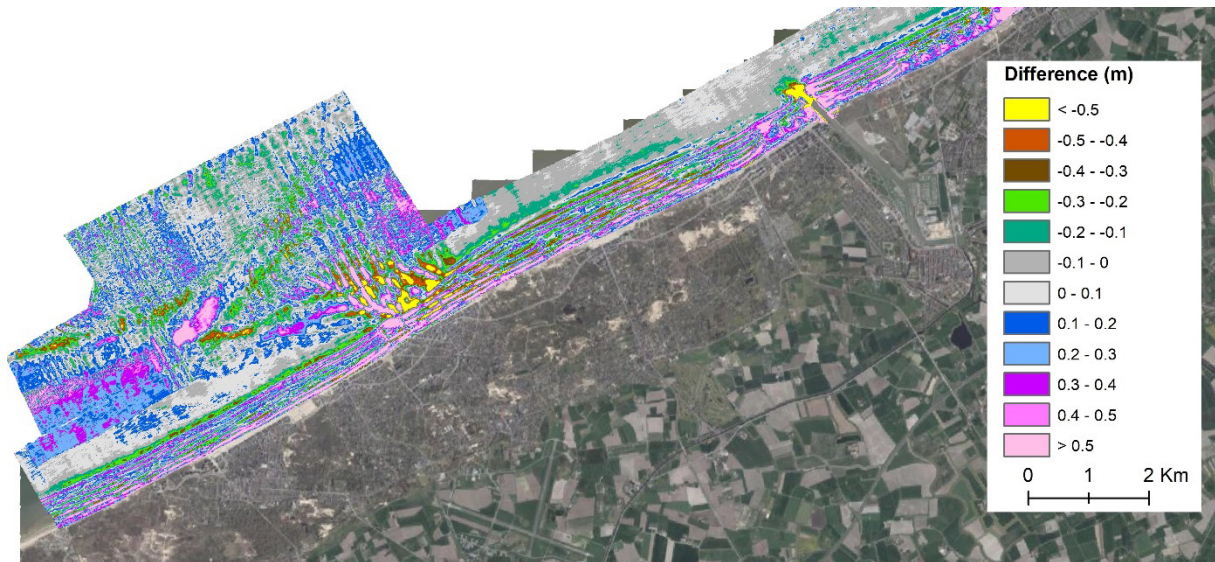
Results of the observed bed evolution of 1 year between 2013-2014 covering the offshore zone



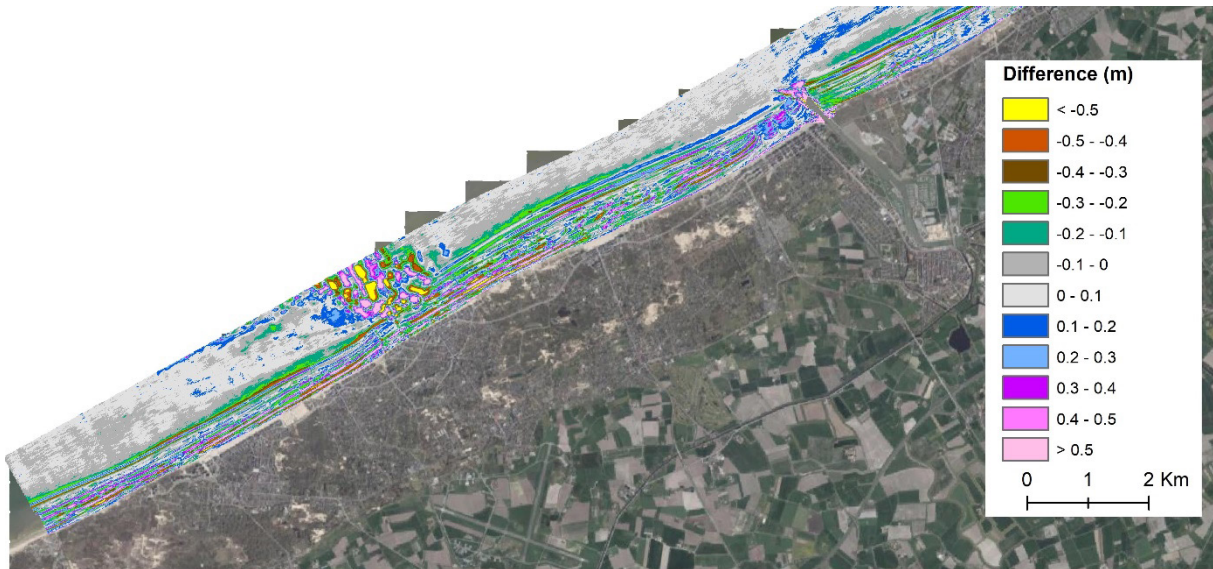
Difference between Scaldis model of the wave and tidal processes simulation (swc005V13a) and observed bed evolution for the onshore zone



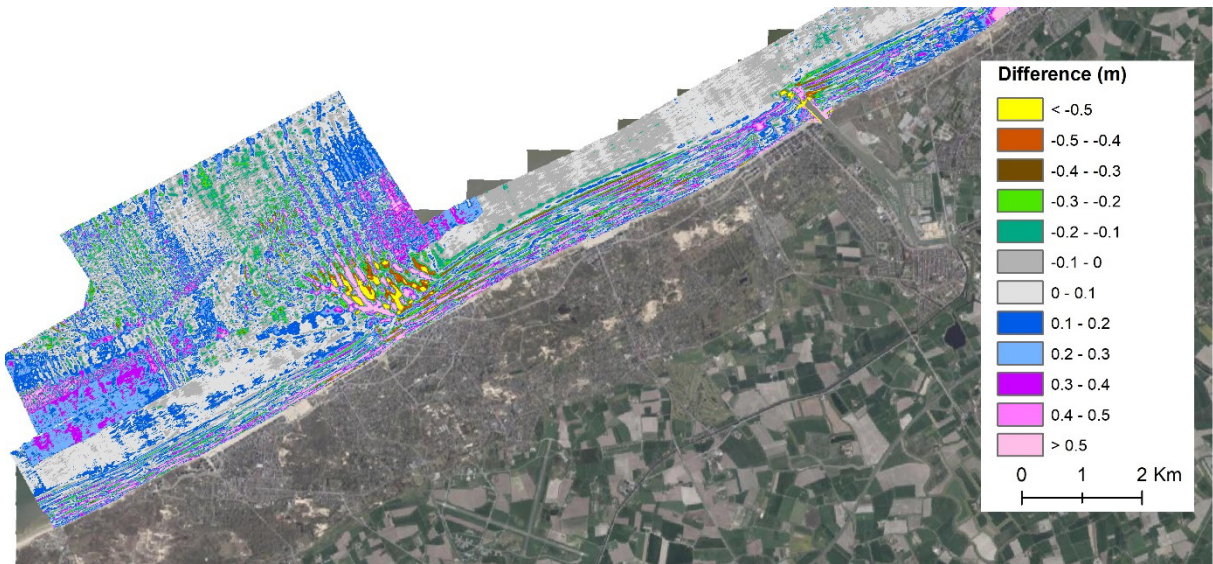
Difference between Scaldis model of the wave and tidal processes simulation (swc005V13a) and observed bed evolution for the offshore zone



Difference between Scaldis model of the tidal processes simulation (sed084) and observed bed evolution for the onshore zone

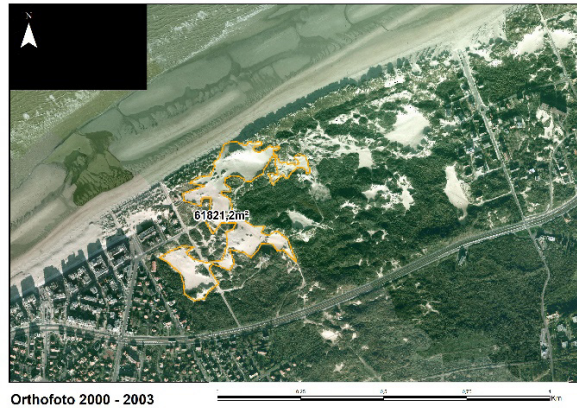
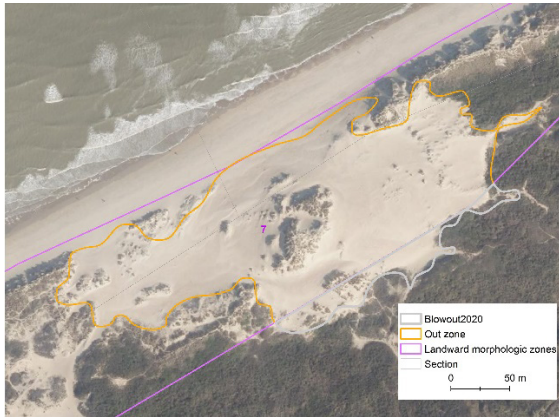


Difference between Scaldis model of the tidal processes simulation (sed084) and observed bed evolution for the offshore zone



Appendix E

Observations of the blowout evolution located in the landward zone 4



Year	Blowout area (m ²)	Blowout volume (m ³)
2000 - 2003	61821	421200 based DEM in 2007
2008 - 2011	36415	423538 based DEM in 2012
2015	37267	449907 based DEM in 2015
2020	40855	474896 based DEM in 2021

Availability: aerial images in 2000-2003, 2008-2011, 2015, 2020; DTM in 2007, 2012, 2015, 2018 and 2021

Data saved in: P:\20_017-kstInmdlWstKs\3_Uitvoering\Morphology\01_Data\Blowout_SCHIPGAT_KoksijdeDuinen

Appendix F

Volumetric changes of the morphological of the landward and active zones

Landward boundary		Diff 2000-2007			Diff 2007-2011			Diff 2011-2015			Diff 2015-2020			Diff 2000-2020		
Unit	Section	Vol/yr	Vol/area (Gain (m/y	Vol/yr	Vol/area (Gain (m/y	Vol/yr	Vol/area (Gain (m/y	Vol/yr	Vol/area (Gain (m/y	Vol/yr	Vol/area (Gain (m/y	Vol/yr	Vol/area (Gain (m/y	Vol/yr	Vol/area (Gain (m/y	
Zone 1	T1-7						3448.33	0.13	0.03	6472	0.30	0.06	2585	0.48	0.02	
Zone 2	T8-9	-293	-0.07	-0.01	-718	-0.10	-0.02	-771	-0.11	-0.03	699	0.12	0.02	-229	-0.15	-0.01
Zone 3	T10-13	-508	-0.06	-0.01	-287	-0.02	0.00	-291	-0.02	-0.01	2019	0.17	0.03	204	0.07	0.00
Zone 4	T14-18	-474	-0.03	0.00	-1072	-0.04	-0.01	3825	0.16	0.04	7086	0.36	0.07	2145	0.44	0.02
Zone 5	T19-26	1726	0.16	0.02	3795	0.20	0.05	4416	0.24	0.06	7830	0.52	0.11	4184	1.13	0.06
Zone 6	T27-33	1846	0.26	0.04	3549	0.28	0.07	2412	0.20	0.05	3784	0.38	0.08	2773	1.12	0.06
Zone 7	T34-43	458	0.01	0.00	2048	0.03	0.01	762	0.01	0.00	9802	0.20	0.04	3139	0.26	0.01
Zone 8	T44	471	0.10	0.01	-366	-0.04	-0.01	1600	0.19	0.05	596	0.09	0.02	565	0.33	0.02
Zone 9	T45-59	21310	0.47	0.07	27189	0.34	0.09	14817	0.19	0.05	22217	0.34	0.07	21348	1.33	0.07
Zone 10-1	T60-64	-2888	-0.50	-0.07	8531	0.82	0.21	6100	0.60	0.15	1967	0.24	0.05	2395	1.17	0.06
Active zone		Diff 2000-2007			Diff 2007-2011			Diff 2011-2015			Diff 2015-2020			Diff 2000-2020		
Unit	Section	Vol/yr	Vol/area (Gain (m/y	Vol/yr	Vol/area (Gain (m/y	Vol/yr	Vol/area (Gain (m/y	Vol/yr	Vol/area (Gain (m/y	Vol/yr	Vol/area (Gain (m/y	Vol/yr	Vol/area (Gain (m/y	Vol/yr	Vol/area (Gain (m/y	
Zone 1	T1-7						12835.16	0.05	0.01	22190	0.10	0.02	13809	0.26	0.01	
Zone 2	T8-9	-3463	-0.08	-0.01	-278	0.00	0.00	-991	-0.01	0.00	8853	0.15	0.03	712	0.05	0.00
Zone 3	T10-13	-14481	-0.20	-0.03	-4702	-0.04	-0.01	-5796	-0.05	-0.01	6338	0.06	0.01	-5629	-0.23	-0.01
Zone 4	T14-18	-22653	-0.23	-0.03	-12777	-0.07	-0.02	-13574	-0.08	-0.02	22286	0.16	0.03	-7736	-0.22	-0.01
Zone 5	T19-26	-4066	-0.02	0.00	4733	0.02	0.00	16803	0.06	0.01	26497	0.11	0.02	9453	0.16	0.01
Zone 6	T27-33	27018	0.15	0.02	23811	0.07	0.02	26656	0.09	0.02	38591	0.15	0.03	29125	0.46	0.02
Zone 7	T34-43	-29604	-0.07	-0.01	23699	0.03	0.01	-13888	-0.02	0.00	4695	0.01	0.00	-7369	-0.05	0.00
Zone 8	T44	2307	0.04	0.01	-1556	-0.02	0.00	-2186	-0.02	-0.01	336	0.00	0.00	142	0.01	0.00
Zone 9	T45-59	24158	0.04	0.01	7302	0.01	0.00	21934	0.02	0.01	52138	0.07	0.01	27241	0.14	0.01
Zone 10	T60	371	0.03	0.00	9234	0.39	0.10	-11203	-0.48	-0.12	3836	0.20	0.04	631	0.13	0.01
Zone 11	T61-64	-16060	-0.14	-0.02	111295	0.54	0.14	-54573	-0.27	-0.07	3621	0.02	0.00	6196	0.15	0.01

Appendix G

HWD system onboard (extract in Methodology_HWD.pdf)

1 Werking HWD ¹

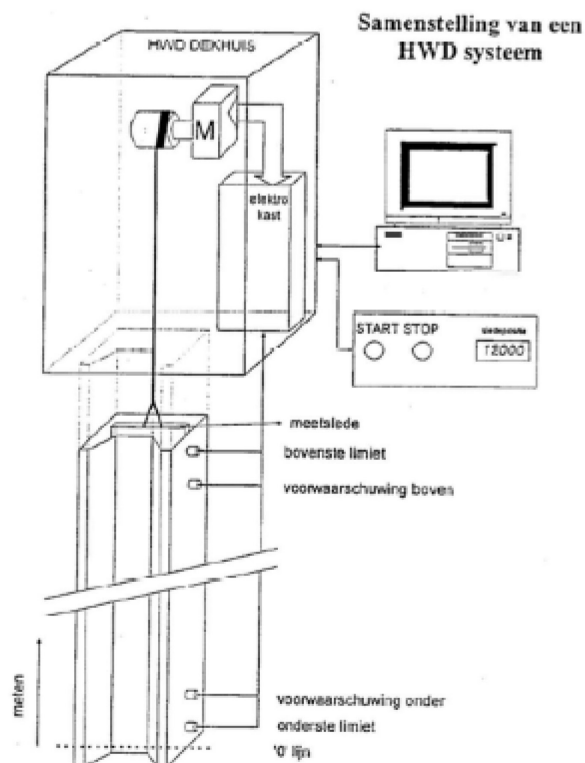
De HWD is ontworpen als installatie voor een nauwkeurige meting van de tonnen droge stof (TDS).

1.1 Samenstelling van het toestel

De installatie bestaat uit

- Minstens één waterdichte stalen meetkoker met een U-profiel, vertikaal opgesteld in laadruim van het schip en uitgerust met een geleidingsprofiel met een op- en neergaande meetslede, voorzien van een nucleair systeem voor het meten van de densiteit van de baggerspecie.
- Minstens één stalen dekhuis waarin o.a. het elektro-mechanisch aandrijfsysteem is ingebouwd.
- Een PC-installatie met randapparatuur op de brug.

Figuur 1 Samenstelling van een HWD-systeem

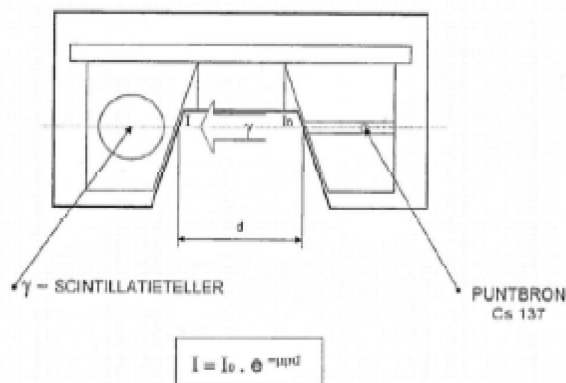


Figuur 2 HWD aan boord van de Sebastiano Caboto: voor- en achteraanzicht.



Op de Sebastiano Caboto bevindt het meetsysteem zich centraal in de beun. Bovenaan (groen) is er het HWD dekhuis. Onderaan is er de waterdichte meetkoker met U-profiel. Er is geen bijkomende bevestiging van de koker voorzien. Enkel onderaan de koker en ter hoogte van het dekhuis is er een bevestiging.

Figuur 4 Principe densiteitsmeter

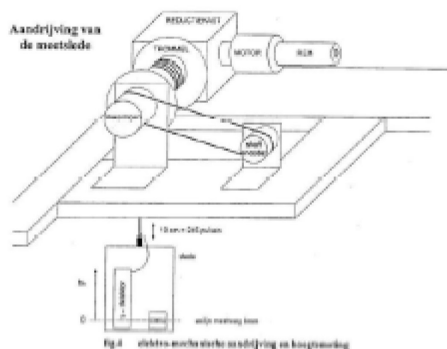


Op basis van de verhouding tussen de oorspronkelijke straling en de residuele straling kan (in combinatie ervan) de dichtheid en absorptiecoëfficiënt van de specie afgeleid worden.

1.2.2 De positiebepaling

De slede met de densiteitsmeter is gemonteerd op een slede die in de koker op en neer gaat. Door de lengtemeting van de kabel kan de positie van de slede en dus ook van de densiteitsmeter bepaald worden.

Figuur 5 Elektromechanische aandrijving en hoogtemeting



De meting begint onderaan op de koker. Bij elke meting gaat de slede tot beneden in de koker en wordt het nulpunt opnieuw bepaald.

1.2.3 De berekening van de gemiddelde dichtheid

De meting gebeurt continue van beneden naar boven.

De laadtabel van de volume-inhoud van de schepen is beschreven aan de hand van hoogtevensters van 10 cm. Door de koker te ijken volgens de vensters in deze laadtabel kan ook het volume op die hoogte (op dat hoogte venster) worden gekoppeld met de gemeten dichtheiden (met een afwijking tot 2%).

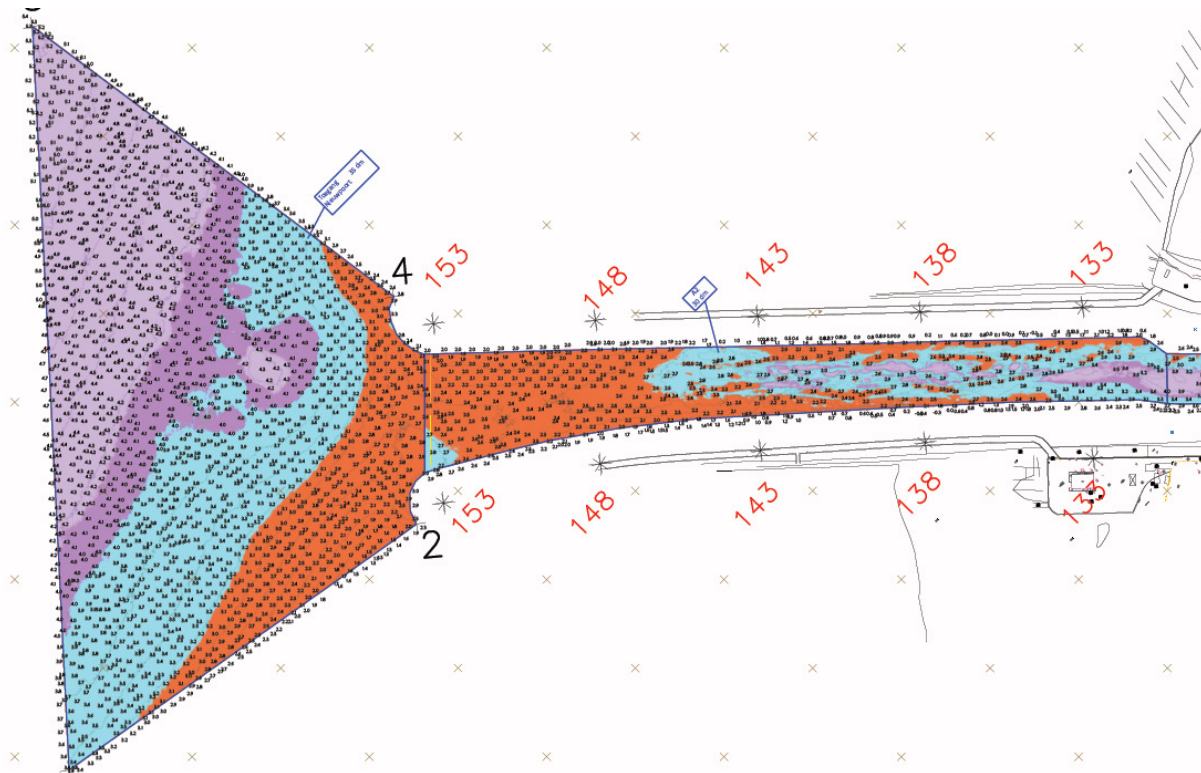
Door per volume de gemeten dichtheid bepalen en met deze verhouding rekening te houden kan (behalve het totale volume) de gemiddelde dichtheid in de beun berekend worden.

Op eenzelfde manier kan ook de tonnen droge stof worden berekend.

Appendix H

Typical pre-dredging bathymetric survey (here on 15/04/2021).

Shallow area (orange colour) means fresh deposition. The deposited area is attached to the west side of the entrance of the harbour.



baggerwerken met sleeppopperzuiger	
zone TG - A2 - A1 - B1 - B2 - B3.1	
vanaf 0.3 m boven streefdiepte	
van 0.3 m boven tot 0.5 m onder streefdiepte	
van 0.5 m tot 0.7 m onder streefdiepte	
vanaf 0.7 m onder streefdiepte	

Found here:

P:\20_017-kstInmdlWstKs\3_Uitvoering\Morphology\01_Data\NieuwpoortHarbour\Map_IN-survey NPT

DEPARTMENT **MOBILITY & PUBLIC WORKS**
Flanders hydraulics Research

Berchemlei 115, 2140 Antwerp

T +32 (0)3 224 60 35

F +32 (0)3 224 60 36

waterbouwkundiglabo@vlaanderen.be

www.flandershydraulicsresearch.be